



National Library
of Canada

Acquisitions and
Bibliographic Services Branch

395 Wellington Street
Ottawa, Ontario
K1A 0N4

Bibliothèque nationale
du Canada

Direction des acquisitions et
des services bibliographiques

395 rue Wellington
Ottawa (Ontario)
K1A 0N4

NOTICE

The quality of this microform is heavily dependent upon the quality of the original thesis submitted for microfilming. Every effort has been made to ensure the highest quality of reproduction possible.

If pages are missing, contact the university which granted the degree.

Some pages may have indistinct print especially if the original pages were typed with a poor typewriter ribbon or if the university sent us an inferior photocopy.

Reproduction in full or in part of this microform is governed by the Canadian Copyright Act, R.S.C. 1970, c. C-30, and subsequent amendments.

AVIS

La qualité de cette microforme dépend grandement de la qualité de la thèse soumise au microfilmage. Nous avons tout fait pour assurer une qualité supérieure de reproduction.

S'il manque des pages, veuillez communiquer avec l'université qui a conféré le grade.

La qualité d'impression de certaines pages peut laisser à désirer, surtout si les pages originales ont été dactylographiées à l'aide d'un ruban usé ou si l'université nous a fait parvenir une photocopie de qualité inférieure.

La reproduction, même partielle, de cette microforme est soumise à la Loi canadienne sur le droit d'auteur, SRC 1970, c. C-30, et ses amendements subséquents.

**A New Code Division
Multiple Access Scheme**

Premkumar Balasubramanian

**A Thesis
in
The Department
of
Electrical and Computer Engineering**

**Presented in Partial Fulfillment of the Requirements
for the Degree of Master of Applied Science at
Concordia University
Montréal, Québec, Canada**

May 1992

© Premkumar Balasubramanian, 1992



National Library
of Canada

Acquisitions and
Bibliographic Services Branch

395 Wellington Street
Ottawa, Ontario
K1A 0N4

Bibliothèque nationale
du Canada

Direction des acquisitions et
des services bibliographiques

395, rue Wellington
Ottawa (Ontario)
K1A 0N4

Notice: Not to be reprinted

Notice: Not to be reprinted

The author has granted an irrevocable non-exclusive licence allowing the National Library of Canada to reproduce, loan, distribute or sell copies of his/her thesis by any means and in any form or format, making this thesis available to interested persons.

L'auteur a accordé une licence irrévocable et non exclusive permettant à la Bibliothèque nationale du Canada de reproduire, prêter, distribuer ou vendre des copies de sa thèse de quelque manière et sous quelque forme que ce soit pour mettre des exemplaires de cette thèse à la disposition des personnes intéressées.

The author retains ownership of the copyright in his/her thesis. Neither the thesis nor substantial extracts from it may be printed or otherwise reproduced without his/her permission.

L'auteur conserve la propriété du droit d'auteur qui protège sa thèse. Ni la thèse ni des extraits substantiels de celle-ci ne doivent être imprimés ou autrement reproduits sans son autorisation.

ISBN 0-315-84705-0

Canada

ABSTRACT

A new Code Division Multiple Access scheme

Premkumar Balasubramanian

In this thesis we evaluate by performance analysis and computer simulation the bit error and throughput characteristics of a new Code Division Multiple Access scheme. The new technique considered is of the Modified SUGAR/DS type. In this multiple access scheme, user signals may arrive in a code asynchronous fashion at the receiver. Each user is identified by an orthogonal waveform and a Gold code. The analytical results show the possibility of gaining a minimum of 2 dB in Signal-to-Noise Ratio by splitting the users into three or more groups in a PSK/DS Spread Spectrum network. Both the chip synchronous and asynchronous cases are investigated. Also the uniform and optimal cases of dividing the total number of users into orthogonal groups are analyzed. Superior bit error and network data throughput results were observed in the different fading and FEC environments involved. By computer simulation we evaluate the bit error probability as a function of the number of users.

ACKNOWLEDGEMENTS

I would like to express my sincere gratitude to Dr.A.K. Elhakeem for his guidance and support throughout the course of my thesis work. This work was born from his ideas and he provided constructive suggestions to enable me to demonstrate this new technique by mathematical analysis and computer simulation. He was always available for consultation and he provided the necessary moral support to enable me to complete my M.A.Sc. program. I am grateful to him for all his sincere efforts. Our work was acknowledged by the acceptance of our work entitled "Modified SUGAR/DS, A new code division multiple access scheme" by IEEE Journal on selected areas in communication.

Throughout my educational efforts my family has provided me ample moral support and I am grateful to them for their patience and understanding. Finally I would like to express my gratitude to Caroline for her understanding and my friends who cheered me up.

TABLE OF CONTENTS

LIST OF FIGURES AND TABLES	vi
LIST OF SYMBOLS	x
CHAPTER 1: INTRODUCTION	1
1.1 Spread Spectrum Communication	1
1.2 Direct Sequence Systems (DS)	1
1.3 Frequency Hopping Systems (FH)	3
1.4 Time Hopping Systems (TH)	3
1.5 Chirp Systems	4
1.6 Scope of Thesis	5
CHAPTER 2: DESIGN AND ANALYSIS OF A NEW CODE DIVISION MULTIPLE ACCESS SCHEME	11
2.1 Introduction	11
2.2 System Description	11
2.3 Mathematical Analysis	13
2.4 The case of propagation delays, not multiples of chip duration ($\tau_k \neq iT_c$)	25
2.5 Analytical Results	27
CHAPTER 3: SIMULATION STUDY OF THE SUGAR SYSTEM	47
3.1 Introduction	47
3.2 Simulation study of the SUGAR system under multipath fading	49
3.3 Simulation study of the SUGAR system under fading	50
3.4 Simulation results	51
3.5 Analytical vs Simulation Results	52
3.6 Gold Codes	52
CHAPTER 4: SUMMARY AND CONCLUSIONS	62
4.1 Conclusions	62
4.2 Suggestions and Future Work	62
REFERENCES	64
APPENDIX	67

LIST OF FIGURES

Figure 1.1	Block diagram of a direct sequence transmitter and receiver	7
Figure 1.2	Block diagram of a frequency hopping transmitter and receiver	8
Figure 1.3	Power spectrum of a FH spread spectrum signal	10
Figure 1.4	Block diagram of a time hopping transmitter and receiver	9
Figure 1.5	Time hopping waveform	10
Figure 2.1	Generic Modified SUGAR/DS transmitter for use in CDMA Mobile or Indoor Communications (Centralized or Distributed Access)	30
Figure 2.2	Generic receiver bank of a modified SUGARW mobile or indoor CDMA system	31
Figure 2.3	Probability of bit error vs. number of users for conventional Spread Spectrum and Modified SUGAR systems for code length $L = 127$ (no fading and no coding).	32
Figure 2.4	Probability of bit error vs. number of users for conventional Spread Spectrum and Modified SUGAR systems for code length $L = 511$ (no fading and no coding).	32
Figure 2.5	Probability of bit error vs. number of users for conventional Spread Spectrum and Modified SUGAR systems for code length $L = 2047$ (no fading and no coding).	33
Figure 2.6	Throughput vs. number of users for conventional Spread Spectrum and Modified SUGAR systems for $L = 127$ and packet sizes $N=128$ and 256, for data communication (no fading and no coding).	33
Figure 2.7	Throughput vs. number of users for conventional Spread Spectrum and Modified SUGAR systems for $L = 511$ and packet sizes $N=128$ and 256, for data communication (no fading and no coding).	34
Figure 2.8	Throughput vs. number of users for conventional Spread Spectrum and Modified SUGAR systems for $L = 2047$ and packet sizes $N=128$ and 256, for data communication (no fading and no coding).	34
Figure 2.9	Probability of bit error vs. number of users for conventional Spread Spectrum and Modified SUGAR systems for $L = 127$ (combined modulation coding and no fading). Other FEC coding parameters as in Reference [9].	35
Figure 2.10	Probability of bit error vs. number of users for conventional Spread Spectrum and Modified SUGAR systems for $L = 511$ (combined modulation coding and no fading). Other FEC coding parameters as in Reference [9].	35
Figure 2.11	Probability of bit error vs. number of users for conventional Spread	

	Spectrum and Modified SUGAR systems for $L = 2047$ (combined modulation coding and no fading). Other FEC coding parameters as in Reference [9].	36
Figure 2.12	Throughput vs. number of users for conventional Spread Spectrum and Modified SUGAR systems for $L = 127$ and packet sizes $N=128$ and 256 , for data communication (combined modulation coding and no fading).	36
Figure 2.13	Throughput vs. number of users for conventional Spread Spectrum and Modified SUGAR systems for $L = 511$ and packet sizes $N=128$ and 256 , for data communication (combined modulation coding and no fading).	37
Figure 2.14	Throughput vs. number of users for conventional Spread Spectrum and Modified SUGAR systems for $L = 2047$ and packet sizes $N=128$ and 256 , for data communication (combined modulation coding and no fading).	37
Figure 2.15	Probability of bit error vs. number of users for conventional Spread Spectrum and Modified SUGAR systems for code length $L = 127$ (Rayleigh fading and no coding).	38
Figure 2.16	Probability of bit error vs. number of users for conventional Spread Spectrum and Modified SUGAR systems for code length $L = 511$ (Rayleigh fading and no coding).	38
Figure 2.17	Probability of bit error vs. number of users for conventional Spread Spectrum and Modified SUGAR systems for code length $L = 2047$ (Rayleigh fading and no coding).	39
Figure 2.18	Throughput vs. number of users for conventional Spread Spectrum and Modified SUGAR systems for $L = 127$ and packet size $N=128$, for data communication (Rayleigh fading and no coding).	39
Figure 2.19	Throughput vs. number of users for conventional Spread Spectrum and Modified SUGAR systems for $L = 511$ and packet size $N=128$, for data communication (Rayleigh fading and no coding).	40
Figure 2.20	Throughput vs. number of users for conventional Spread Spectrum and Modified SUGAR systems for $L = 2047$ and packet size $N=128$, for data communication (Rayleigh fading and no coding).	40
Figure 2.21	Probability of bit error vs. number of users for conventional Spread Spectrum and Modified SUGAR systems for $L = 127$ (Combined modulation coding and Rician fading, $BW=0.1$). Other FEC coding parameters as in Reference [9].	41
Figure 2.22	Probability of bit error vs. number of users for conventional Spread Spectrum and Modified SUGAR systems for $L = 511$ (Combined modulation coding and Rician fading, $BW=0.1$). Other FEC coding parameters as in Reference [9].	41
Figure 2.23	Probability of bit error vs. number of users for conventional Spread Spectrum and Modified SUGAR systems for $L = 2047$ (Combined modulation coding and Rician fading, $BW=0.1$). Other FEC coding	

	parameters as in Reference [9].	42
Figure 2.24	Throughput vs. number of users, for conventional Spread Spectrum and Modified SUGAR systems for $L = 127$ and packet sizes $N=128$ and 256, for data communication (combined modulation coding and Rician fading, $BW=0.1$).	42
Figure 2.25	Throughput vs. number of users, for conventional Spread Spectrum and Modified SUGAR systems for $L = 511$ and packet sizes $N=128$ and 256, for data communication (combined modulation coding and Rician fading, $BW=0.1$).	43
Figure 2.26	Throughput vs. number of users, for conventional Spread Spectrum and Modified SUGAR systems for $L = 2047$ and packet sizes $N=128$ and 256, for data communication (combined modulation coding and Rician fading, $BW=0.1$).	43
Figure 2.27	Probability of bit error vs. number of users for,conventional Spread Spectrum and Modified SUGAR systems for $L = 255$ (Reed-Solomon coding and Rayleigh fading). Other FEC coding parameters as in Reference [10].	44
Figure 2.28	Probability of bit error vs. number of users for,conventional Spread Spectrum and Modified SUGAR systems for $L = 511$ (Reed-Solomon coding and Rayleigh fading). Other FEC coding parameters as in Reference [10].	44
Figure 2.29	Probability of bit error vs. number of users for,conventional Spread Spectrum and Modified SUGAR systems for $L = 2047$ (Reed-Solomon coding and Rayleigh fading). Other FEC coding parameters as in Reference [10].	45
Figure 2.30	Throughput vs. number of users, for conventional Spread Spectrum and Modified SUGAR systems for $L = 255$ and packet sizes $N=128$ and 256, for data communication (Reed-Solomon coding and Rayleigh fading).	45
Figure 2.31	Throughput vs. number of users, for conventional Spread Spectrum and Modified SUGAR systems for $L = 511$ and packet sizes $N=128$ and 256, for data communication (Reed-Solomon coding and Rayleigh fading).	46
Figure 2.32	Throughput vs. number of users, for conventional Spread Spectrum and Modified SUGAR systems for $L = 2047$ and packet sizes $N=128$ and 256, for data communication (Reed-Solomon coding and Rayleigh fading).	46
Figure 3.1	Simulation model of a Code Division Multiple Access system	54
Figure 3.2	A typical Gold code generator consisting of two Linear Feedback Shift Registers	55
Figure 3.3	Radio wave channel model at waveform level[7]	56
Figure 3.4	Simulation results of probability of bit error vs. number of users for asynchronous spread spectrum and Modifed SUGAR systems	

	for $L=127$ (no coding, no fading)	57
Figure 3.5	Simulation results of probability of bit error vs. number of users for synchronous classic spread spectrum and Modified SUGAR systems for $L=127$ (no coding, no fading)	58
Figure 3.6	Simulation results of probability of bit error vs. number of users for asynchronous classic spread spectrum and Modified SUGAR44 systems for $L=511$ (no coding, no fading)	59
Figure 3.7	Simulation results of probability of bit error vs. number of users for asynchronous classic spread spectrum and Modified SUGAR systems for $L=127$ (Ricean fading, no coding)	60
Figs. (A-1 to A-4)	Switching function cross-correlation for 2 users in groups 4,4. $\{b_0, b_1\}$ are the two data bits of the interfering user k4 overlapping the received bit of the intended user.	71
Figs. (A-5 to A-8)	Switching function cross-correlation for 2 users in groups 4,2. $\{b_0, b_1\}$ are the two data bits of the interfering user k2 overlapping the received bit of the intended user.	75
Figs. (A-9 to A-12)	Switching function cross-correlation for 2 users in groups 4,1. $\{b_0, b_1\}$ are the two data bits of the interfering user k1 overlapping the received bit of the intended user.	79
Figs. (A-13 to A-16)	Switching function cross-correlation for 2 users in groups 1,2. $\{b_0, b_1\}$ are the two data bits of the interfering user k1 overlapping the received bit of the intended user.	83
Figs. (A-17 to A-20)	Switching function cross-correlation for 2 users in groups 2,2. $\{b_0, b_1\}$ are the two data bits of the interfering user k2 overlapping the received bit of the intended user.	87
Figs (A-21 to A-24)	Switching function cross-correlation for 2 users in groups 1,1. $\{b_0, b_1\}$ are the two data bits of the interfering user k1 overlapping the received bit of the intended user.	92
Table 2.1	Average Gold code cross-correlation power for different generator lengths.	30

LIST OF SYMBOLS

T_b	Bit duration
T_c	Gold code chip
n_s	Number of subcodes per data bit
$d_{m,l}(t)$	Data bit of the m^{th} user of the l^{th} group
$S_{m,l}(t)$	Switching function of the m^{th} user of the l^{th} group
$C_{m,l}(t)$	Gold code of the m^{th} user of the l^{th} group
$\tau_{m,l}$	Random delay of the m^{th} user of the l^{th} group
ω_c	Common carrier
M_i	Number of users in group i, i=1,2,4
M	Total number of users
P	Signal power
$\phi_{m,l}$	Random phase of the m^{th} user with respect to another user in the l^{th} group
L	Gold code length
n	Length of code generator
R_{sg}	Average Gold code cross-correlation power
P_b	Bit error probability
P_c	Probability of correct packet reception
η	Throughput efficiency
N	Number of bits per packet
W	Spread Spectrum bandwidth

R_b	Bit rate
SNR	Signal-to-Noise ratio
erfc	Complementary error function

INTRODUCTION

1.1 Spread Spectrum Communication

Spread Spectrum communication is a modulation/demodulation technique in which the transmitted signal energy occupies a channel bandwidth that is larger than the information bit rate and the demodulation is achieved by correlation of the received signal with a replica of the code used in the transmitter to spread the information signal. These techniques, through the properties of coded modulation, can provide systems that produce low interference to other systems, have interference rejection capability, provide multiple access capability, antijam capability, improved spectral efficiency and have other useful capabilities.

Spread spectrum techniques are divided into four basic types.

1-Direct Sequence (DS)

2-Frequency Hopping (FH)

3-Time Hopping (TH)

4-Chirp

Hybrid systems combine two or more of the above techniques. One reason for using hybrid techniques is that some of the advantages of different spreading techniques can be utilized in a single system.

1.2 Direct Sequence Systems (DS)

Direct sequence systems are the best known and most widely used spread spectrum systems. In this technique, the data-modulated carrier is directly modulated by a wideband signal or code. The codes employed are just long sequences of ones and zeros at bit rates usually in the range from one to a few tens of MHz. Fig. 1.1 shows a block diagram of a Binary Phase Shift Keying (BPSK) direct sequence spread spectrum

transmitter and receiver.

Ideal BPSK modulation results in instantaneous phase changes of the carrier by 180 degrees and can be mathematically represented as a multiplication of the carrier by a function $c(t)$ which takes on the values ± 1 . The constant envelope data-modulated carrier is given by

$$s_d(t) = \sqrt{2P} \cos[\omega_o t + \theta_d(t)] \quad (1.1)$$

where P is the power, ω_o is the radian frequency and $\theta_d(t)$ is the modulated data. BPSK spreading is achieved by simply multiplying $s_d(t)$ by a function $c(t)$ representing the spreading waveform. Thus the transmitted signal is

$$s_t(t) = \sqrt{2P} c(t) \cos[\omega_o t + \theta_d(t)] \quad (1.2)$$

This signal is transmitted via a distortionless path having transmission delay T_d . The signal is received in multiaccess interference and/or Gaussian noise. Demodulation is accomplished in part by mixing with the spreading code appropriately delayed as shown in Figure 1.1. The correlation of the received signal with the delayed spreading waveform is called despreading. The signal component at the output of the despreading mixer is

$$\sqrt{2P} c(t-T_d) c(t-\hat{T}_d) \cos[\omega_o t + \theta_d(t-T_d) + \phi] \quad (1.3)$$

where \hat{T}_d is the receiver's best estimate of the transmission delay. Since $c(t) = \pm 1$, the product $c(t-T_d) c(t-\hat{T}_d)$ will be unity if $\hat{T}_d = T_d$, that is if the spreading code at the receiver is synchronized with the spreading code at the transmitter. When correctly synchronized, the signal component of the output of the receiver despreading mixer is equal to $s_d(t)$ except for a random phase ϕ , and $s_d(t)$ can be demodulated using a conventional coherent phase demodulator.

An important parameter that is sometimes useful in specifying the performance of a spread spectrum signal in the presence of interference is known as the processing gain. The processing gain G_p is frequently defined as the ratio of the spreading code rate to the data bit rate. Hence

$$G_b = \frac{R_c}{R_b} \quad (1.4)$$

1.3 Frequency Hopping (FH)

This is a spreading technique in which the carrier is frequency shifted in a pattern determined by a digital code sequence, thus widening the spectrum of the data-modulated carrier. The hopped frequency and hopping rate are determined by the Pseudo Random (PN) sequence and code rate respectively. The code clock rate is usually lower than that of the DS code rate, usually in the order of a few hundred kilobits per second.

Figure 2.2 shows a simplified block diagram of a frequency hopping system. Spreading of the spectrum is obtained by changing the carrier frequency over the whole available band, according to a PN sequence. The bandwidth over which the energy is spread is essentially independent of the code clock rate and can be chosen by a combination of the number and size of frequency hops.

At the receiver a frequency synthesizer driven by a PN code generator generates a frequency shifted reference signal, which is multiplied by the incoming signal in a mixer. A signal with the same bandwidth as the local reference would have twice the reference bandwidth at the Intermediate Frequency (IF). The IF then can reject all of the undesired signals that lie outside its bandwidth. Almost all the undesired signals' power is rejected whereas the desired signal is enhanced by being correlated with the local reference.

As in Direct Sequence spread spectrum modulation, the processing gain for a FH system is defined as

$$G_P = \frac{W_s}{W_d} \quad (1.5)$$

where W_s is the total FH band and W_d is the data bandwidth.

1.4 Time Hopping (TH)

In time hopping systems, the spreading is achieved by compressing the information signal in the time domain. That is, the time hopping systems control their transmission time and period with a code sequence in the same way that frequency hopping systems control their frequencies. A typical TH system is shown in Fig. 1.4. A time hopping waveform is shown in Fig. 1.5, where the time axis is divided into intervals known as frames and each of these frames is subdivided into M time slots. During each slot in a frame the carrier will be modulated with a message by any modulation method. Time slot is chosen for a given frame by means of a PN code generator.

Time hopping may be used in reducing interference between systems in TDM. Interference among simultaneous users in a time hopping system can be minimized by coordinating the times at which each user can transmit a signal, which also avoids the problem of very strong signals at a receiver swamping out the effects of weaker signals. In a non-coordinated system, overlapping transmission bursts will result in message errors, and for this it will normally require the use of error-correction coding to restore the proper message bits. The advantages of TH system are high bandwidth efficiency and its implementation is simpler than that of a FH system. The disadvantages are long acquisition time and the need for error correction.

1.5 Chirp Systems

Frequency-modulation pulse compression or chirp is a technique in which a carrier is swept linearly over a wide range of frequencies during a given pulse. This technique of spectrum spreading was developed a number of years ago to improve radar operation by obtaining the resolution of a short pulse, but with the detection capability of a long pulse. A long transmitted pulse is suitably modulated and the receiver is designed to act on the modulation to compress the pulse into a much shorter one. In this technique each transmitted signal element gives a change of frequency with time. Each received signal element is operated by a matched filter, which coherently combines the signal spectral components into a narrow signal of increased amplitude. The advantage

of this technique for radar systems is that significant power reduction is possible. Also chirp waveforms are less affected by Doppler shifts due to motion of the target relative to the radar and this is often significant when high velocity targets must be catered for. Specifically the chirp waveform suffers very little Doppler-induced correlation loss relative to PN-spread symbols of the same time duration. However, the chirp waveforms have the property that the apparent time of arrival shifts as a function of Doppler offset. Because of this chirp modulation is used in jam-resistant communication and pulse compression radars.

The receiver used for chirp signals is a matched filter, matched to the angular rate of change of the transmitting frequency-sweep signal. The transmitted frequency-swept chirp signal is like that produced by a common laboratory sweep generator, that is because most chirp systems use a linear sweep pattern. Any pattern suitable to the requirement of a matching receive filter is suitable. In communication systems the receiver signal processing is similar to that used in chirp radar. The main difference is that in the communication system, both upward and downward frequency sweeps have to be detected, whereas in radar application only sweeps in one direction are used. At the receiver, two matched filters are used, one matched to the mark chirp signal and the other to the space chirp signal, where mark and space are used to represent "ones and zeros" in digital communication. Chirp systems possess certain advantages, namely significant power reduction is possible and coding is not normally used.

1.6 Scope of Thesis

The thesis is organized as follows:

In chapter 2, introduction to the new CDMA system is given and mathematical development of the performance measures is analyzed through several equations. The results of the analytical work are illustrated through several graphs, plotted under varying channel conditions. In particular bit error rate and throughput efficiency as functions of number of users for various Gold code lengths and packet lengths are examined in

several graphs.

Chapter 3 presents the computer model and performance of SUGAR/DS system through computer simulation. The simulation results are explained.

Chapter 4 summarizes the results of the research work and offers suggestions for further research. The entire thesis is well supported by diagrams and tables, where necessary.

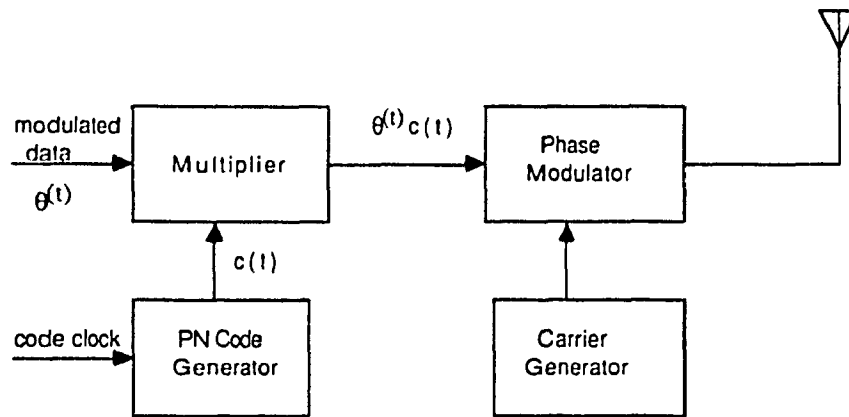


Fig.(1.1a) Block diagram of a direct sequence transmitter

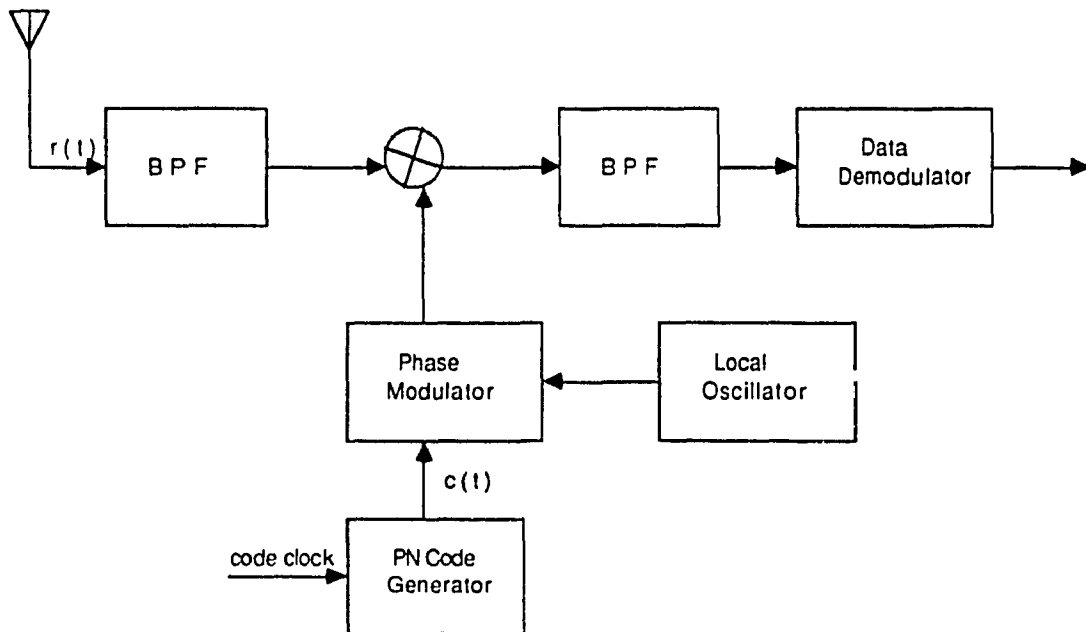


Fig. (1.1b) Block diagram of a direct sequence receiver

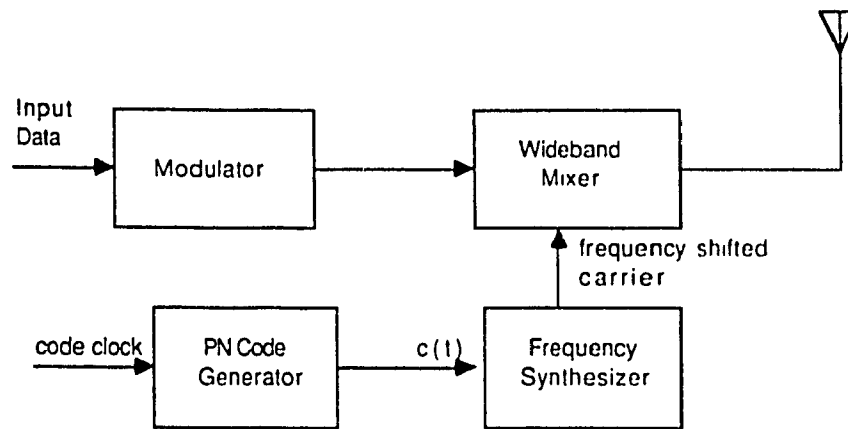


Fig.(1.2a) Block diagram of a frequency hopping transmitter

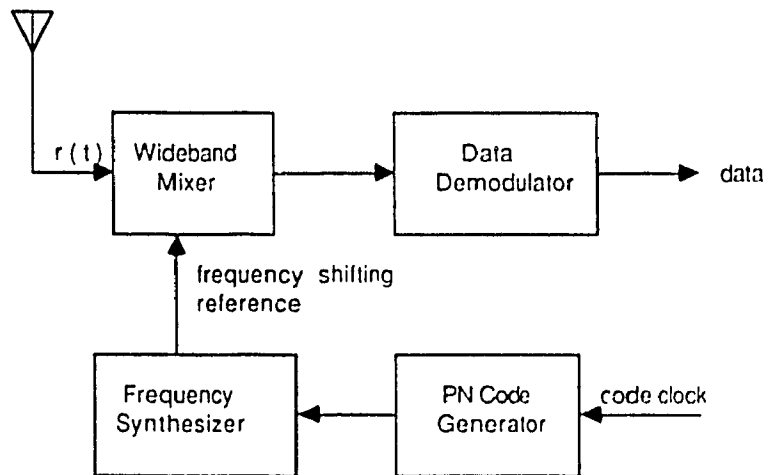


Fig. (1.2b) Block diagram of a frequency hopping receiver

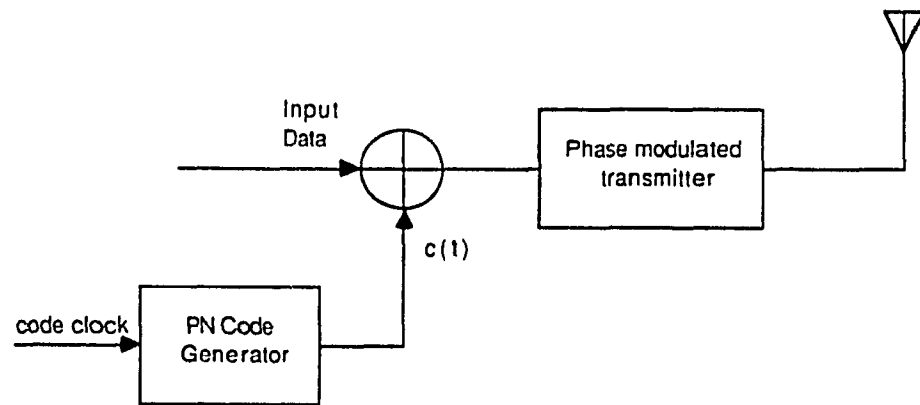


Fig.(1.4a) Block diagram of a time hopping transmitter

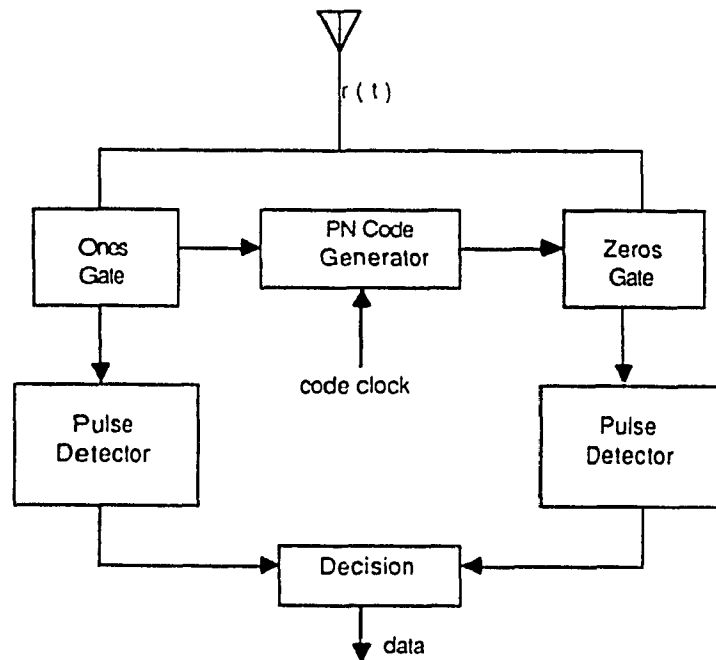


Fig. (1.4b) Block diagram of a time hopping receiver

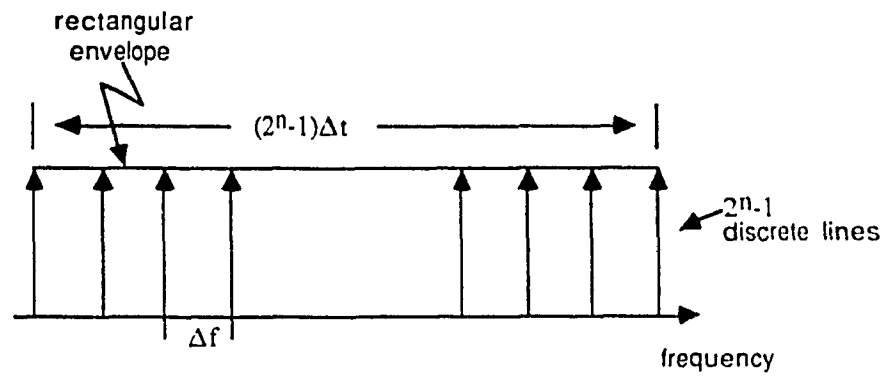


Fig.(1.3) Power spectrum of a FH spread spectrum signal

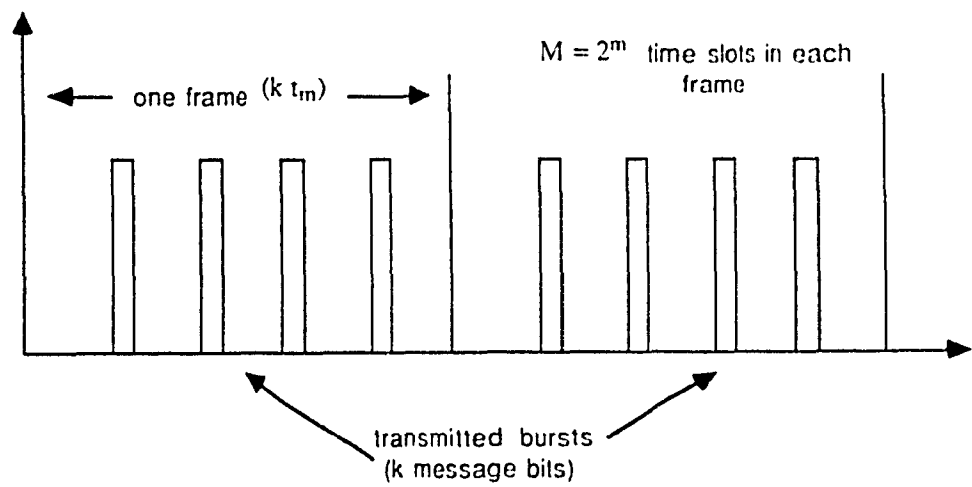


Fig. (1.5) Time hopping waveform

Chapter Two

Design and analysis of a new Code Division Multiple Access scheme

2.1 Introduction

Using Code Division Multiple Access (CDMA) as a multiple access technique in digital radio networks provides several desirable features. In a network with a large number of simple stations with a mixed traffic of digital voice and data, CDMA provides a simple multi-access protocol. Other advantages are immunity to fading and jamming, privacy of data, improved multipath propagation etc. It may also require less peak transmitted power than Time Division Multiple Access (TDMA) and less RF stability and accuracy than required in Frequency Division Multiple Access (FDMA) [18]. Furthermore, in CDMA as opposed to TDMA, no global synchronization is required.

In a digital radio network with a large number of stations, m out of n users may simultaneously access the shared channel at random with no reservation or network control necessary. The number of simultaneous users m is determined by the processing gain of the system and the acceptable level of mutual interference.

The basic problem in CDMA networks, as far as data transmission is concerned, is low throughput efficiency and code acquisition problems. The acquisition problem is partially solved by parallel matched filtering at the receiver[1] while the more serious problem of low throughput is taken care of by the orthogonality of the proposed waveforms.

The thesis assumes that code acquisition and synchronization have been achieved and considers only the communication performance where probability of bit error and throughput efficiency are performance measures.

2.2 System Description

The uplink communication technique (from user to base station) is a new random access technique, Modified SUGAR/DS. The downlink (from base station to users) is the Time Division Multiplexing (TDM) access technique. The modified SUGAR system is basically a combined modulation/access technique where the digital data bits (voice or data or video) of T_b seconds each are modulated by the carrier(ω_c), a pseudo noise generated by combining of two feed back shift registers generator each of chip duration, T_c seconds and one of M orthogonal signals over T_b (preferably square orthogonal signals) as shown in Figure 2.1.

The total user population is divided into three groups(1,2,4). Users of one group will have different Gold codes but all users in one group will have the same orthogonal waveform. On the radio channel, signals of the three groups of users are summed and the base station demodulates the signals of all active users and relays the information to various destinations in a TDM scheme after remodulation (using differential PSK, say). Packet mode is assumed and hence the system is transparent to the service kind, i.e., all packets at the receiver are treated the same as far as packet detection, decoding, ARQ and retransmissions are concerned. Each user is identified by a pseudorandom code (Gold code) and an orthogonal waveform (switching function), thus guaranteeing selective identification.

User signals may arrive in an asynchronous fashion at the base station, but user cross-correlation is still a minimum compared to the Classic spread spectrum system. For the Modified SUGAR system, the bit period is split over 4 subcode periods, each having a repetitive shorter Gold code. At the base station, the interfering signals (on average) will be split among three user groups with equal probability and the cross-correlation and hence bit error and packet detection success will be optimized.

Following reception at a user station (Figure 2.2), the total received signal is carrier-recovered, mixed and integrated over one bit period with the switching function and user Gold code. Subsequent threshold detection (we could use PSK or DPSK

demodulation) yields the information signals, after which FEC decoding could further minimize bit errors. Diversity combining could also be used (eg., antenna diversity to combat AWGN and fading) to further improve bit errors. Also any ARQ technique could be used to detect packet errors and ask for retransmission.

The previous system(SUGARW system), does not need acquisition. The modified SUGAR system does not go from acquisition to data reception and vice versa, as in classic systems. Acquisition and data modulation overlap in time, and hence throughput capacity is not wasted in that system. This was achieved by having the receiver acquiring and demodulating simultaneously in two banks, one based on old code epoch and the other based on a new epoch found by parallel matched filtering.

Analysis of the new system, Modified SUGAR/DS, shows superior performance against existing state of the art techniques. However, it may suffer a fairness problem (users in group 1 are slightly better off) necessitating the frequent changes or reassignment of orthogonal waveforms to users on a slow basis.

2.3 Mathematical Analysis

Figure 2.1 shows the transmitter and receiver block diagrams of one of the users of the third group (group 4). Without losing generality, we assume $\tau_{1,4} = \theta_{1,4} = 0$ (delay and phase of the intended user are zero since the user is assumed synchronized to the received code (both coarse and fine synchronization)). The data bits, switching functions, and the code chips of the m^{th} user of l^{th} group are given by

$$d_{m,l}(t-nT_b) = \pm 1, \quad nT_b < t \leq (n+1)T_b \quad (2.1)$$

$$S_{m,l}(t-rT_b/n_s) = \pm 1, \quad rT_b/n_s < t \leq (r+1)T_b/n_s \quad (2.2)$$

$$C_{m,l}(t-mT_c) = \pm 1, \quad mT_c < t \leq (m+1)T_c \quad (2.3)$$

The switching functions and data for various groups are shown in Fig(2.1) and $T_b, n_s, r, \tau_{m,l}$ are the data bit duration, the number of subcodes per data bit duration, the r^{th}

subcode identity and the random delay of m^{th} user signal received at the receiver of the first user of group l . The received signal is now given by (following steps similar to those of [4]):

$$\begin{aligned}
 r(t) = & \sqrt{2P} d_{1,4}(t-nT_b) S_{1,4}(t-jT_b/n_s) C_{1,4}(t-mT_c) \cos(\omega_c t) + n(t) \\
 & + \sum_{\substack{k=2 \\ M_1}}^{k=4} \sqrt{2P} d_{k,4}(t-nT_b) S_{k,4}(t+\tau_{k,4}-jT_b/n_s) C_{k,4}(t+\tau_{k,4}-mT_c) \cos(\omega_c t + \theta_{k,4}) \\
 & + \sum_{\substack{k=1 \\ M_1}}^{k=2} \sqrt{2P} d_{k,2}(t-nT_b+\tau_{k,2}) S_{k,2}(t-jT_b/n_s+\tau_{k,2}) C_{k,2}(t+\tau_{k,2}-mT_c) \cos(\omega_c t + \theta_{k,2}) \\
 & + \sum_{k=1} \sqrt{2P} d_{k,1}(t-nT_b+\tau_{k,1}) S_{k,1}(t-jT_b/n_s+\tau_{k,1}) C_{k,1}(t+\tau_{k,1}-mT_c) \cos(\omega_c t + \theta_{k,1})
 \end{aligned} \quad (2.4)$$

where

$$\theta_{m,l} = \phi_{m,l} + \omega_c \tau_{m,l} \quad (2.5)$$

$\omega_c, T_c, P, M_1, M_2, M_4$ are respectively, the common carrier of all users, the DS chip duration, the signal power (assumed the same for all user signals), and the number of users in the three groups. $d_{i,j}$, $S_{i,j}$, $C_{i,j}$ are the data bit, the switching function, and the Gold Code chip of the i^{th} user of group j respectively. $\phi_{m,l}$ is the random phase of the m^{th} user with respect to another user in the l^{th} group. $n(t)$ is the received AWGN of double sided density equal to N_0 . The three sums of (2.4) represent all interference from the three groups.

Note: In this thesis, and contrary to [5] where $\tau_{m,l}$ could assume any value, we assumed a chip synchronous multiaccess system, i.e., all $\tau_{m,l} = nT_c$ similar to many recent proposals[6]. Removing this assumption results in better bit SNR but more required Spread Spectrum bandwidth. Also it is left as an easy exercise for the reader to see that the Spread Spectrum bandwidth of our Modified SUGAR DS/PSK system is a few percentage points above that required by a classic DS/PSK system following the same lines as in [7].

At this point it is important to note that though the switching functions are orthogonal by themselves, the multiplication function $S_{m,l}(t) \cdot C_{m,l}(t)$ are not orthogonal for

different l . (Please refer to the Appendix). However it is the area under the square of the multiplication functions that gives the powers of multiuser interferences. Without our switching functions, and if all users are in one group as in classic systems, this power will be given by the well-known cross-correlation properties of Gold codes (2.12,2.13). In our approach, this Gold code cross-correlation of (2.13) becomes multiplied by the cross-correlation envelope of the switching functions $ff_{m,l}(\tau)$ as in (2.18) and (2.19), etc. The appendix shows clearly that for all τ , the average cross-correlation envelope is not zero, but it is much less than that of the equivalent classic system, i.e.,

for example, compare from (A-13), $y_4 = \frac{16L^2T_c^2}{9}$ to the corresponding $16L^2T_c^2$ of the classic system. This cuts down the variance of the multiuser interference, as can be evidenced by comparing equations (2.26-2.28) to the denominator of equation (2.36), which is the variance of the classic case.

It is to be noted that the first line of equation (2.4) is empty of τ, θ since the term corresponds to the intended signal ($\tau_{1,4} = \theta_{1,4} = 0$). While specific values for M_1, M_2, M_4 depend on the traffic conditions, network topology, code assignment policy, etc., we assume for the first phase of this research that they have equal values, i.e.,

$$M_1 = M_2 = M_4 = M/3 \quad (2.6)$$

At the receiver, $r(t)$ is multiplied by the reference signal, defined in four subcode intervals ($j=0,1,2,3$), yielding for the j^{th} subcode interval

$$a_{1,j,4} = \int_{jT_b/4}^{(j+1)T_b/4} r(t) S_{1,4}(t-jT_b/4) C_{1,4}(t-mT_c) \cos \omega_c t \, dt \quad (2.7)$$

The substitution $n_s=4$ was made the four received subcode sections corresponding to one bit which are appropriately multiplied by the reference signals (consisting of the code, the switching function and the carrier), after which summing yields

$$\begin{aligned}
 y_4(t) &= \sum_{j=0}^3 a_{1,j,4} = \sqrt{P/2} T_b d_{1,4} + \sum_{j=0}^3 \sqrt{P/2} \cdot \\
 &\left\{ \begin{aligned} &M_1 \int_{jT_b/4}^{(j+1)T_b/4} \sum_{k=2}^4 \cos \theta_{k,4} \int_{jT_b/4}^{(j+1)T_b/4} d_{k,4}(t-nT_b+\tau_{k,4}) S_{1,4}(t-jT_b/4) S_{k,4}(t-jT_b/4+\tau_{k,4}) \\ &C_{1,4}(t-mT_c) C_{k,4}(t-mT_c+\tau_{k,4}) dt \\ &M_2 + \sum_{k=2}^4 \cos \theta_{k,2,4} \int_{jT_b/4}^{(j+1)T_b/4} d_{k,2,2}(t-nT_b+\tau_{k,2,4}) S_{1,4}(t-jT_b/4) S_{k,2,2}(t-jT_b/4+\tau_{k,2,4}) \\ &C_{1,4}(t-mT_c) C_{k,2,2}(t-mT_c+\tau_{k,2,4}) dt \\ &M_3 + \sum_{k=1}^4 \cos \theta_{k,1,4} \int_{jT_b/4}^{(j+1)T_b/4} d_{k,1,1}(t-nT_b+\tau_{k,1,4}) S_{1,4}(t-jT_b/4) S_{k,1,1}(t-jT_b/4+\tau_{k,1,4}) \\ &C_{1,4}(t-mT_c) C_{k,1,1}(t-mT_c+\tau_{k,1,4}) dt \end{aligned} \right\} \\
 &+ \int_0^{T_b} n(t) S_{1,4}(t-jT_b/4) C_{1,4}(t-mT_c) \cos \omega_c t dt \quad (2.8)
 \end{aligned}$$

For given values of the delays $\tau_{k,1,4}$, $\tau_{k,2,4}$, $\tau_{k,4,4}$ and knowing the user identity, the switching function takes only ± 1 values. For data bits $d_{k,1,1}$, $d_{k,2,2}$, $d_{k,4,4}$ all terms within the integrands in (2.8) yields only fixed ± 1 depending on the delay situation, data bits, etc., as explained, and the only remaining terms under the integral will be the code cross correlation terms (such as $C_{1,4}(t-mT_c) C_{k,1,1}(t-mT_c+\tau_{k,1,4})$). Also, since the switching functions and data terms are much slower than the code, they can be taken outside the integrators. This simplifying assumption appears over and over in the literature (see for e.g., [7], page 337). It is justified whenever one fourth of the bit period (the smallest period in which the switching function S_4 remains constant) is a multiple of the chip period T_c . In this thesis the ratio $T_b/4T_c$ was set equal to 32, thus guaranteeing that the Gold code cross-correlation assumes its full code period. For example, in moving from (2.8) to (2.9) we have taken $S_{m,l}(t) d_{m,l}$ outside the integrators. However the integration is only over a period equal to $T_b/4$, i.e., the minimum amount over which $S_{m,l}(t) d_{m,l}(t)$ remains constant. Now assigning the data and switching functions, fixed values for each

scenario (see the Appendix) and averaging over all data possibilities (all scenarios), we obtain the average cross correlation.

Now defining the following periodic estimate cross correlation functions (periodic in the sense that the integrations in (2.9) give the same final values at $j=0,1,2,3$ since the same short Gold Codes are repeated for each user four times in each bit).

$$CC_{4,4}(\tau_{k4,4}) = \int_{\substack{(j+1)T_b/4 \\ jT_b/4}}^{(j+1)T_b/4} C_{1,4}(t-mT_c) C_{k4,4}(t-mT_c+\tau_{k4,4}) dt \quad (2.9a)$$

$$CC_{2,4}(\tau_{k2,4}) = \int_{\substack{jT_b/4 \\ (j+1)T_b/4}}^{jT_b/4} C_{1,4}(t-mT_c) C_{k2,2}(t-mT_c+\tau_{k2,4}) dt \quad (2.9b)$$

$$CC_{1,4}(\tau_{k1,4}) = \int_{jT_b/4}^{(j+1)T_b/4} C_{1,4}(t-mT_c) C_{k1,1}(t-mT_c+\tau_{k1,4}) dt \quad (2.9c)$$

Also given certain values for the data, user switching function scenarios we define the following quantities. (see the Appendix)

$$f_{k4,4}(j; \tau_{k4,4}; d_{k4,4}; S_{1,4}; S_{k4,4}) = d_{k4,4}(t-nT_b+\tau_{k4,4}) S_{1,4}(t-jT_b/4) S_{k4,4}(t-jT_b/4+\tau_{k4,4}) \quad (2.10a)$$

$$f_{k2,4}(j; \tau_{k2,4}; d_{k2,2}; S_{1,4}; S_{k2,2}) = d_{k2,2}(t-nT_b+\tau_{k2,4}) S_{1,4}(t-jT_b/4) S_{k2,2}(t-jT_b/4+\tau_{k2,4}) \quad (2.10b)$$

$$f_{k1,4}(j; \tau_{k1,4}; d_{k1,1}; S_{1,4}; S_{k1,1}) = d_{k1,1}(t-nT_b+\tau_{k1,4}) S_{1,4}(t-jT_b/4) S_{k1,1}(t-jT_b/4+\tau_{k1,4}) \quad (2.10c)$$

Substituting (2.9), (2.10) into (2.8), exchanging the order of the summation, and recalling the periodicity of the four subcodes used within each bit, (they are actually one short Gold Code repeated $n_s=4$ times!) it is easy to see that the quantities $C(.)$ in (2.9) assume the same value for all j . Also assuming that the propagation path delays $\tau_{k1,4}, \tau_{k2,4}, \tau_{k4,4}$ remain constant at least for a few data bits, which is a very reasonable assumption, we finally obtain for $y(t)$

$$\begin{aligned} y_4(t) \Big|_{\tau_{k1,4}, \tau_{k2,4}, \tau_{k4,4}} = & \sqrt{P/2} \left[T_b d_{1,4} + \sum_{k4=2}^{M_4} \cos\theta_{k4,4} CC_{4,4}(\tau_{k4,4}) \sum_{j=0}^3 f_{k4,4}(j; \tau_{k4,4}; d_{k4,4}; S_{1,4}; S_{k4,4}) \right. \\ & + \sum_{\substack{k2=1 \\ M_2}}^{M_2} \cos\theta_{k2,4} CC_{2,4}(\tau_{k2,4}) \sum_{j=0}^3 f_{k2,4}(j; \tau_{k2,4}; d_{k2,2}; S_{1,4}; S_{k2,2}) \\ & \left. + \sum_{\substack{k1=1 \\ M_1}}^{M_1} \cos\theta_{k1,4} CC_{1,4}(\tau_{k1,4}) \sum_{j=0}^3 f_{k1,4}(j; \tau_{k1,4}; d_{k1,1}; S_{1,4}; S_{k1,1}) \right] + n_4(t) \quad (2.11) \end{aligned}$$

where the conditioning on the LHS of (2.11) is over all delays, data, phases and switching functions of the users in all groups and where $n'(t)$ remains essentially an AWGN after multiplying $n(t)$ by the reference signal.

Another well justified assumption is that the time averages in (2.9) can be replaced by ensemble averages (ergodicity) with the well known Gold Codes cross correlation $CC_{\dots}(\dots)$ (based on whole subcode length) taking one of the following three values[8].

$$CC_{\dots}(\dots) = \frac{-t(L)}{L} \begin{cases} \text{occurring with probability } 0.25 & (n \text{ odd}) \\ \text{occurring with probability } 0.125 & (n \text{ even}) \end{cases} \quad (2.12a)$$

$$= \frac{-1}{L} \begin{cases} \text{occurring with probability } 0.5 & (n \text{ odd}) \\ \text{occurring with probability } 0.75 & (n \text{ even}) \end{cases} \quad (2.12b)$$

$$= \frac{t(L) - 2}{L} \begin{cases} \text{occurring with probability } 0.25 & (n \text{ odd}) \\ \text{occurring with probability } 0.125 & (n \text{ even}) \end{cases} \quad (2.12c)$$

where

$$t(L) = 1 + 2^{0.5(n+1)}, \quad n \text{ odd} \quad (2.13a)$$

$$= 1 + 2^{0.5(n+2)}, \quad n \text{ even} \quad (2.13b)$$

and $L = (2^n - 1) =$ Gold Code length and n is the length of the code generating LFSR.

It is important to recall at this point that the length of the shift register of the equivalent classic DS system is $n' = n + 2$, since each data bit encloses 4 repeated shorter Gold Codes in the Modified SUGAR system and only one longer Gold Code in the classic system.

The assumption of $y(T_b)$ being Gaussian is typical in the literature and justified by the Central Limit Theorem and the statistical nature of the various $CC_{\dots}(\dots)$, $f(\dots)$ and $(\cos\theta)$ terms in (2.11). Now taking the average of (2.11) and noting that the expected values of $\bar{n}(t)$ and $CC_{\dots}(\dots)$ and $f(\dots)$ (from the Appendix), we obtain

$$E\{y(T_b)\} = \sqrt{P/2} T_b d_{1,4} \quad (2.14)$$

For clarity we drop the arguments of $f(\dots)$ and $CC_{\dots}(\dots)$ functions and define

$$ff_{4,4}(\tau_{k4,4}) = \sum_{j=0}^3 f_{k4,4}(j; \tau_{k4,4}; d_{k4,4}; S_{1,4}; S_{k4,4}) \quad (2.15)$$

$$ff_{2,4}(\tau_{k,2,4}) = \sum_{j=0}^3 f_{k,2,4}(j; \tau_{k,2,4}; d_{k,2,2}; S_{1,4}; S_{k,2,2}) \quad (2.16)$$

$$ff_{1,4}(\tau_{k,1,4}) = \sum_{j=0}^3 f_{k,1,4}(j; \tau_{k,1,4}; d_{k,1,1}; S_{1,4}; S_{k,1,1}) \quad (2.17)$$

Each of the function $ff(.)$ (evaluated in the Appendix) above represents the envelope of the cross correlation of the interfering user and the local receiver reference signal. Each $ff(.)$ is the sum of 4 functions over 4 consecutive Gold Code periods.

In the analysis that follows, we assume that acquisition and synchronization problems have been solved, i.e., at a certain receiver we have an exact replica of the code and switching function of the intended signal being received. It is possible, especially in a mobile environment, to lose code acquisition from time to time. In this case one might use central station pilot tones and/or matched filtering techniques to aid the process of reacquiring the code. During this reacquisition period, which should be shorter than data transmission period, it is debatable to say that the acquisition performance will be slightly poorer than that of the classic system (which uses only Gold codes). Yes, during code acquisition our intended signal waveform of the multiplication function $S_{m,l}(t) \cdot C_{m,l}(t)$ is not as nice as the triangular auto-correlation waveform of Gold code alone. However the multiuser interference has been cut to a great extent by using our orthogonal function approach, thus offsetting the small reduction in the intended signal component (for example, the auto-correlation mentioned above for a user in group 1 goes down from $16L^2T_c^2 \cdot CC_{...}(...)$ (in a classic system) to $\frac{32}{3}L^2T_c^2 \cdot CC_{...}(...)$ i.e. a reduction of 1/3. However cross-correlation between our user and other users in his group goes down by the same amount. The same argument applies for other users of other groups during code acquisition.

Also even in classic systems, acquisition is a difficult problem in a network environment. The acquisition performance degradation is restricted only to this period and does not lend itself to modulation or data transmission period once the local code

and received codes are synchronized. It will be seen shortly from the Appendix that the auto-correlation of the multiplication function of the Gold code and switching functions is an irregular function, though not similar in form to the well-familiar triangular auto-correlation waveform of a Gold code. It exhibits much better cross-correlation properties between users of the same group or different groups with a little bit of sacrifice on the self autocorrelation component of each user (only during acquisition).

Now evaluating the mean square value of $y_4(T_b)$ and subtracting the signal power $E^2(y_4(T_b))$ (noting the independence of the $\cos\theta_k$ terms), and that $E[\cos\theta_k] = 0$, $E[n'(T_b)] = 0$, $E(\cos^2\theta = 1/2)$, we obtain the variance $\sigma_{y_4}^2$ as

$$\begin{aligned} \sigma_{y_4}^2 = & (P/4) \sum_{k=2}^{M_4} ff_{4,4}^2(\tau_{k4,4}) CC_{4,4}^2(\tau_{k4,4}) + (P/4) \sum_{k=2}^{M_2} ff_{2,4}^2(\tau_{k2,4}) CC_{2,4}^2(\tau_{k2,4}) \\ & + (P/4) \sum_{k=1}^{M_1} ff_{1,4}^2(\tau_{k1,4}) CC_{1,4}^2(\tau_{k1,4}) + \sigma_n^2 \end{aligned} \quad (2.18)$$

Note that the multiplication of the delayed switching functions in (2.15)-(2.17) are independent of the user number since all users in a certain group k_1 or k_2 or k_4 have the same orthogonal function. Also note that all users having Gold Codes of the same length will have the same cross correlation properties (see (2.12), (2.13)) irrespective of the fact that the number of network users may be divided into several Gold code families. Now we can safely take $CC(.)$ and $ff(.)$ terms in (2.18) outside the summations and combining with (2.14), we obtain the signal-to-noise ratio (SNR) at the subsequent PSK demodulator, i.e.,

$$\begin{aligned} SNR_{y_4} \Big|_{\tau} = & (P/2)T_b^2 \left[(P/4)(M_4-1)ff_{4,4}^2(\tau_{k4,4}) CC_{4,4}^2(\tau_{k4,4}) + (P/4)M_2ff_{2,4}^2(\tau_{k2,4}) CC_{2,4}^2(\tau_{k2,4}) \right. \\ & \left. + (P/4)M_1ff_{1,4}^2(\tau_{k1,4}) CC_{1,4}^2(\tau_{k1,4}) + \sigma_n^2 \right] \end{aligned} \quad (2.19)$$

where

$$\sigma_n^2 = \frac{N_o T_b}{4} \quad (2.20)$$

It is typical in the literature to assume that the multiplicative processes $CC(.)$ are wide-sense stationary and ergodic, in which case the time averages in (2.9) are replaced by the statistical averages in (2.11). Now assuming that $CC(.)$ takes one of the three values in (2.12) with equal probability and that the random delays are uniformly distributed in the range $[0, T_b]$, substituting the denominator of (2.19) with $T_b = 4LT_c$, where L is the length of one short Gold Code and averaging over all L delays and all three values of cross correlation in (2.12), we obtain

$$\sigma_{v_i}^2 = \frac{P}{4} R_{sg} \frac{1}{4L} \cdot \left[(M_4-1) \sum_{\tau_{4,4}=0}^{4LT_c} ff_{4,4}^2(\tau_{k4,4}) + M_2 \sum_{\tau_{2,2}=0}^{4LT_c} ff_{2,2}^2(\tau_{k2,2}) + M_1 \sum_{\tau_{1,1}=0}^{4LT_c} ff_{1,1}^2(\tau_{k1,1}) \right] + \sigma_n^2 \quad (2.21)$$

Similarly, following the same steps in (2.1)-(2.21), it is easy to see that the variances at one of the user receivers of the second and first groups are given by

$$\sigma_{v_i}^2 = \frac{P}{4} \frac{R_{sg}}{4L} \left[(M_1) \sum_{\tau_{1,1}=0}^{4LT_c} ff_{1,1}^2(\tau_{k1,1}) + (M_2-1) \sum_{\tau_{2,2}=0}^{4LT_c} ff_{2,2}^2(\tau_{k2,2}) + M_4 \sum_{\tau_{4,4}=0}^{4LT_c} ff_{4,4}^2(\tau_{k4,2}) \right] + \sigma_n^2 \quad (2.22)$$

$$\sigma_{v_i}^2 = \frac{P}{4} \frac{R_{sg}}{4L} \left[(M_1-1) \sum_{\tau_{1,1}=0}^{4LT_c} ff_{1,1}^2(\tau_{k1,1}) + M_2 \sum_{\tau_{2,2}=0}^{4LT_c} ff_{2,2}^2(\tau_{k2,1}) + M_4 \sum_{\tau_{4,4}=0}^{4LT_c} ff_{4,4}^2(\tau_{k4,1}) \right] + \sigma_n^2 \quad (2.23)$$

where R_{sg} = average short Gold Code cross correlation power (over all probabilities and cross-correlations in (2.12)). This is given by

$$R_{sg} = \frac{t^2(n) - 2t(n) + 3}{2L^2} \quad n \text{ odd}$$

$$R_{sg} = \frac{t^2(n) - 2t(n) + 5}{4L^2} \quad n \text{ even} \quad (2.24)$$

For comparison purposes, it is easy to see that the variance in the case of a classic DS system (no switching function) (See also Appendix), is given by

$$\sigma_{v_i}^2 = \frac{P}{4} R'_{sg} 16L^2 T_c^2 M + \sigma_n^2 \quad (2.25)$$

where $n' = (n+2)$ = equivalent longer DS Gold Code generator length

$L' = (2^{n+2}-1)$ =equivalent longer DS Gold code length

and $(16L^2)$ is the effective cross correlation envelope of the continuous (+1) switching function equivalent to the case of a DS system. Table 2.1 shows the values of R_{sg} , R'_{sg} for different Gold code lengths. One way of looking at the switching cross correlation function is the fact that it models a time varying waveform by which the Gold Code cross correlation interference multiplies.

For classic systems it is a constant time window resulting in the term $(16L^2T_c^2)$ ((2.24)). For the Modified SUGAR/DS system it is much less than that $(16L^2)$ (see equations A4-A9). Now substitutions from (A4-A9) into (2.21)-(2.23) and approximating (M_4-1) by M_4 , (M_2-1) by M_2 , (M_1-1) by M_1 , we get

$$\sigma_{y_4}^2 = \frac{P}{4} R_{sg} T_c^2 \left[\frac{2M_1 L^2}{3} + \frac{2M_2 L^2}{3} + 4M_4 L^2 \right] + \sigma_n^2 \quad (2.26)$$

$$\sigma_{y_2}^2 = \frac{P}{4} R_{sg} T_c^2 \left[\frac{8M_1 L^2}{3} + \frac{16}{3} M_2 L^2 + \frac{2M_4 L^2}{3} \right] + \sigma_n^2 \quad (2.27)$$

$$\sigma_{y_1}^2 = \frac{P}{4} R_{sg} T_c^2 \left[\frac{32}{3} M_1 L^2 + \frac{8}{3} M_2 L^2 + \frac{2M_4 L^2}{3} \right] + \sigma_n^2 \quad (2.28)$$

In the balanced group case $M_1 = M_2 = M_4 = \frac{M}{3}$, we obtain

$$\sigma_{y_4}^2 \approx \frac{P}{4} R_{sg} T_c^2 \frac{16}{9} L^2 M + \sigma_n^2 \quad (2.29)$$

$$\sigma_{y_2}^2 \approx \frac{P}{4} R_{sg} T_c^2 \frac{26}{9} L^2 M + \sigma_n^2 \quad (2.30)$$

$$\sigma_{y_1}^2 \approx \frac{P}{4} R_{sg} T_c^2 \frac{42}{9} L^2 M + \sigma_n^2 \quad (2.31)$$

The SNR of average and individual Modified SUGAR/DS systems and the SNR of the classic system are then given by

$$SNR_{y_4} = \frac{(P/2) T_b^2}{(P/4) R_{sg} T_c^2 \frac{28}{9} L^2 M + \sigma_n^2} \quad (2.32)$$

$$= \frac{102}{10MR_{sg} + (2\sigma_n^2/PT_b^2)} \approx \frac{10.2}{MR_{sg}}$$

AWGN is neglected because the main interference is from among the simultaneous users, represented by R_{sg} . Thus,

$$SNR_{y_4} = \frac{(P/2)T_b^2}{(P/4)R_{sg}T_c^2 \frac{16}{9}L^2M + \sigma_n^2} \approx \frac{18}{MR_{sg}} \quad (2.33)$$

$$SNR_{y_2} = \frac{10.99}{MR_{sg}} \quad (2.34)$$

$$SNR_{y_1} = \frac{(P/2)T_b^2}{(P/4)R_{sg}T_c^2 \frac{42}{9}L^2M + \sigma_n^2} \approx \frac{6.85}{MR_{sg}} \quad (2.35)$$

$$SNR_{y_i} = \frac{(P/2)T_b^2}{(P/4)R'_{sg}T_c^2 16L^2M + \sigma_n^2} \approx \frac{2}{MR'_{sg}} \quad (2.36)$$

We recall that since $n' = n+2$ from (2.24), (2.25), it is easy to obtain a relationship between R_{sg} and R'_{sg} for Gold Codes of different length L . Now dividing, we obtain

$$\left[\frac{R'_{sg}}{R_{sg}} \right] \approx \frac{1}{4} \text{ and hence}$$

$$\left[\frac{SNR_{y_4}}{SNR_{y_i}} \right] \approx 2.25 \quad (2.37)$$

$$\left[\frac{SNR_{y_2}}{SNR_{y_i}} \right] \approx 1.37 \quad (2.38)$$

$$\left[\frac{SNR_{y_1}}{SNR_{y_i}} \right] \approx 0.86 \quad (2.39)$$

$$\left[\frac{SNR_{y_4}}{SNR_{y_i}} \right] \approx 1.28 \quad (2.40)$$

The above equations tell us clearly that an asynchronous Modified SUGAR system has about 1 dB improvement in signal to multiaccess interference ratio, a clear advantage over the classic system. The worst group (group 1) is worse than the classic system, however the best group has about 3 dB improvement(all compared to the classic system).

The above, of course, assumes negligible AWGN ($\sigma_n^2 = 0$) which is naturally dominated by the like user interference terms. To improve these performances, we try to optimize the assignment of orthogonal groups to users (optimal code assignment policy) rather than assuming $M_1 = M_2 = M_4 = \frac{M}{3}$. It is easily seen that optimizing the average of equations (2.29)-(2.31) is a simple constrained nonlinear programming problem. From (2.26)-(2.28), we get

$$\begin{aligned}\sigma_{y_a}^2 &= \frac{(\sigma_{y_4}^2 + \sigma_{y_2}^2 + \sigma_{y_1}^2)}{3} \\ &= \frac{PR_{sg}T_c^2L^2}{36} \left[16M_4 + 26M_2 + 42M_1 \right] + \sigma_n^2\end{aligned}\quad (2.41)$$

Trying for example,

$$M_1 = \frac{M}{6}, M_2 = \frac{M}{3}, M_4 = \frac{M}{2}\quad (2.42)$$

we get from (2.26)-(2.28)

$$\sigma_{y_a}^2 = \frac{P}{4} R_{sg}T_c^2(2.63)L^2M\quad (2.43)$$

A more systematic way of optimally assigning users to orthogonal groups proceeds as

follows: denote $\alpha_1 = \frac{M_1}{M}$, $\alpha_2 = \frac{M_2}{M}$, $\alpha_4 = \frac{M_4}{M}$. Substituting into (2.26),(2.27),(2.28)

results in

$$\begin{aligned}\sigma_{y_a}^2 &= (\alpha_4\sigma_{y_4}^2 + \alpha_2\sigma_{y_2}^2 + \alpha_1\sigma_{y_1}^2) \\ &= \frac{P}{4} R_{sg}T_c^2L^2M \left[\frac{2\alpha_4\alpha_1}{3} + 2\frac{\alpha_2\alpha_4}{3} + 4\alpha_4^2 + \frac{8\alpha_2\alpha_1}{3} + \frac{16}{3}\alpha_2^2 + \frac{2\alpha_2\alpha_4}{3} + \frac{32}{3}\alpha_1^2 + \frac{8}{3}\alpha_2\alpha_1 + \frac{2\alpha_1\alpha_4}{3} \right]\end{aligned}\quad (2.44)$$

A straight minimization yields

$$\alpha_1 = 0.11, \alpha_2 = 0.34, \alpha_4 = 0.55 \quad \text{and} \quad \sigma_{y_a}^2 = \frac{P}{4} R_{sg} T_c^2 L^2 M \quad (2.45)$$

These values lead to the following new results.

$$SNR_{y_4} = \frac{(P/2)T_b^2}{(P/4)R_{sg}T_c^2(2.5)L^2M + \sigma_n^2} \approx \frac{12.8}{MR_{sg}} \quad (2.46)$$

$$SNR_{y_2} = \frac{(P/2)T_b^2}{(P/4)R_{sg}T_c^2(2.47)L^2M + \sigma_n^2} \approx \frac{12.96}{MR_{sg}} \quad (2.47)$$

$$SNR_{y_1} = \frac{(P/2)T_b^2}{(P/4)R_{sg}T_c^2(2.45)L^2M + \sigma_n^2} \approx \frac{13.06}{MR_{sg}} \quad (2.48)$$

$$SNR_{y_a} = \frac{(P/2)T_b^2}{(P/4)R_{sg}T_c^2(2.49)L^2M + \sigma_n^2} \approx \frac{12.85}{MR_{sg}} \quad (2.49)$$

$$\left[\frac{SNR_{y_4}}{SNR_{y_i}} \right] = 1.6 \quad \text{or} \quad \approx 2.04 \text{ dB} \quad (2.50)$$

$$\left[\frac{SNR_{y_2}}{SNR_{y_i}} \right] = 1.62 \quad \text{or} \quad \approx 2.09 \text{ dB} \quad (2.51)$$

$$\left[\frac{SNR_{y_1}}{SNR_{y_i}} \right] = 1.63 \quad \text{or} \quad \approx 2.12 \text{ dB} \quad (2.52)$$

$$\left[\frac{SNR_{y_a}}{SNR_{y_i}} \right] = 1.6 \quad \text{or} \quad \approx 2.04 \text{ dB} \quad (2.53)$$

which shows a clear 2 dB improvement of our Modified SUGAR/DS system over the classic system.

2.4 The case of propagation delays, not multiples of chip duration ($\tau_k \neq iT_c$):

All the results of (2.26-2.53) and the appendix pertain to the case of synchronous chip

transmission, i.e., all random delays τ_k of all users are assumed to be multiples of the chip duration T_c . For the chip asynchronous case, $\tau_k \neq nT_c$, all the variances are scaled down by a factor of 2/3 due to more spreading that takes place and all signal-to-noise ratios in all equations (2.26-2.53) get multiplied by 3/2 (including the classic system). Thus the SNR advantages of Modified SUGAR systems over the classic system remain the same.

Having obtained the average SNR of the classic and Modified SUGAR systems, it is academic to compute the final bit error probability of PSK used, i.e., the equal group population case is taken as the lower bound on performance.

$$P_b = \frac{1}{2} \operatorname{erfc} \sqrt{\text{SNR}} \quad (2.54)$$

where the value of SNR depends on the system selected, number of users, Gold code lengths, etc. (thermal noise, being insignificant, was ignored in the results of this thesis). For data communications, packet transmission mode is assumed, and the probability of correct packet reception is given by

$$P_c = (1 - P_b)^N \quad (2.55)$$

where N=number of bits per packet.

The throughput or bandwidth efficiency is given by

$$\eta = \frac{M \cdot (1 - P_b)^N R_b}{W} = \frac{M (1 - P_b)^N}{L} \quad (2.56)$$

where $L = (T_b/T_c)$ is the Spread Spectrum processing gain or code length and W and R_b are respectively, the SS bandwidth and bit rate. The η in (2.56) defines the useful obtained bit rate from all users divided by the used Spread Spectrum bandwidth. This η is a worst case, in the sense that it assumes stream users with no speech silence, no load variations, etc.

The above equations (2.54)-(2.56) assume no fading, no coding environment. The results of Rayleigh fading can easily be obtained from any reference eg. [9] (assuming

the SNR in (2.32-2.36, 2.54) are in an Additive White Gaussian Noise environment and PSK detection.

The results will also show the superior performance under different types of fading and FEC, obtained by superimposing our SNRs or P_b from this thesis on the results of references [10] - [12]. Careful mapping of our SNR to the SNR of these references, as well as, changing L in all SNR to reflect the processing gain loss due to the use of FEC , i.e.,

$$L' = L * (FEC \text{ code rate}) \quad (2.57)$$

replaces L in all equations in this paper, except in (56).

2.5 ANALYTICAL RESULTS

The bit error rate P_b and throughput efficiency are computed as functions of number of users (M) for various Gold code lengths L , packet lengths N for both the classic and modified SUGAR systems.

Figures 2.3 to 2.5 show the clear SNR advantages of our modified SUGAR system for code lengths $L=127,511,2047$ in a no coding and no fading environment. Figures 2.6,2.7 and 2.8 show the high throughput efficiency (η) of the Modified SUGAR system, as compared to the classic system. Maximum η is 0.58 for the Modified SUGAR while the best η for the classic system is 0.4. It is important to note that η of the classic system goes down faster with increasing load(M) than in the Modified SUGAR, thus yielding a more graceful degradation and an enhanced network stability. Also short packets yield better efficiency for all system parameters, as evidenced from the values of throughput efficiency for packet sizes of $N=128$ and $N=256$. These figures also show that increasing the code length L extends the load range (working values of M) but this does not affect the maximum η obtained.

Under Trellis coding and no fading, figures 2.9 to 2.14 depict similar but improved results where we have used the same FEC coding parameters as in [9]. For example, for

the Modified SUGAR system $\eta_{\max} = 0.8$, while $\eta_{\max} = 0.5$ for the classic system. Under Rayleigh fading and no FEC used, figures 2.15 to 2.20 show the degrading effects of fading on both systems. However, η values are still higher in the Modified SUGAR system (eg. $\eta_{\max} = 0.05$ for Modified SUGAR, $\eta_{\max} = 0.015$ for classic DS system). Both systems degrade rapidly in throughput efficiency η with increasing load, but they preserve their relative performances as in figures (2.3-2.8).

Results of the two systems' performance under Rician fading and Combined Modulation coding are depicted in figures 2.21 to 2.26. The superior throughput efficiency of Modified SUGAR still prevails ($\eta_{\max} = 0.35$ for Modified SUGAR with $N=128$). The flatness in the Modified SUGAR throughput curve indicates the excellent graceful degradation with increasing load.

Finally, the results under Rayleigh fading and Reed-Solomon coding are shown in figures (2.27-2.32). The FEC coding parameters (generator word lengths, rates etc.) used are the same as in Reference [10]. The inherent throughput loss due to use of FEC is accounted for (see equation(2.57)). Figure 2.32 shows throughput efficiency for code length $L=2047$. Both the systems behave identically at low loads, but the modified SUGAR system performs better at higher loads.

	$t(L)$	R_{sg}	$n' = n + 2$	R'_{sg}
L=31, n=5	9	0.03434	7	0.00799
L=63, n=6	17	0.01638	8	0.00395
L=127, n=7	17	0.00799	9	0.001964
L=255, n=8	33	0.00395	10	0.000979
L=511, n=9	33	0.001964	11	0.000489
L=1023, n=10	65	0.000979	12	0.000244
L=2047, n=11	65	0.000489	13	0.000122
L=4095, n=12	129	0.000244	14	0.000061
L=8191, n=13	129	0.000122		
L=16383, n=14	257	0.000061		

TABLE 2.1 Average Gold Code cross-correlation power for different generator lengths

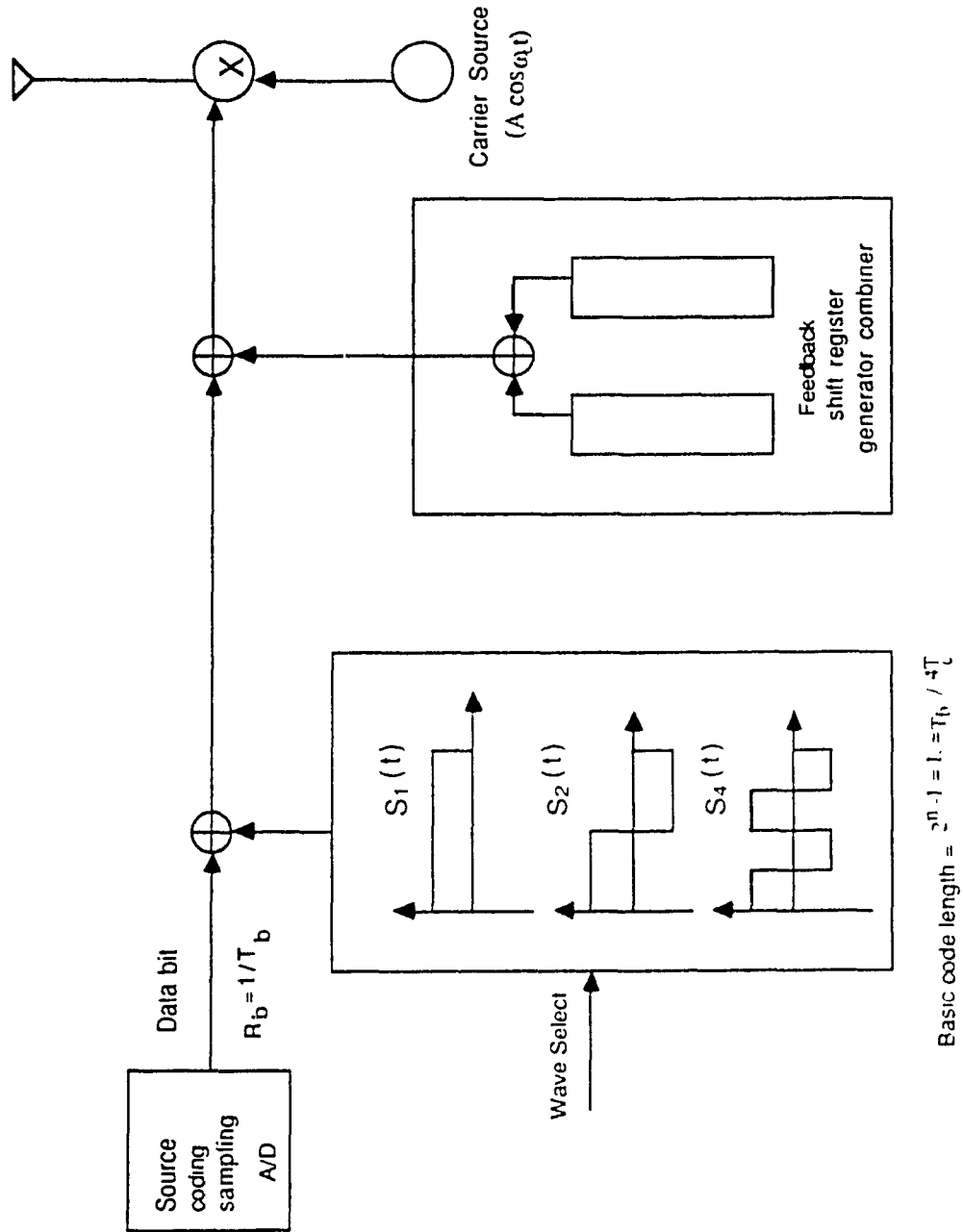


Fig 2 1 Generic (modified SUGARW) transmitter for use in CDMA Mobile or Indoor Communication
Centralized or Distributed Access

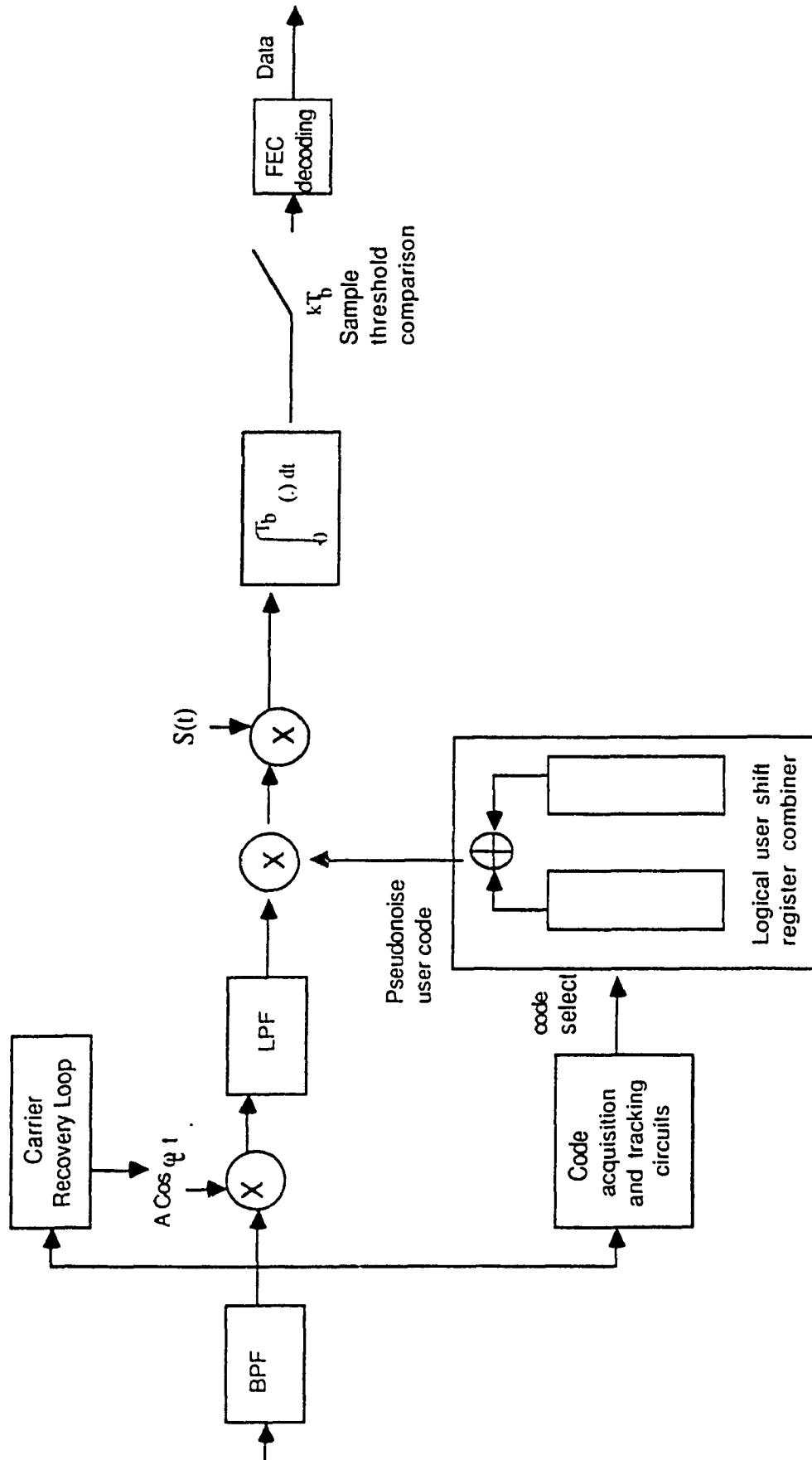


Fig. 2.2 Generic receiver bank of a modified SUGARW mobile or indoor CDMA system

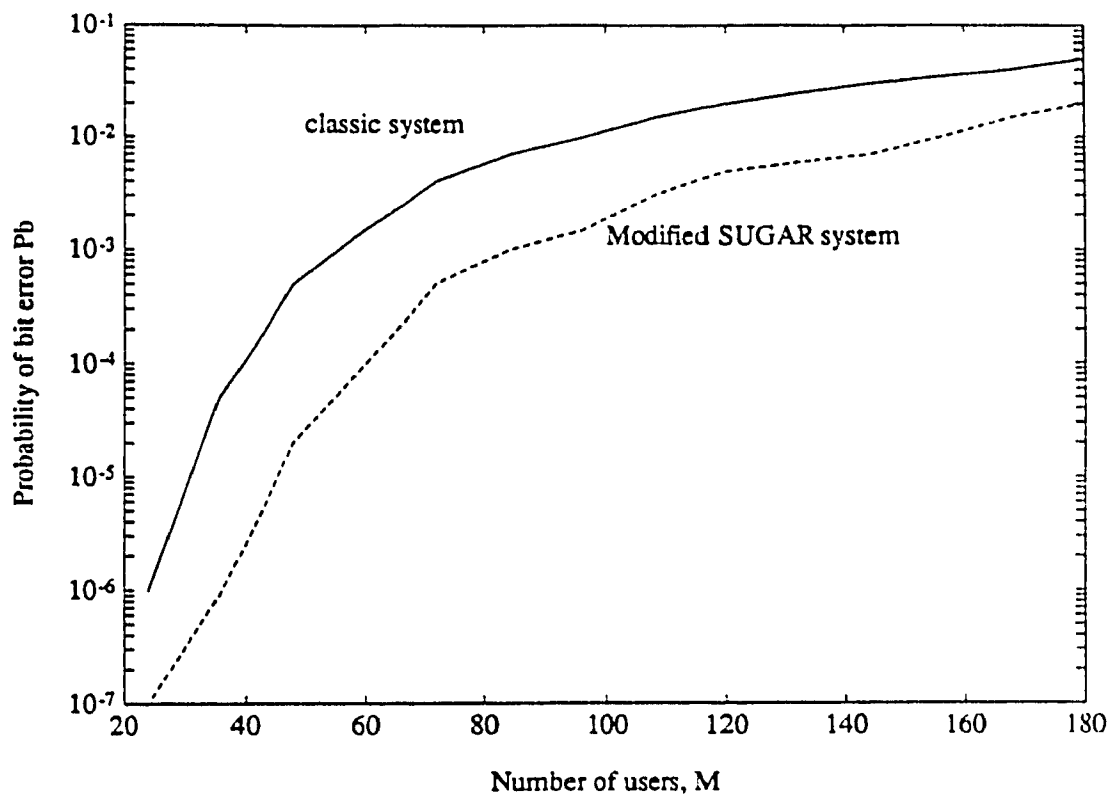


Fig. 2.3 Probability of bit error vs. number of users for conventional Spread Spectrum and Modified SUGAR systems for code length $L = 127$ (no fading and no coding).

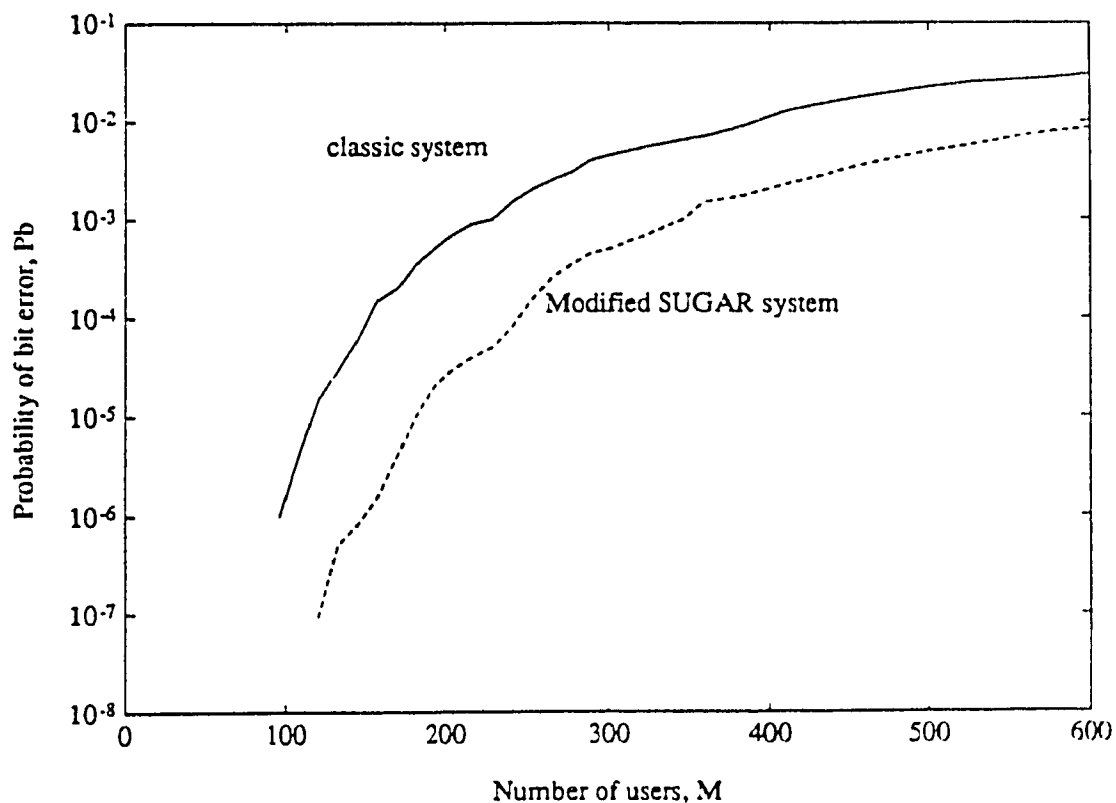


Fig. 2.4 Probability of bit error vs. number of users for conventional Spread Spectrum and Modified SUGAR systems for code length $L = 511$ (no fading and no coding).

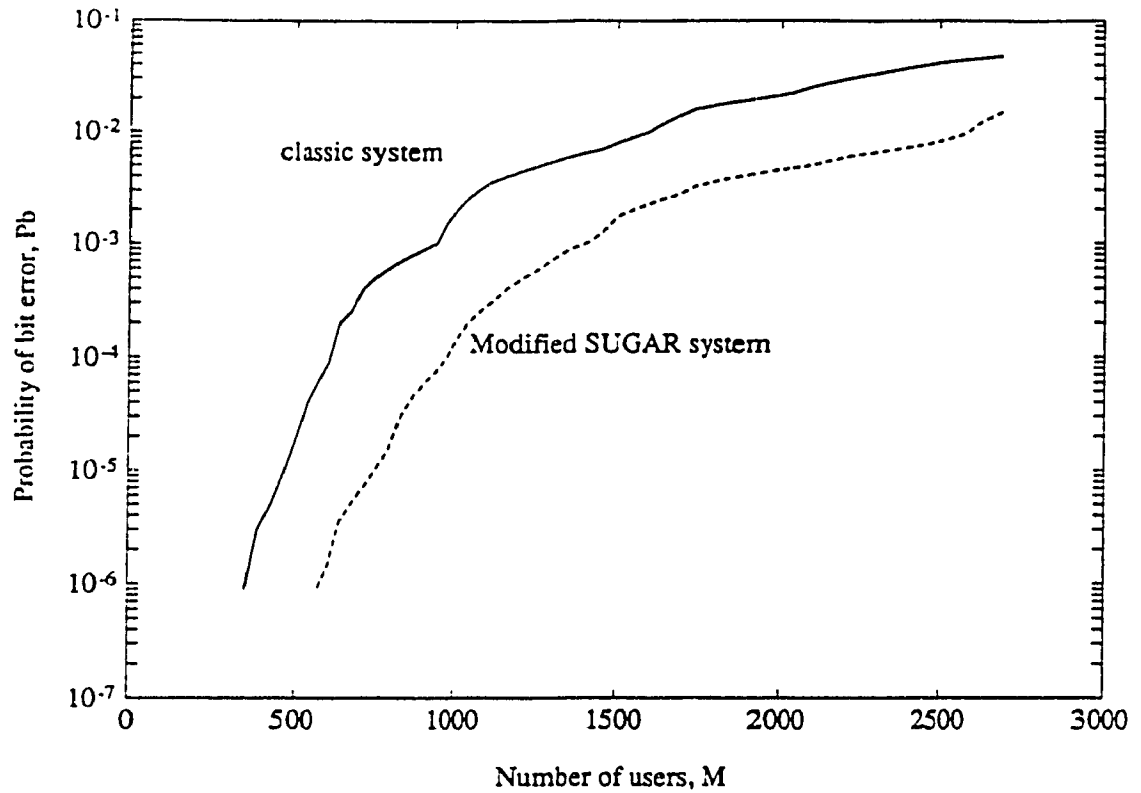


Fig. 2.5 Probability of bit error vs. number of users for conventional Spread Spectrum and Modified SUGAR systems for code length $L = 2047$ (no fading and no coding).

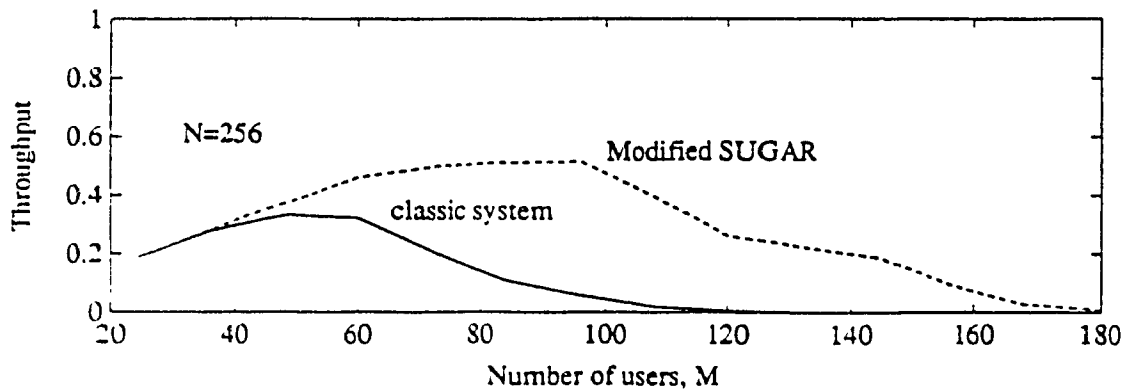
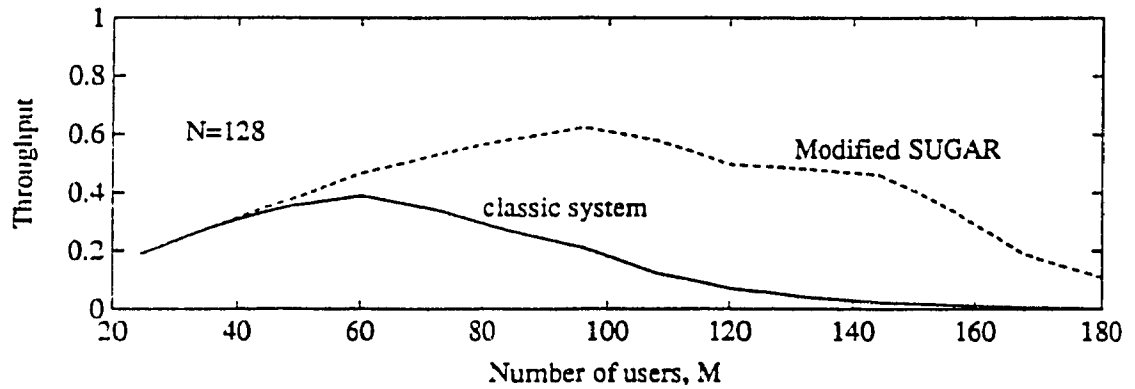


Fig. 2.6 Throughput vs. number of users for conventional Spread Spectrum and Modified SUGAR systems for $L = 127$ and packet sizes $N=128$ and 256 , for data communication (no fading and no coding).

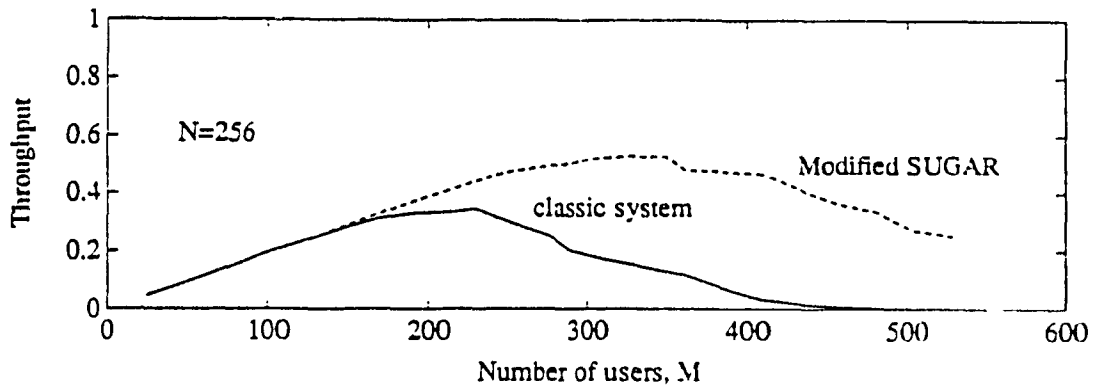
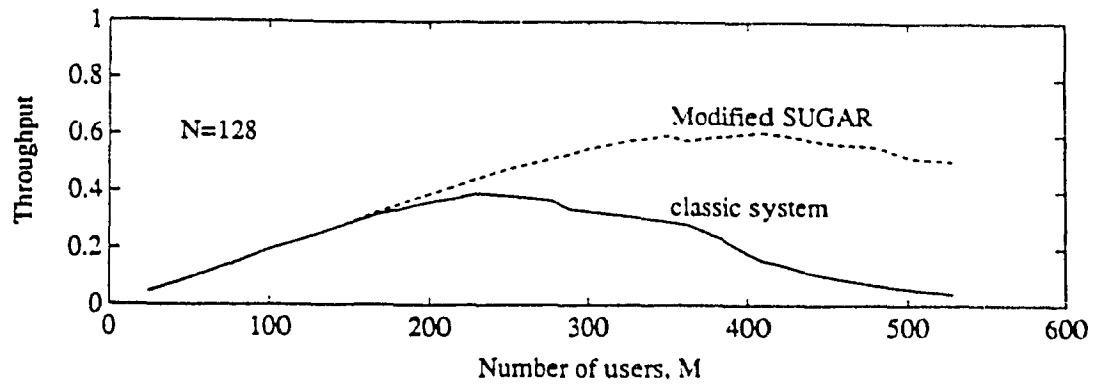


Fig. 2.7 Throughput vs. number of users for conventional Spread Spectrum and Modified SUGAR systems for $L = 511$ and packet sizes $N=128$ and 256 , for data communication (no fading and no coding).

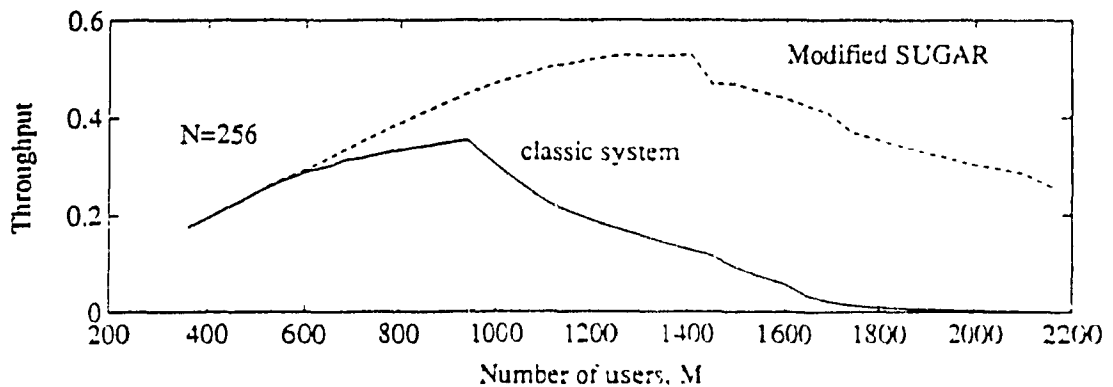
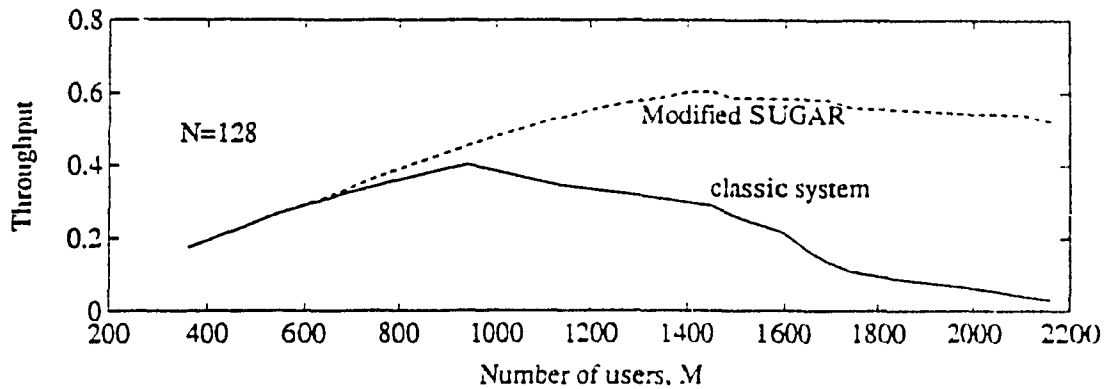


Fig. 2.8 Throughput vs. number of users for conventional Spread Spectrum and Modified SUGAR systems for $L = 2047$ and packet sizes $N=128$ and 256 , for data communication (no fading and no coding).

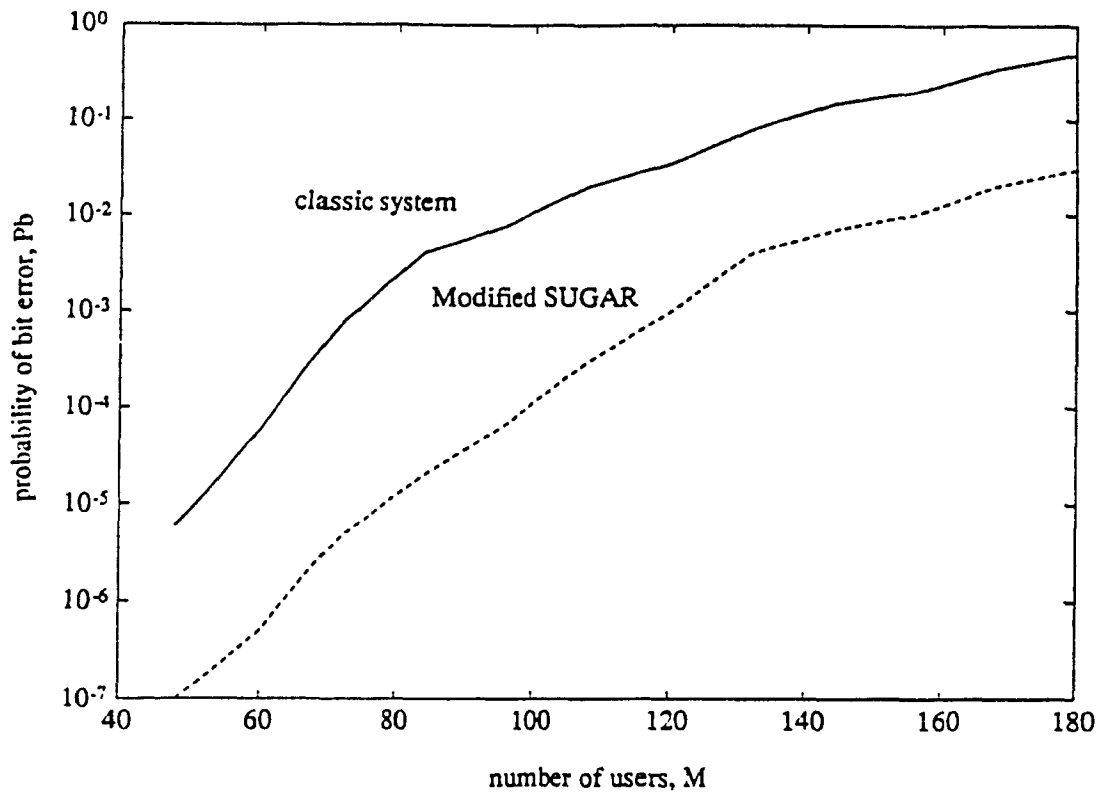


Fig. 2.9 Probability of bit error vs. number of users for conventional Spread Spectrum and Modified SUGAR systems for $L = 127$ (combined modulation coding and no fading). Other FEC coding parameters as in Reference [9].

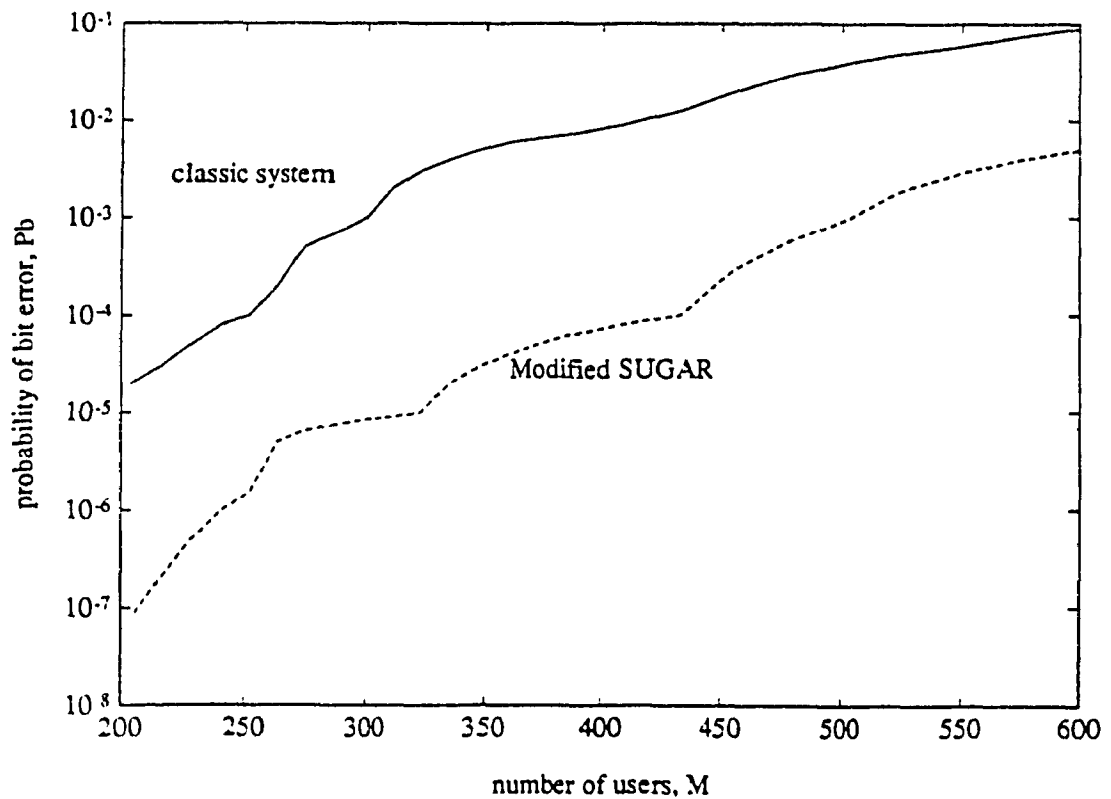


Fig. 2.10 Probability of bit error vs. number of users for conventional Spread Spectrum and Modified SUGAR systems for $L = 511$ (combined modulation coding and no fading). Other FEC coding parameters as in Reference [9].

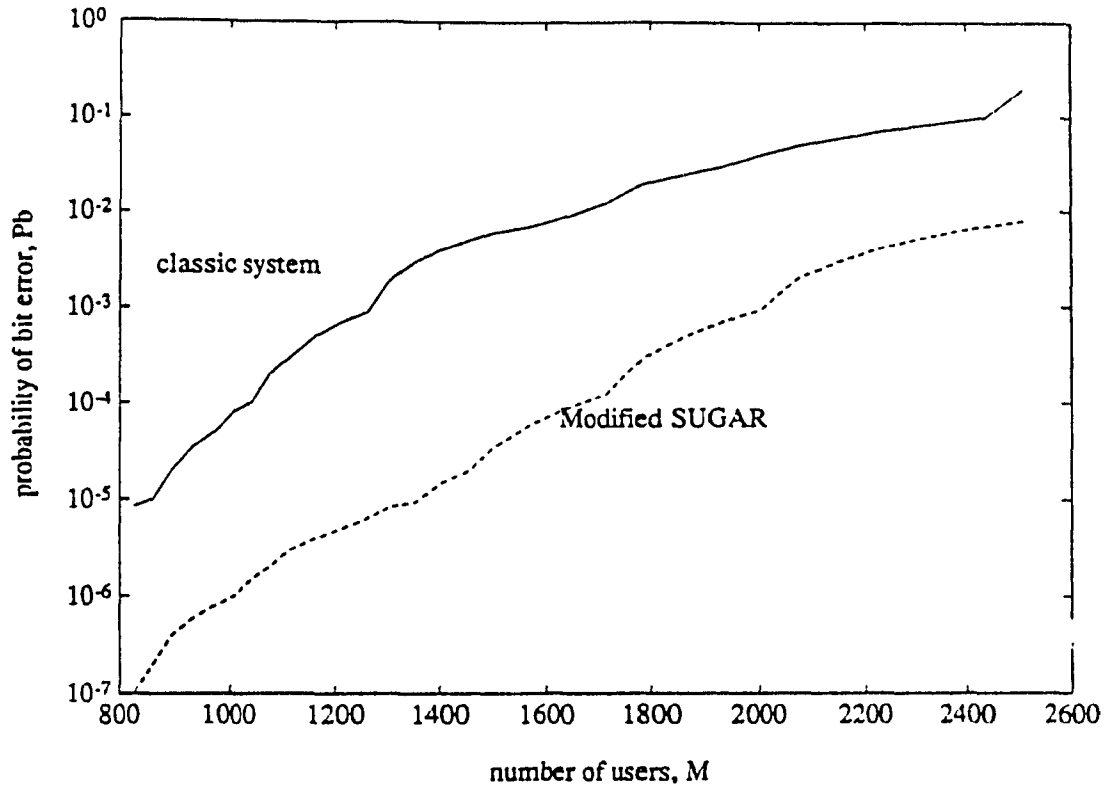


Fig. 2.11 Probability of bit error vs. number of users for conventional Spread Spectrum and Modified SUGAR systems for $L = 2047$ (combined modulation coding and no fading). Other FEC coding parameters as in Reference [9].

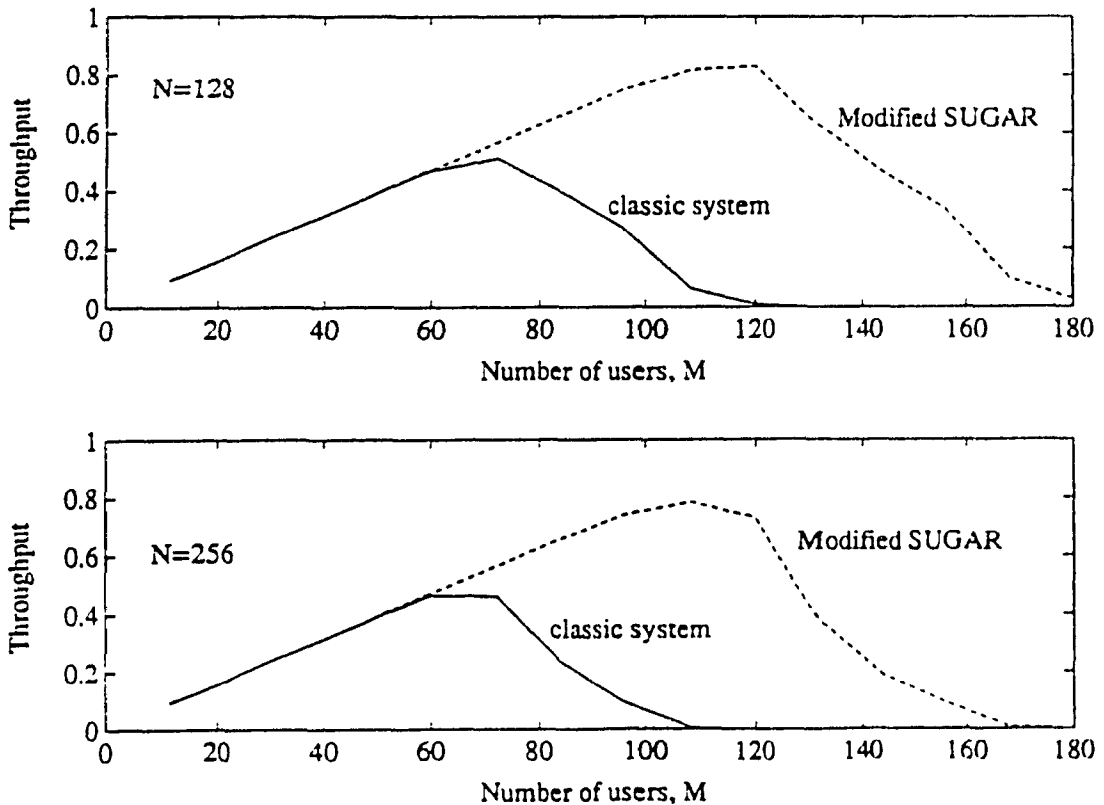


Fig. 2.12 Throughput vs. number of users for conventional Spread Spectrum and Modified SUGAR systems for $L = 127$ and packet sizes $N=128$ and 256 , for data communication (combined modulation coding and no fading).

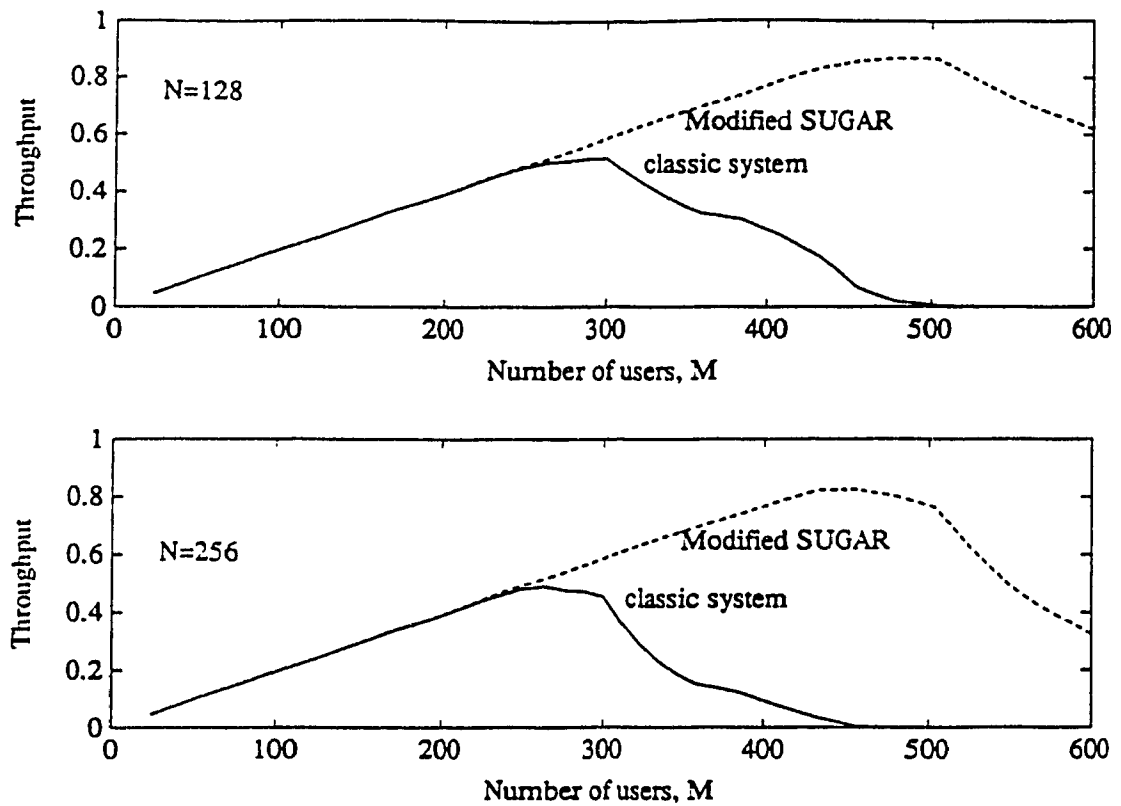


Fig. 2.13 Throughput vs. number of users for conventional Spread Spectrum and Modified SUGAR systems for $L = 511$ and packet sizes $N=128$ and 256 , for data communication (combined modulation coding and no fading).

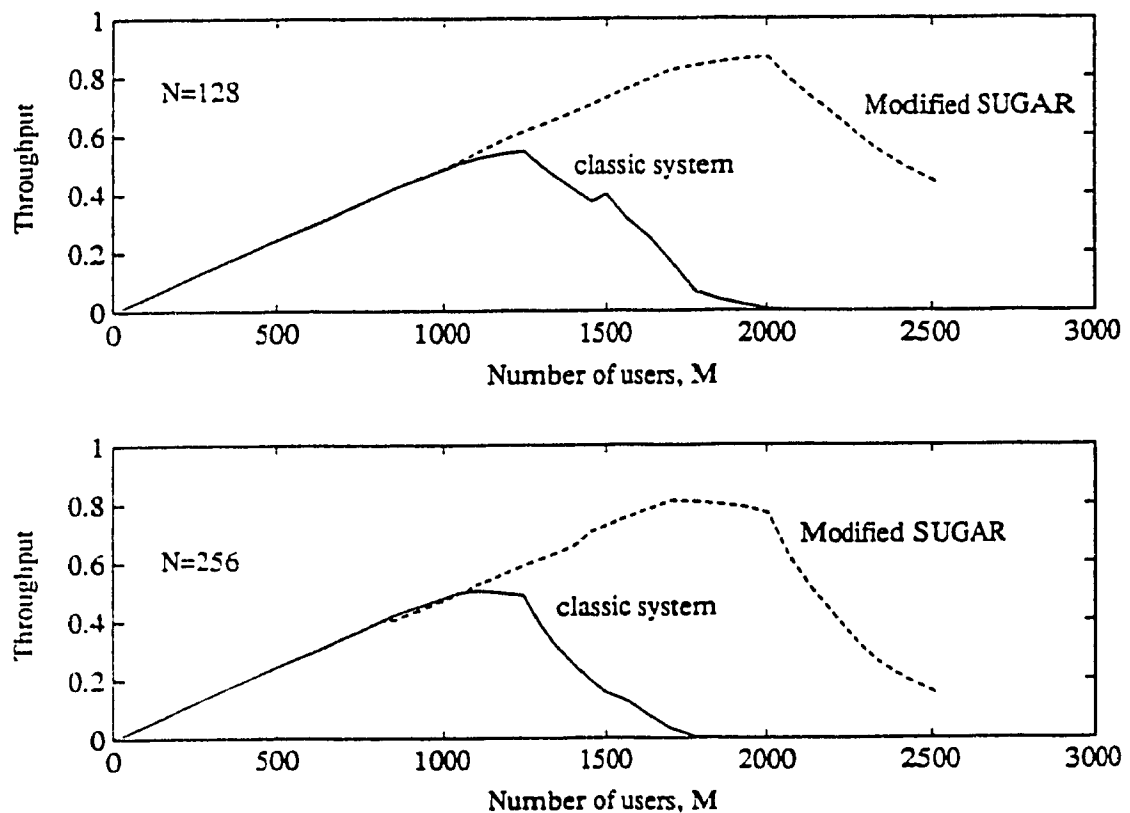


Fig. 2.14 Throughput vs. number of users for conventional Spread Spectrum and Modified SUGAR systems for $L = 2047$ and packet sizes $N=128$ and 256 , for data communication (combined modulation coding and no fading).

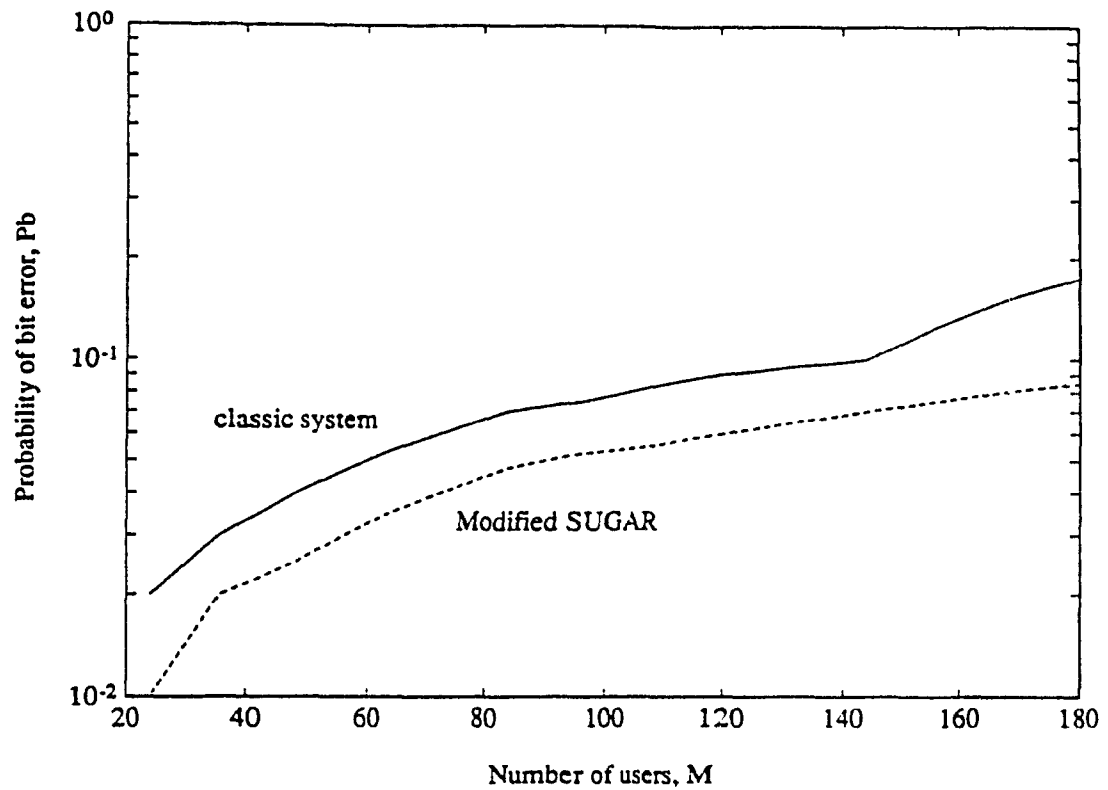


Fig. 2.15 Probability of bit error vs. number of users for conventional Spread Spectrum and Modified SUGAR systems for code length $L = 127$ (Rayleigh fading and no coding).

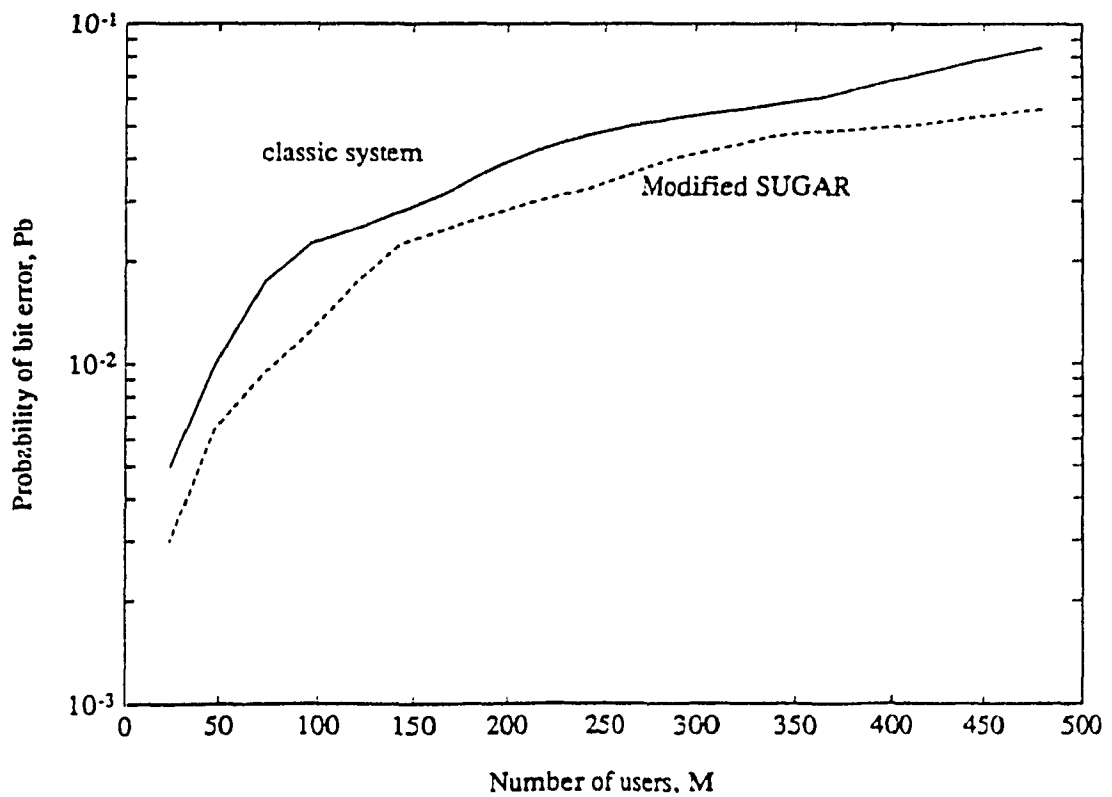


Fig. 2.16 Probability of bit error vs. number of users for conventional Spread Spectrum and Modified SUGAR systems for code length $L = 511$ (Rayleigh fading and no coding).

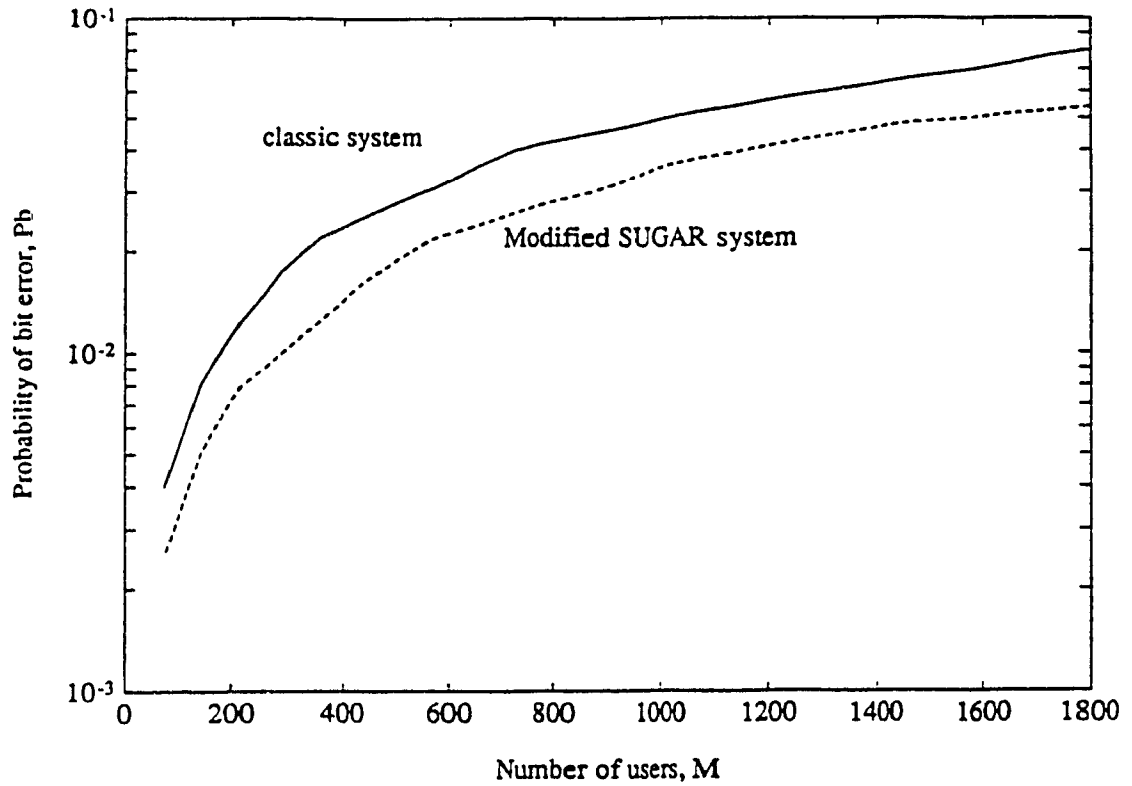


Fig. 2.17 Probability of bit error vs. number of users for conventional Spread Spectrum and Modified SUGAR systems for code length $L = 2047$ (Rayleigh fading and no coding).

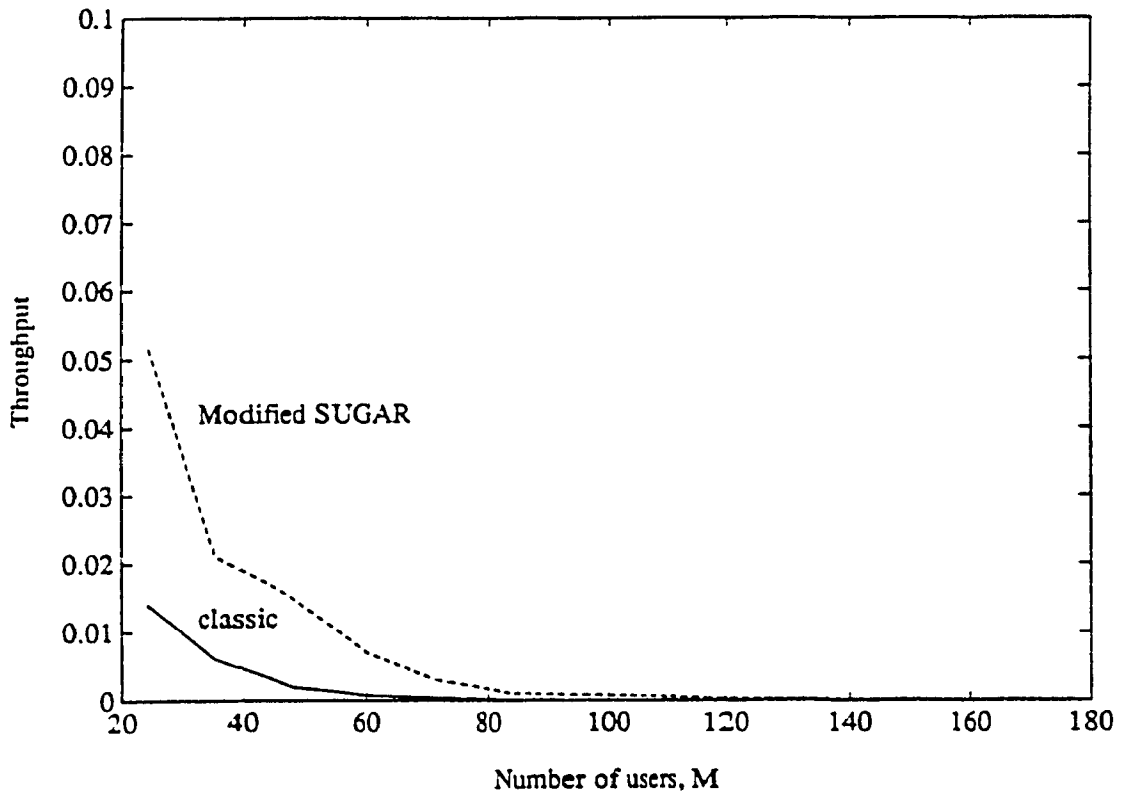


Fig. 2.18 Throughput vs. number of users for conventional Spread Spectrum and Modified SUGAR systems for $L = 127$ and packet size $N=123$, for data communication (Rayleigh fading and no coding).

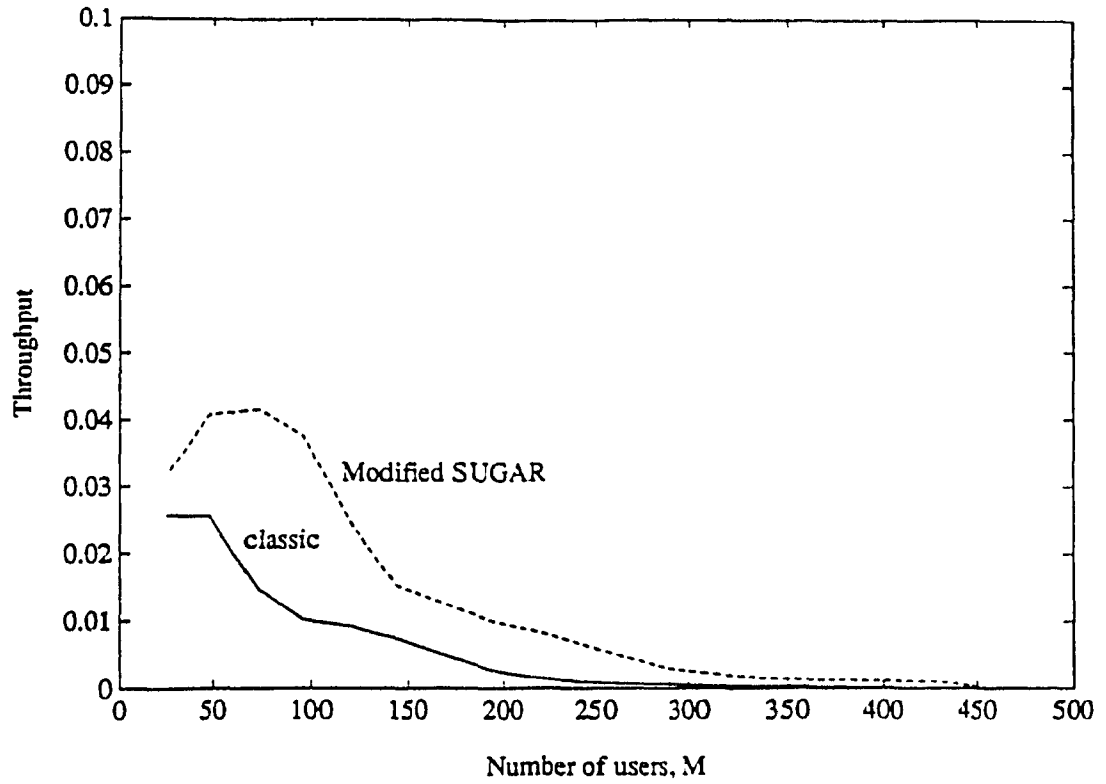


Fig. 2.19 Throughput vs. number of users for conventional Spread Spectrum and Modified SUGAR systems for $L = 511$ and packet size $N=128$, for data communication (Rayleigh fading and no coding).

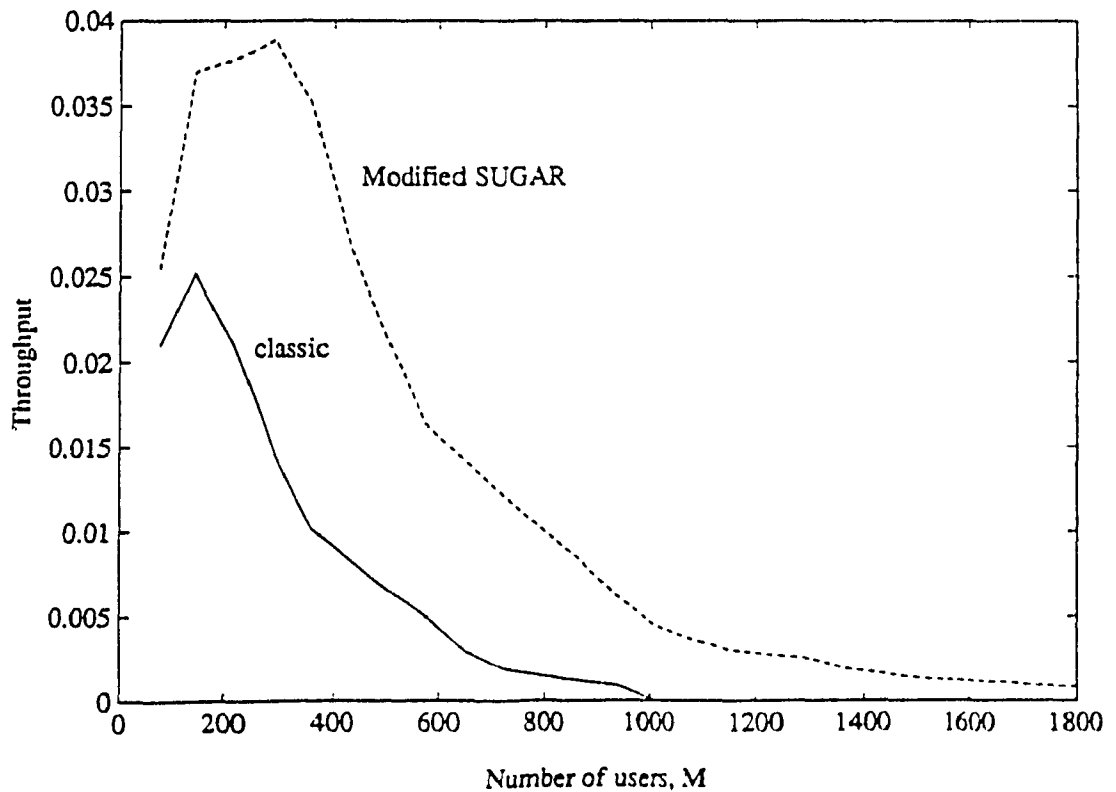


Fig. 2.20 Throughput vs. number of users for conventional Spread Spectrum and Modified SUGAR systems for $L = 2047$ and packet size $N=128$, for data communication (Rayleigh fading and no coding).

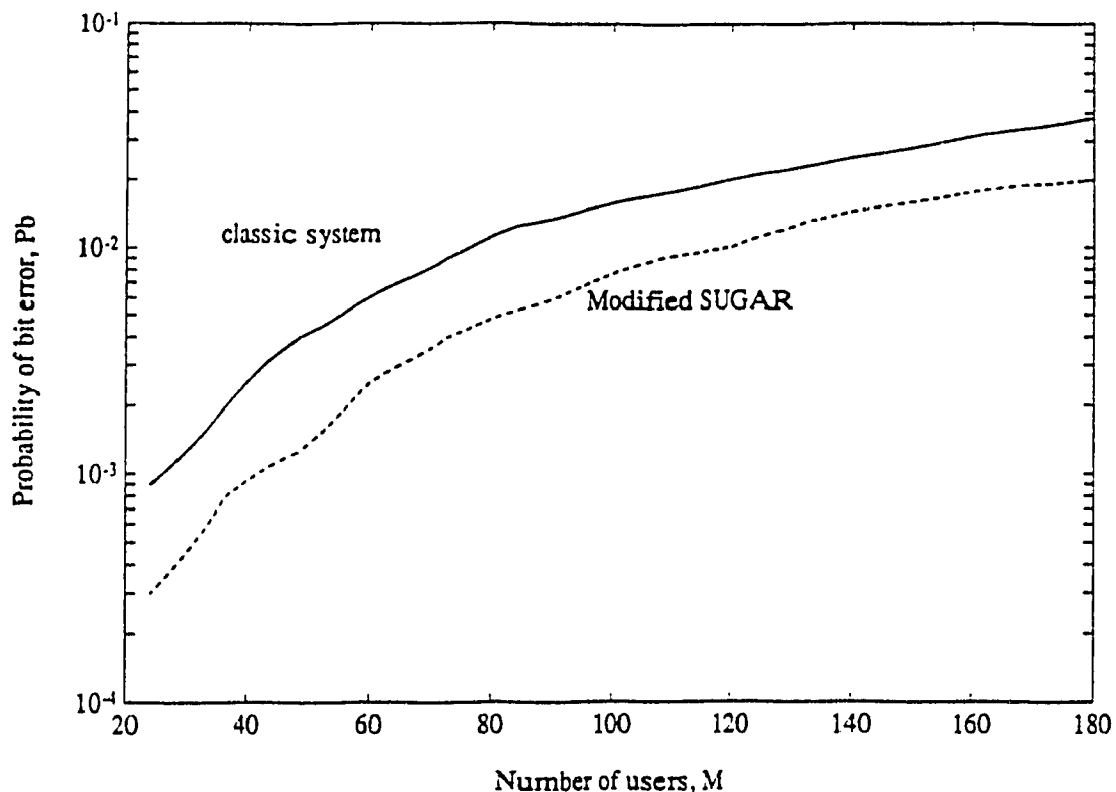


Fig. 2.21 Probability of bit error vs. number of users for conventional Spread Spectrum and Modified SUGAR systems for $L = 127$ (Combined modulation coding and Rician fading, $BW=0.1$). Other FEC coding parameters as in Reference [9].

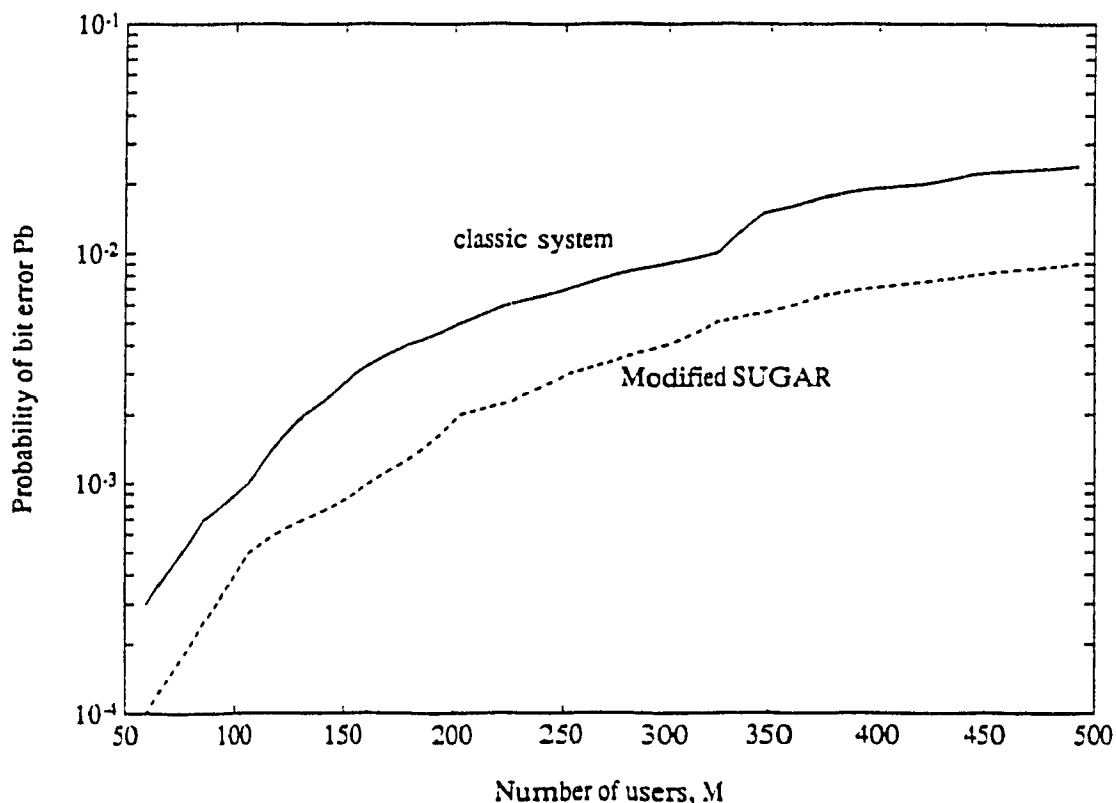


Fig. 2.22 Probability of bit error vs. number of users for conventional Spread Spectrum and Modified SUGAR systems for $L = 511$ (Combined modulation coding and Rician fading, $BW=0.1$). Other FEC coding parameters as in Reference [9].

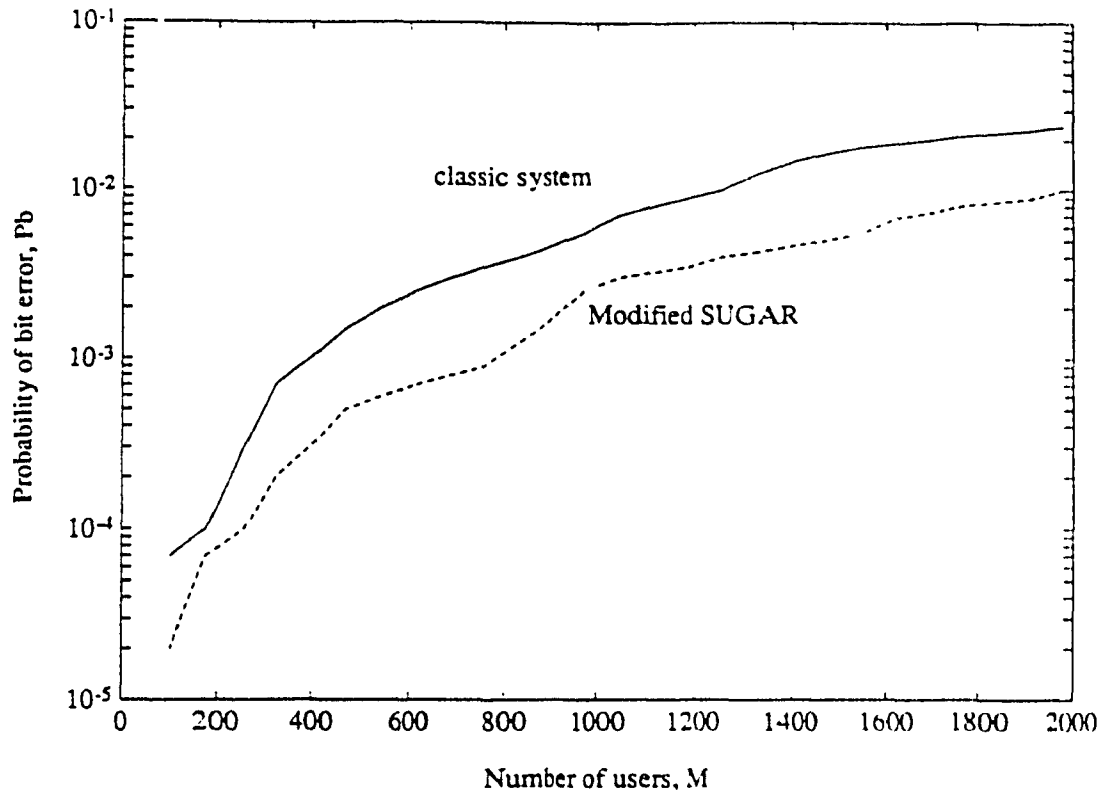


Fig. 2.23 Probability of bit error vs. number of users for conventional Spread Spectrum and Modified SUGAR systems for $L = 2047$ (Combined modulation coding and Rician fading, $BW=0.1$). Other FEC coding parameters as in Reference [9].

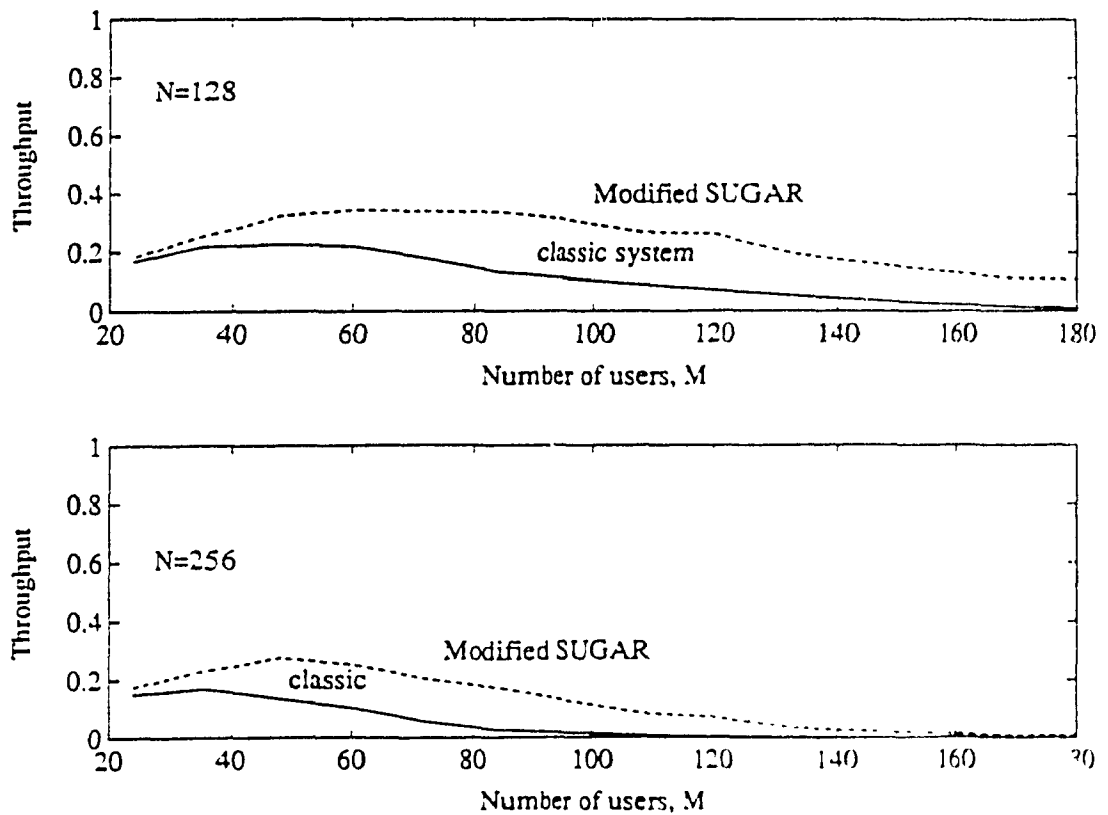


Fig. 2.24 Throughput vs. number of users for conventional Spread Spectrum and Modified SUGAR systems for $L = 127$ and packet sizes $N=128$ and 256, for data communication (combined modulation coding and Rician fading, $BW=0.1$).

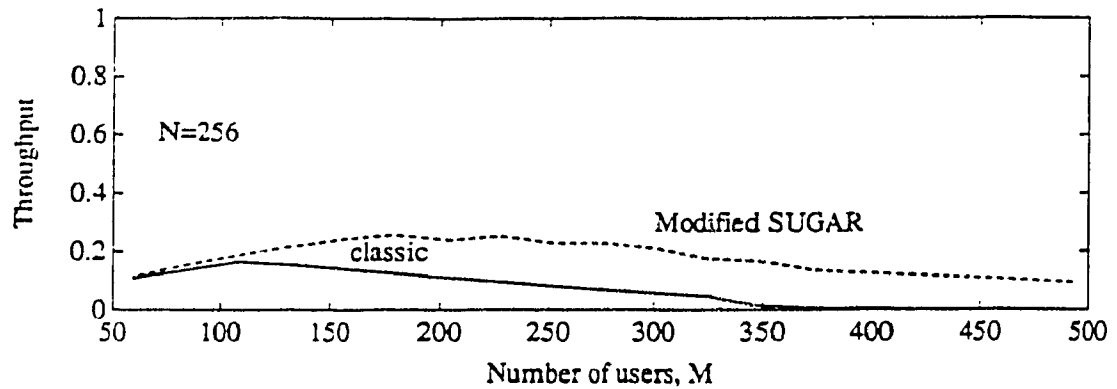
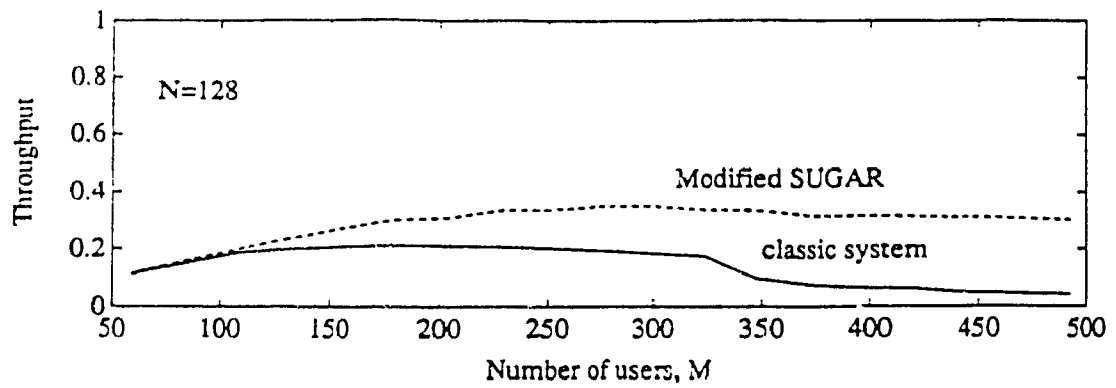


Fig. 2.25 Throughput vs. number of users for conventional Spread Spectrum and Modified SUGAR systems for $L = 511$ and packet sizes $N=128$ and 256 , for data communication (combined modulation coding and Rician fading, $BW=0.1$).

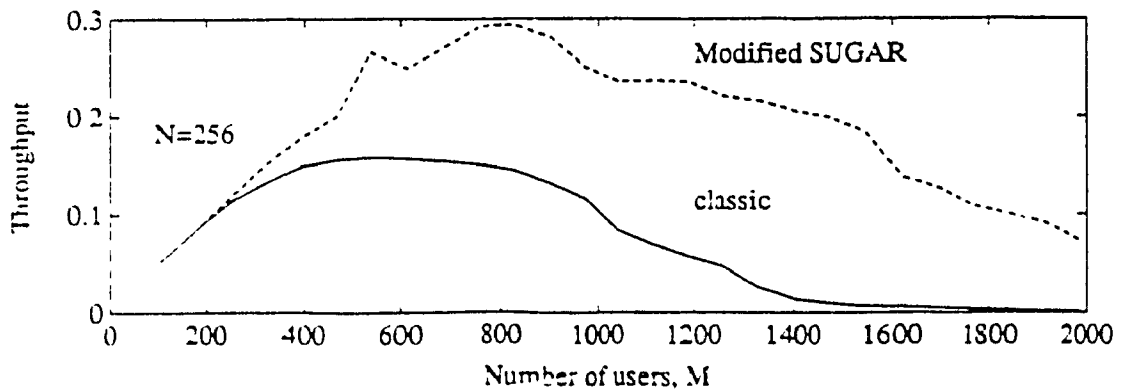
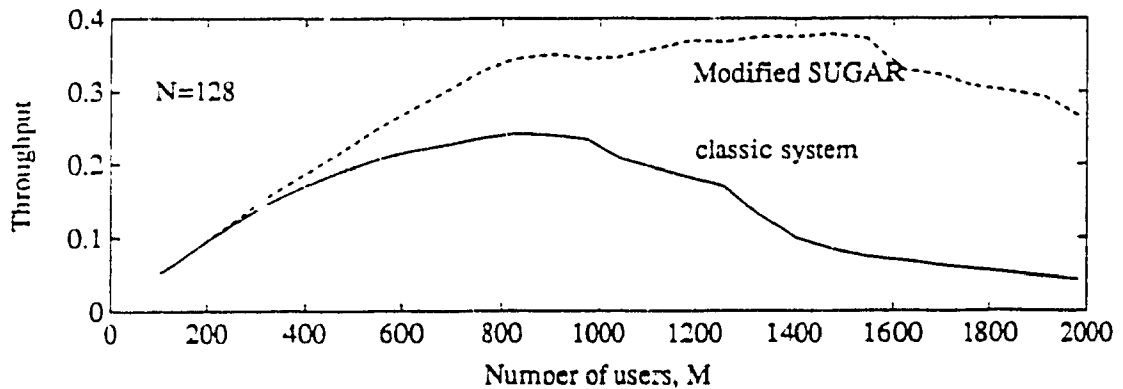


Fig. 2.26 Throughput vs. number of users for conventional Spread Spectrum and Modified SUGAR systems for $L = 2047$ and packet sizes $N=128$ and 256 , for data communication (combined modulation coding and Rician fading, $BW=0.1$).

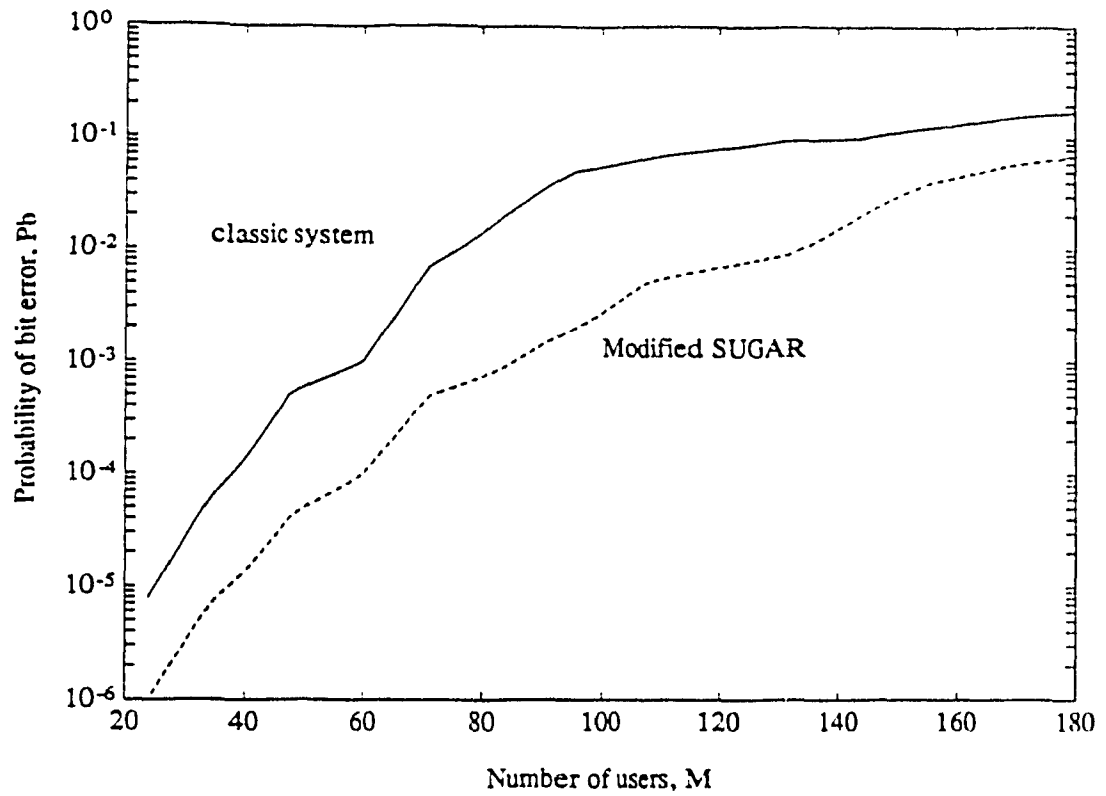


Fig. 2.27 Probability of bit error vs. number of users for conventional Spread Spectrum and Modified SUGAR systems for $L = 255$ (Reed-Solomon coding and Rayleigh fading). Other FEC coding parameters as in Reference [10].

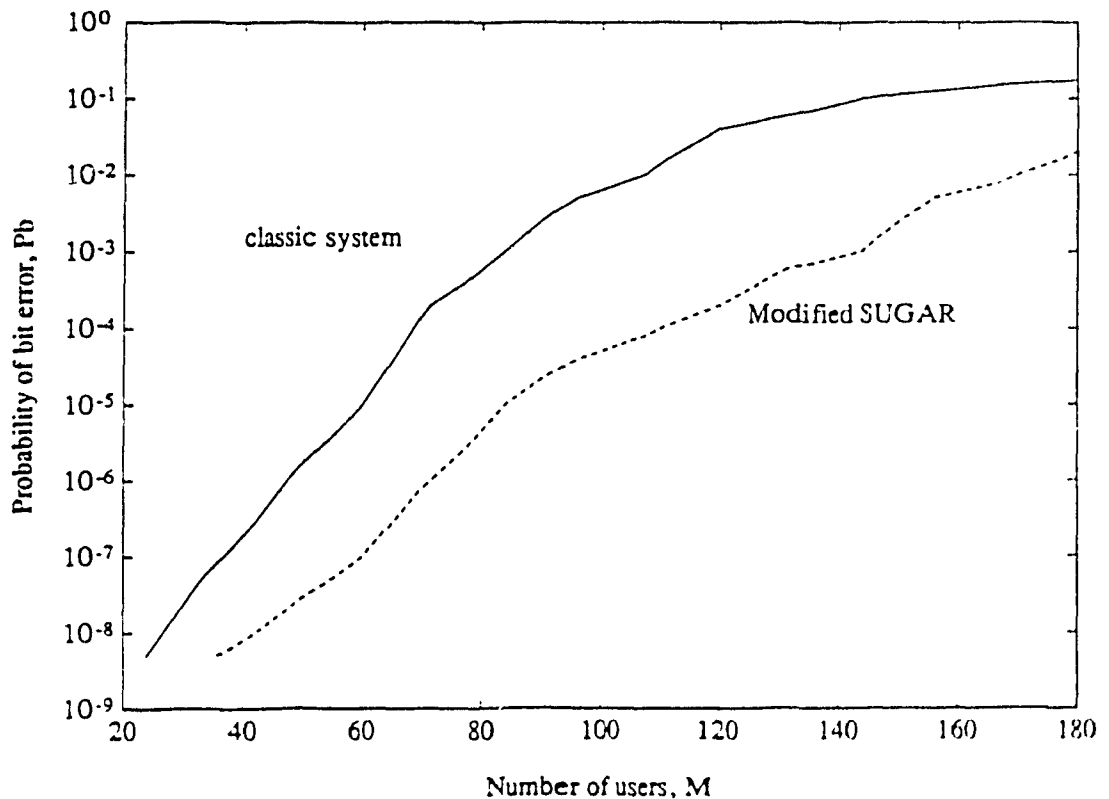


Fig. 2.28 Probability of bit error vs. number of users for conventional Spread Spectrum and Modified SUGAR systems for $L = 511$ (Reed-Solomon coding and Rayleigh fading). Other FEC coding parameters as in Reference [10].

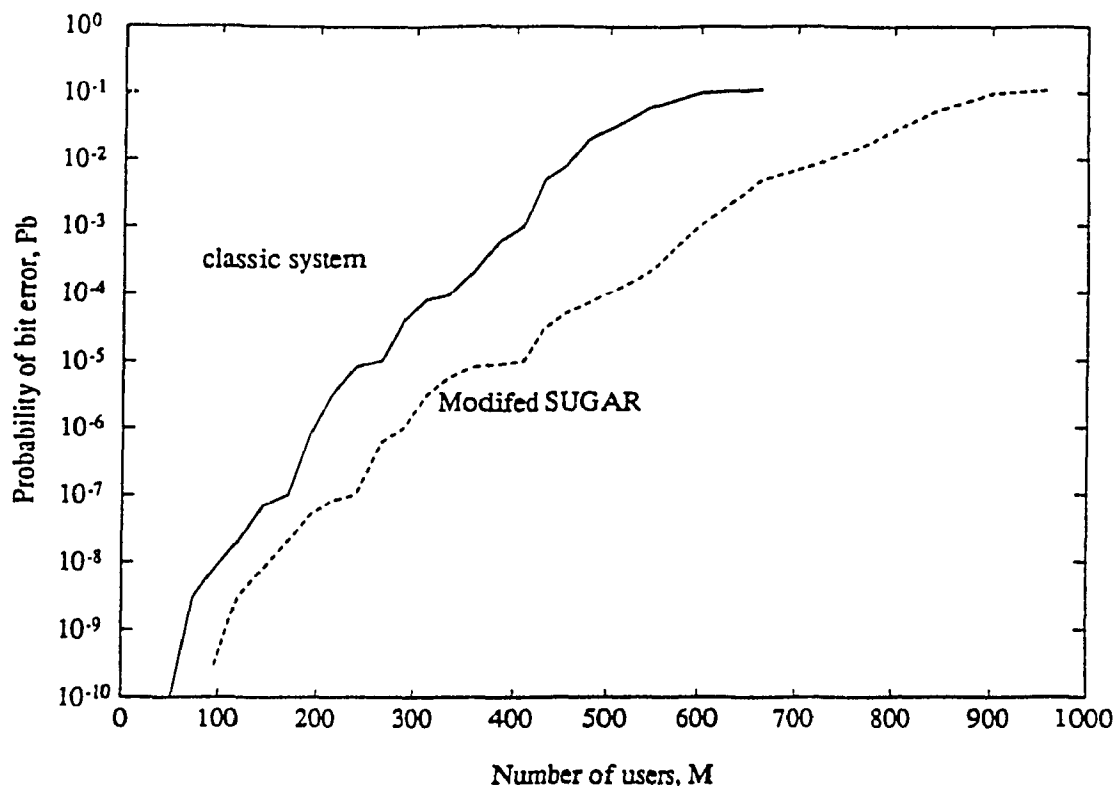


Fig. 2.29 Probability of bit error vs. number of users for conventional Spread Spectrum and Modified SUGAR systems for $L = 2047$ (Reed-Solomon coding and Rayleigh fading). Other FEC coding parameters as in Reference [10].

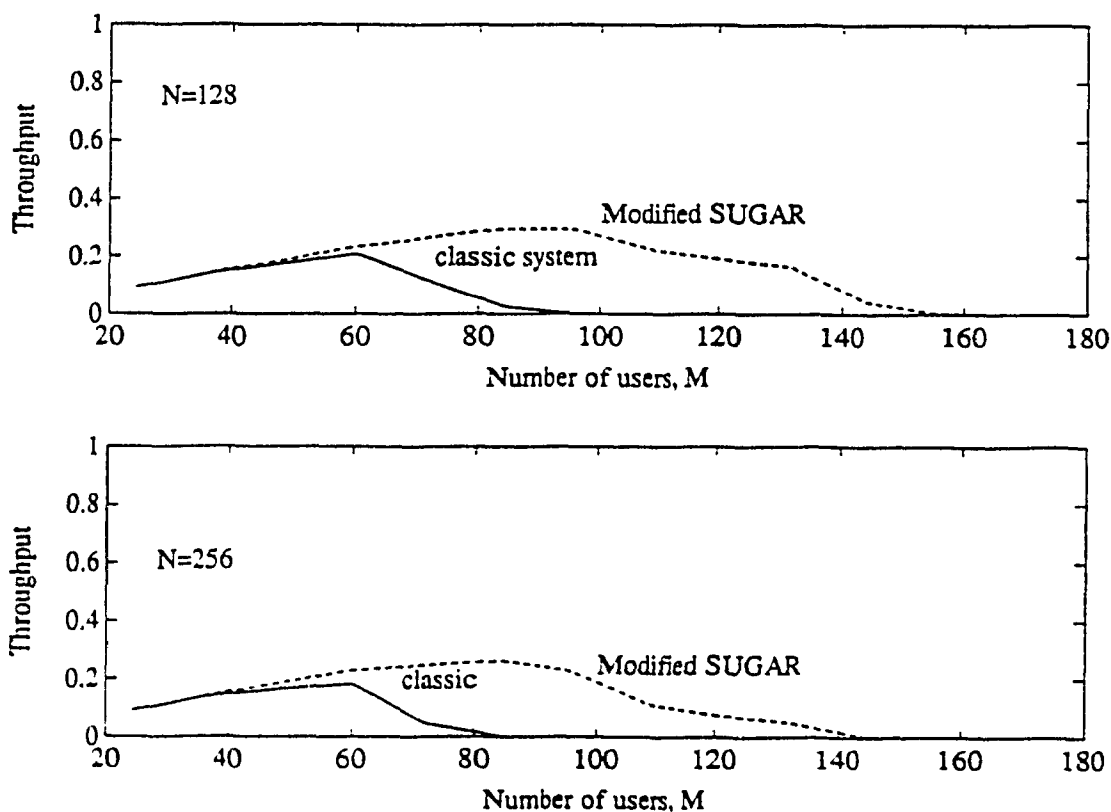


Fig. 2.30 Throughput vs. number of users for conventional Spread Spectrum and Modified SUGAR systems for $L = 255$ and packet sizes $N=128$ and 256 , for data communication (Reed-Solomon coding and Rayleigh fading).

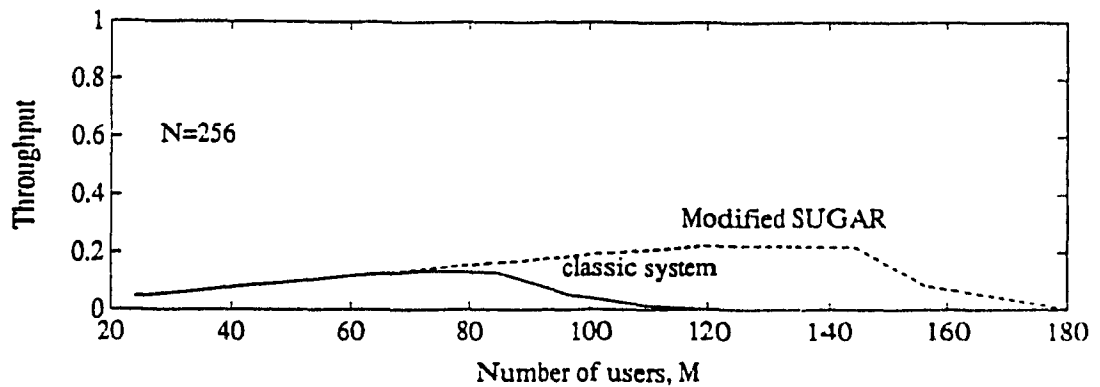
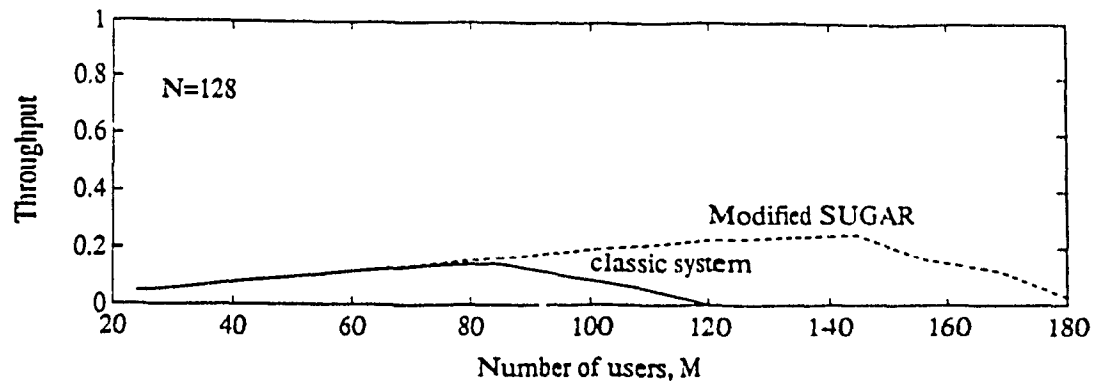


Fig. 2.31 Throughput vs. number of users for conventional Spread Spectrum and Modified SUGAR systems for $L = 511$ and packet sizes $N=128$ and 256 , for data communication (Reed-Solomon coding and Rayleigh fading).

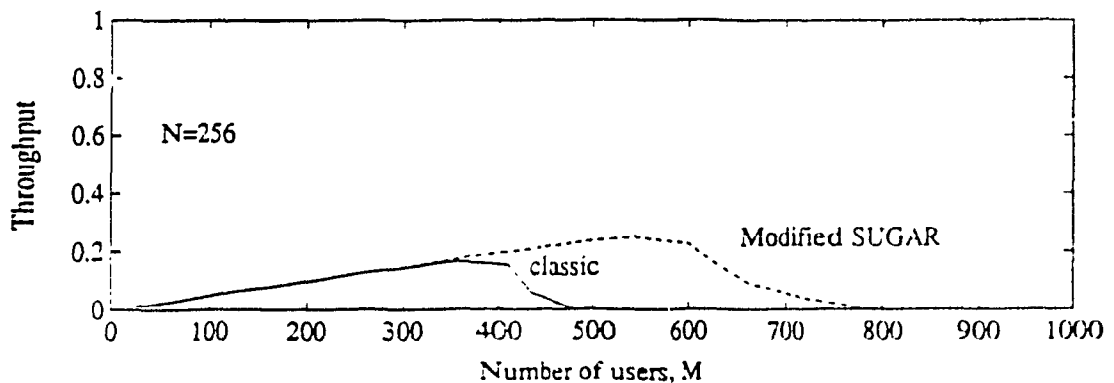
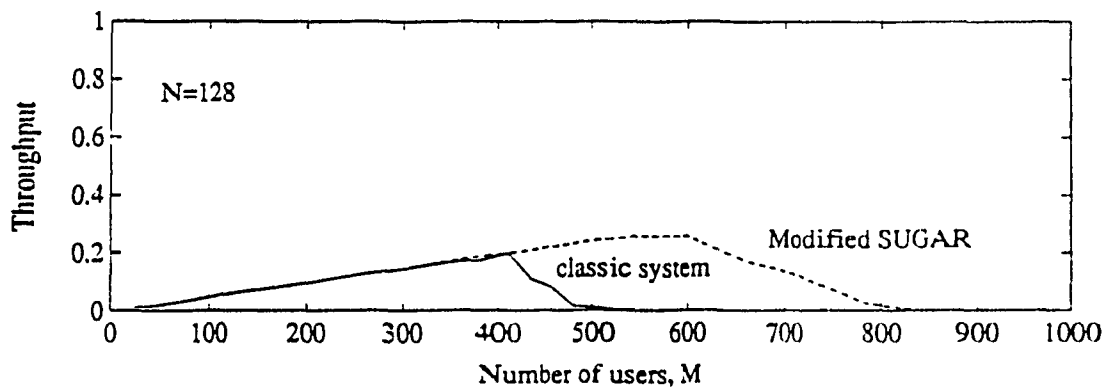


Fig. 2.32 Throughput vs. number of users for conventional Spread Spectrum and Modified SUGAR systems for $L = 2047$ and packet sizes $N=128$ and 256 , for data communication (Reed-Solomon coding and Rayleigh fading).

Simulation study of the SUGAR system

3.1 Introduction

This chapter describes the computer modelling and simulation of the SUGAR system. Simulation is an important cost-effective technique to study any physical system and in our case to corroborate our analytical assumptions and results. The programming language used for this simulation is FORTRAN 77. A computer model of the various subsystems is shown in Figure 3.1.

The general procedure of the simulation program can be outlined as below:

- (1) Generate random delay and random phases for all users in the three groups.
- (2) Initialize the switching functions to reflect the random delays generated above.
Initialize the feedback connections of the Gold code generator.
- (3) Generate random data bits for all users in the three groups.
- (4) The calculation of interference starts with this step. The intended signal component is computed by considering its data over the whole bit period.
- (5) The interference effects of other users on the intended user signal is computed.
- (6) The sum of the intended signal and the total interference is compared against the generated data bit for any user in a group. If they do not match, then an error is recorded.
- (7) The probability of bit error is then computed after all the iterations are completed.

The above steps can be elaborated below:

1. The number of users in this simulated system is divided into three groups with equal users in each group and one user of any group is designated as the intended receiver. The shift register length is fixed for any simulation run - this also determines the number of simultaneous users that the system can support.

Since users may arrive in an asynchronous(unslotted) fashion, we generate random delays and random phases for all users in the system. Note that the delay and phase differences for the intended user is zero. These random values are generated using IMSL routines, in this case random numbers from a uniform (0,1) distribution. These random values are appropriately scaled so that random delay varies between 0 to T_b and phase difference varies from 0 to 2π .

2. The switching functions are initialized to reflect the random delays for each user. The feedback connections of the Gold code generator are initialized to model the two sets of the Linear Feedback Shift Register(LFSR). Arbitrary bits are assigned as initial values of the LFSR. Figure 3.2 shows a typical Gold code generator, modelled in this simulation.

3. In order to examine the number of errors over a stream of data bits, we perform the steps from here repeatedly. In each iteration, we consider 10 data bits and hence in n iterations we can examine $10n$ data bits. Thus in each iteration we generate 10 random data bits for each user in the system. We again use IMSL random number generator to generate these random data bits.

4. We perform the interference calculations by considering 10 data bits at a time. The intended signal component is calculated by considering its data bit over the bit period, i.e., $S(t) = \sqrt{0.5d} \cdot T_b$. For the interfering users (i.e., all other users in the system except the intended user), the signal is sampled at each chip interval iteratively until the whole code period is considered.

5. Thus for each user in one group, the switching function is determined by considering the delay and assignment of that user in any one group i.e. each group has its own switching function.

The Gold code generator is modelled according to Figure 3.2. This Gold code generation is done in a separate subroutine which assigns a Gold code for each call to it. The codes are unique for each user and this gives each user the selective identification

among several users simultaneously accessing the channel. Each user is thus identified by a Gold code and a group of users is identified by a switching function. The assignment of Gold codes can be done in one of several ways.

The effect of adjacent data bits is also considered in our calculation of interference. Thus the multiuser interference is determined by adjacent data bits, the switching function and Gold code. For the intended user, the signal consists only of the data bit since the receiver correlation operation effectively removes the Gold code and switching function. We assume perfect synchronization operation in the receiver.

This interference calculation is similarly carried for all users in the three groups. Note that the above calculation is done for each data bit. For each data bit considered, we compare the generated data bit and the data bit received in the presence of multiuser interference. If the two data bits compared do not match, an error is recorded and we increment a counter for the erroneous data bits received.

6. We now consider the next data bit and repeat steps 4 and 5. After all 10 data bits are considered, we start the next iteration. Thus we repeat steps 3,4 and 5 for each iteration, for n iterations say.

7. After all iterations are completed, the probability of bit error is calculated as:

$$P_b = \frac{\text{Number of received bits in error}}{\text{total number of transmitted bits}}$$

Note that the whole system is modelled by considering the calculation in base band and ignoring AWGN or any fading or multipath propagation effects. Fading and multipath propagation effects are included in variations of this simulation program.

3.2 Simulation of the SUGAR system under multipath fading

The simulation of our SUGAR system under multipath fading is done based on models developed for satellite communication channels from [10]. Signal transmission over radio channels have randomly time-variant impulse responses. The random variations of the signal in terms of amplitude and phase are treated in statistical terms. Hence

there is a penalty to be paid as a consequence of the fading of the received signal. Associated with each path is a propagation delay and an attenuation factor. In our simulation model, we consider one direct path and two multipath components of the signal at two different delays relative to the direct path. The direct path is subjected to a log-normal transformation and the multipath component is Rayleigh distributed. Thus the signal received over these discrete multipaths will have different attenuation and time delay relative to the others. The received signal is

$$S(t) = \alpha r(t) + \beta_1 r(t - \tau_1) + \beta_2 r(t - \tau_2) \quad 0 < \tau_1, \tau_2 < T_p \quad (3.1)$$

where $r(t)$ is the transmitted or line of sight signal.

$$\beta_1 = \left[\gamma_1^2 + X_2^2 \right]^{0.5} \quad \text{where} \quad X_1 = N(0, \sigma_1) \quad \text{and} \quad X_2 = N(0, \sigma_2)$$

where X_1 and X_2 are zero-mean Gaussian random variables, and α is the attenuation factor of the direct path, which has a log-normal distribution. β_1 and β_2 represent attenuation factors due to Rayleigh fading. Note that α , β_1 , β_2 appear as multiplicative factors of their respective signal paths.

In the simulation program, all users are given these attenuation factors by random number generation of log-normal and zero-mean Gaussian deviates. These factors appear in the calculation of both the intended signal and the interfering signals of all other users. We also assume that fading for different signals is statistically independent.

3.3 Simulation of the SUGAR system under fading

In the simple *fading* case, the signal amplitude variations are due to the time-variant characteristics of the channel. This phenomenon causes destructive interference with the signal carrier. We could have Rayleigh fading and Ricean fading. Ricean fading is due to atmospheric effects, especially rain, while Rayleigh fading is due reflections from moving and fixed objects such as tropospheric clouds, buildings, trees, etc.

Rayleigh fading is included in the program by using random number generator. Thus if β is a multiplicative Rayleigh fading component,

$$\beta_1 = \left[X_1^2 + X_2^2 \right]^{0.5} \quad (3.2)$$

where $X_1 = N(0, \sigma_1)$ and $X_2 = N(0, \sigma_2)$, where X_1 and X_2 are zero-mean Gaussian random variables.

Rician fading comes as a multiplicative factor in all signal calculations. Thus

$$\alpha = \left[X_1^2 + X_2^2 \right]^{0.5} \quad (3.3)$$

where $X_1 = N(\gamma_1, \sigma_1)$ and $X_2 = N(\gamma_2, \sigma_2)$ where X_1 and X_2 are normalized Gaussian distributed variables.

Diversity techniques can be used to combat multipath fading. FEC coding can be used to combat these destructive effects as well. These effects can be simulated as well and this is one suggested item for future work on this topic. Figure 3.3 is a simple model of the radio-wave channel at the waveform level[7].

3.4 Simulation Results

The simulation was carried out to calculate the bit error probability (P_b) as a function of the number of simultaneous users (M) for various Gold code lengths, L, for both the classic spread spectrum and Modified SUGAR systems.

Figure 3.4 shows the SNR advantage of the Modified SUGAR system over the classic system for code length L=127 in a no coding, no fading environment. The advantage is clear, especially in the low load ranges. This simulation assumes that the user signals may arrive in an asynchronous or unslotted fashion at the receiver.

When user signals arrive in a synchronous or slotted fashion at the receiver, the performance is expected to be better and is evident from Figure 3.5. The Modified SUGAR system performs better than the classic system by about 2 dB, especially under low loads.

When the code length is increased, the number of simultaneous users that the system can support at an acceptable bit error is also increased. In this simulation with an extended code length ($L=511$), we see the performance of the two systems in a no coding, no fading environment in Figure 3.6.

Finally the bit error probability is computed as a function of M for code length $L=127$ in a Ricean fading environment. The degrading effects of fading on both systems are observed in Figure 3.7.

3.5 Analytical vs Simulation Results

There are inherent drawbacks in the simulation work and hence its results. Due to limitations in computer execution time, the simulation results are not very precise and hence they can only show a general trend in the two systems' performance. In this case, the Modified SUGAR system still performs better than the Classic system, as is evident from the simulation results.

More accurate results can be obtained, for example, for the bit error rate by examining the performance over a greater bit range (e.g., 100,000 bits, compared to 5000 bits in the simulation work). Several IMSL routines were used in the simulation work - they generate only pseudo-random values for the different distributions. Pure random deviates are difficult to generate. Overall the analytical work was done in a step-by-step manner, incorporating our derivations and results from some references. Thus the analytical results are the more accurate of the results obtained by Analysis and Simulation. However, simulation work was useful in understanding the effects of different parameters on the performance of the two systems under study and hence it had its own utility.

3.6 Gold Codes

When channel resources are shared using spread spectrum techniques, all users are permitted to transmit simultaneously using the same band of frequencies. Users are

each assigned a different spreading code so that they can be separated in the receiver despreading process. Hence for a multiple access system, there is a need to find a set of spreading codes or waveforms such that as many users as possible can use the same band of frequencies with as little interference as possible. Gold codes were invented in 1967 at the Magnavox Corporation specifically for multiple access spread spectrum systems.

The receiver despreading operation is a correlation operation with the spreading code of the desired transmitter. A received signal that has been spread using a different spreading code will not be despread and will cause minimal interference with the desired signal. Thus the amount of interference for any single user is related to the cross-correlation between the spreading code of the intended user and those of the interfering users. Relatively large sets of Gold codes exist, which have low cross-correlation properties for sequences of a given length. Thus Gold codes are ideally suited for CDMA applications.

Gold codes have a cross-correlation spectrum which is three-valued, where those three values are

$$\begin{aligned} & \frac{-1}{N} \\ & \frac{-1}{N} \\ & \frac{1}{N} [t(n) - 2] \end{aligned}$$

where

$$t(n) = \begin{cases} 1 + 2^{0.5(n+1)} & \text{for } n \text{ odd} \\ 1 + 2^{0.5(n+2)} & \text{for } n \text{ even} \end{cases}$$

where $N = 2^n - 1$ is the code-period and n is the degree of this m-sequence. n is also the length of the shift-register configuration used in generating the Gold codes. A typical shift-register configuration used to generate a family of Gold codes is shown in Figure 3.2. The period of this sequence is 31 and the generator polynomial of the upper

shift-register combination is expressed as

$$g(D) = 1 + D^2 + D^5$$

while the generator polynomial for the lower one is

$$g(D) = 1 + D^2 + D^3 + D^4 + D^5$$

The complete family of Gold codes for this generator is obtained using different initial loads of the shift register. Given the period N , there are a total of $N+2$ codes in any family of Gold codes. These codes are important since they have well-behaved cross-correlation properties and they offer rapid acquisition possibilities.

A Gold code generator is implemented in a subroutine in the simulation program. Each user is identified by a Gold code besides a switching function. In this simulation, we assign codes to each user sequentially in that family of codes and then reassign the same set of codes if the user population exceeds the maximum number of codes in that family. The assignment of codes to users in different groups is an interesting problem and needs to be investigated further.

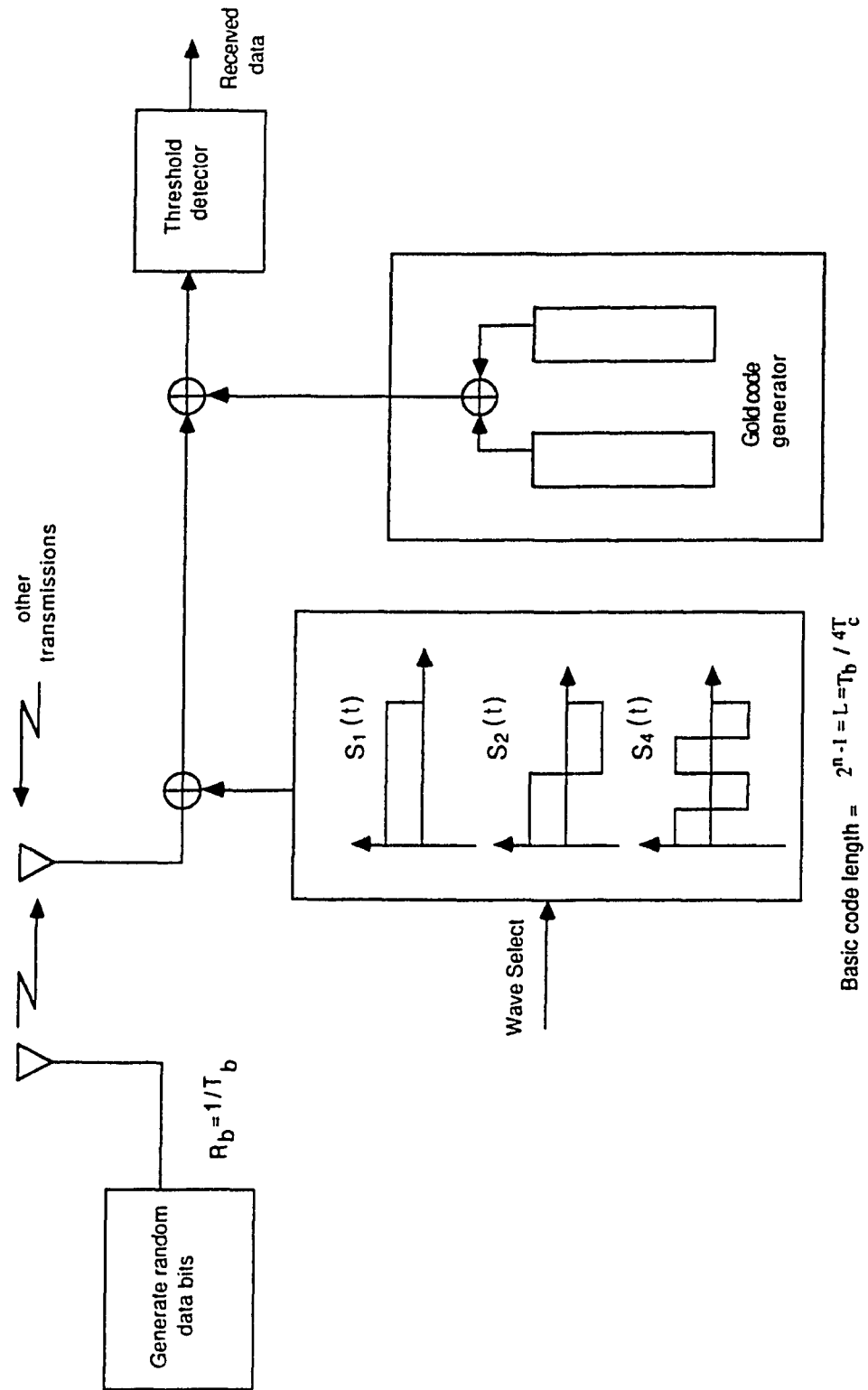


Fig. 3.1 Simulation model of a Code Division Multiple Access system

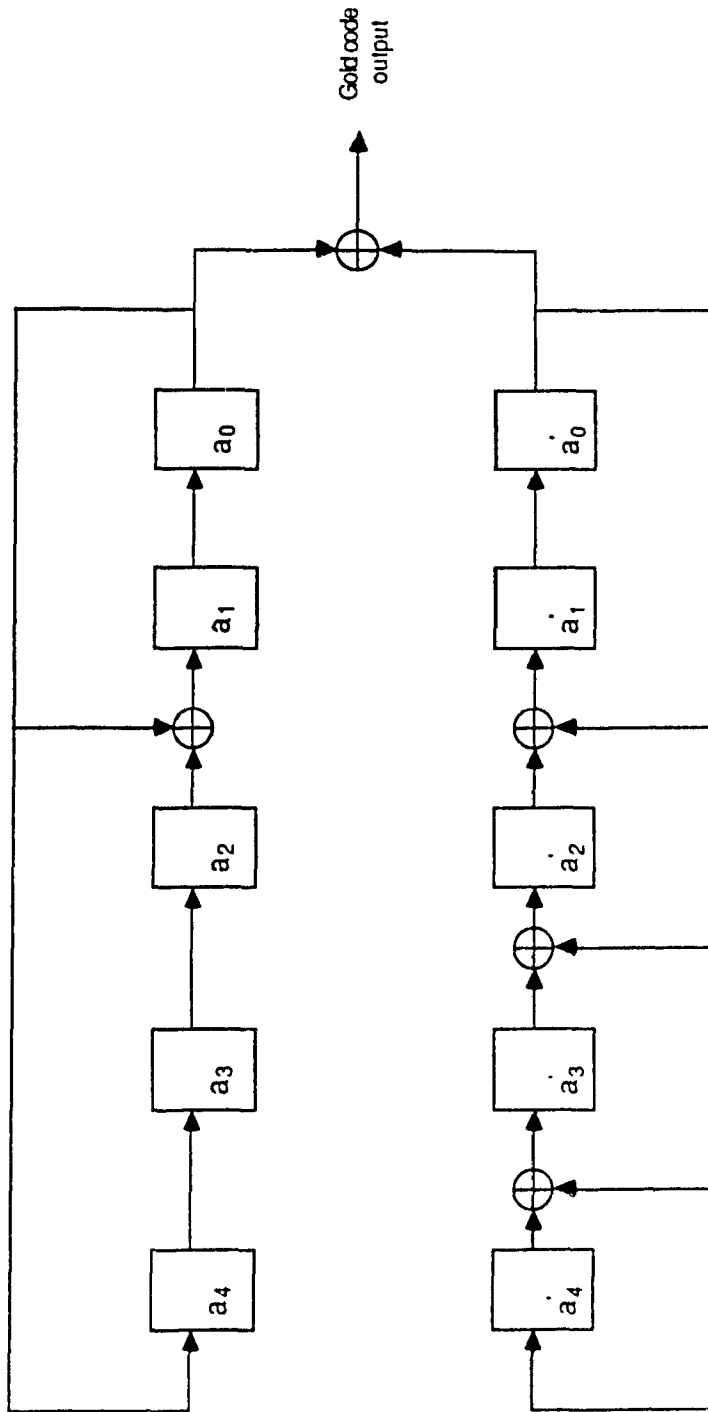


Fig 3.2 A Typical Gold code generator consisting of two Linear Feedback Shift Registers

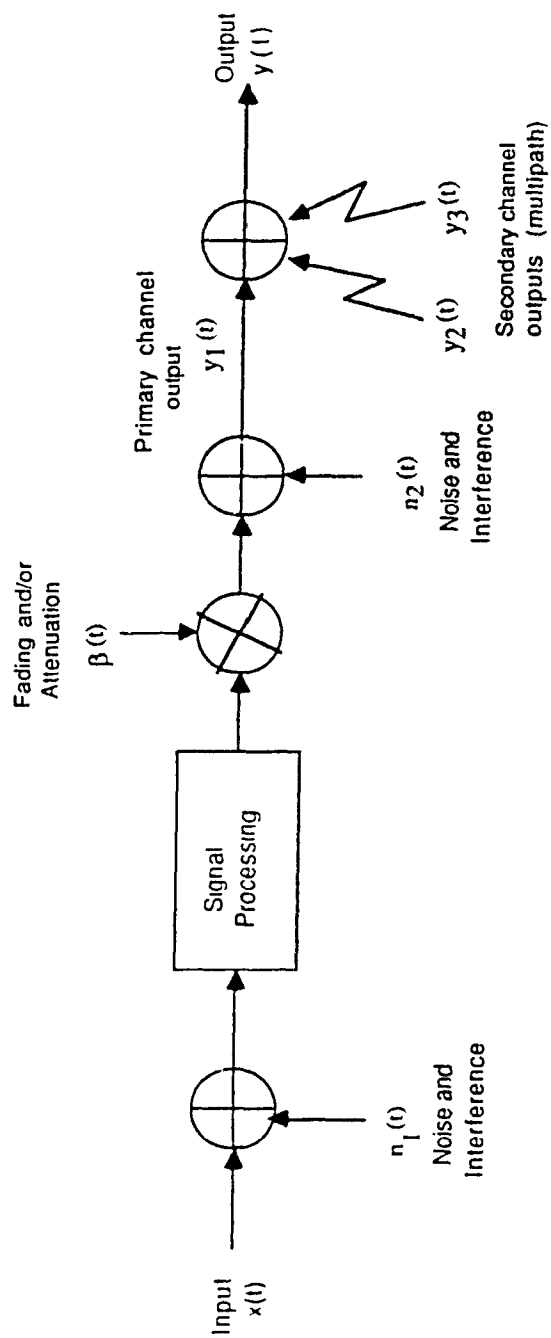


Fig. (3.3) Radio wave channel model at waveform level [7]

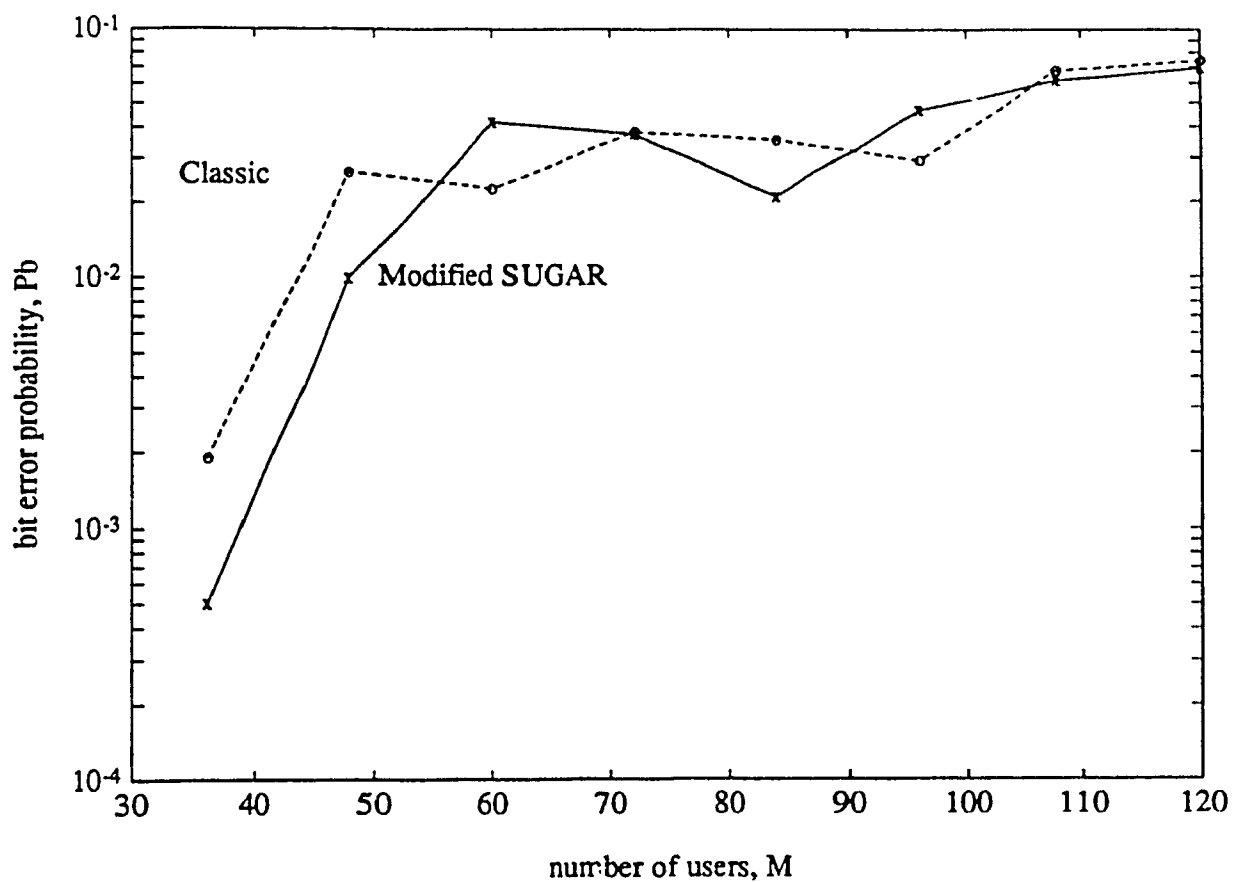


Fig.3.4 Simulation results of Probability of bit error vs. number of users for asynchronous Spread Spectrum and Modified SUGAR systems for $L=127$ (no coding, no fading)

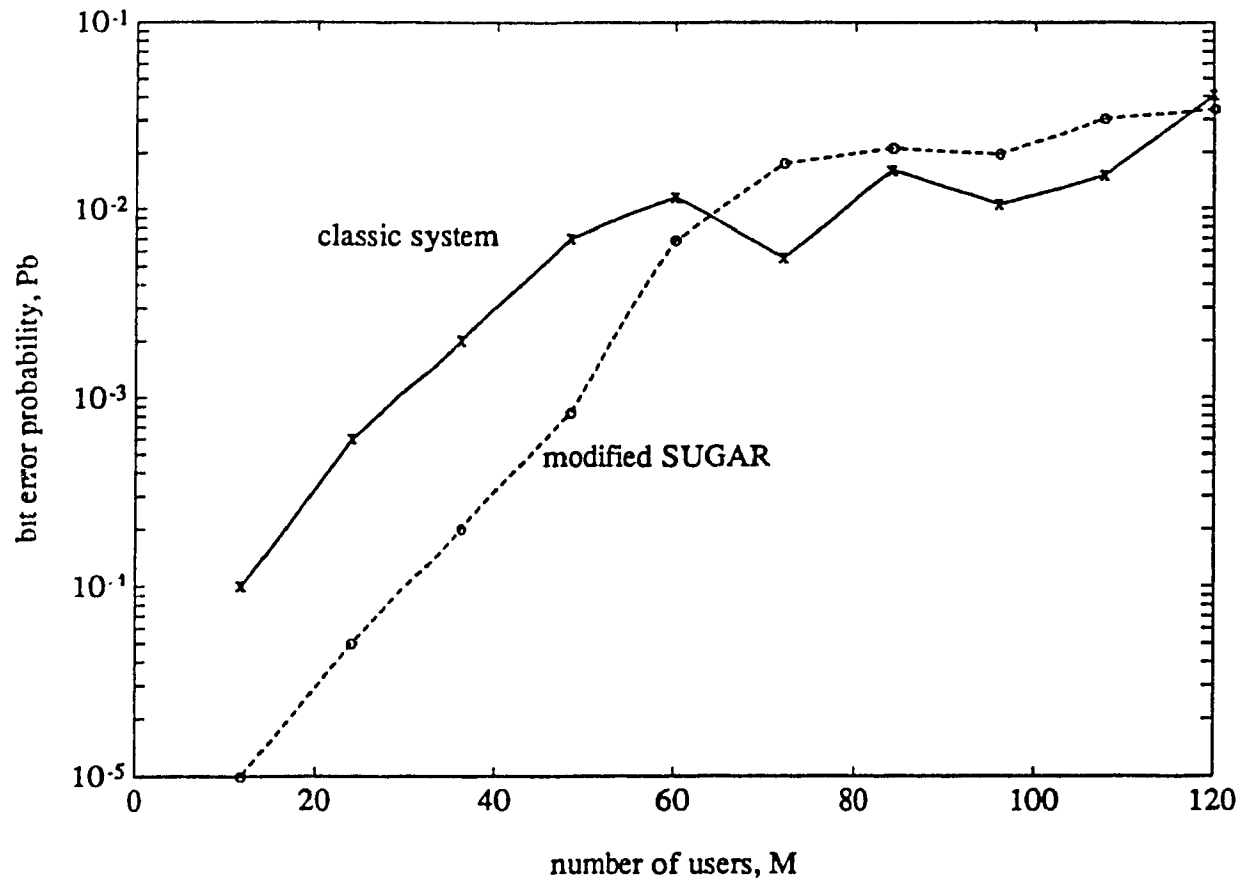


Fig.3.5 Simulation results of Probability of bit error vs. number of users for synchronous classic Spread Spectrum and Modified SUGAR systems for $L=127$ (no coding, no fading)

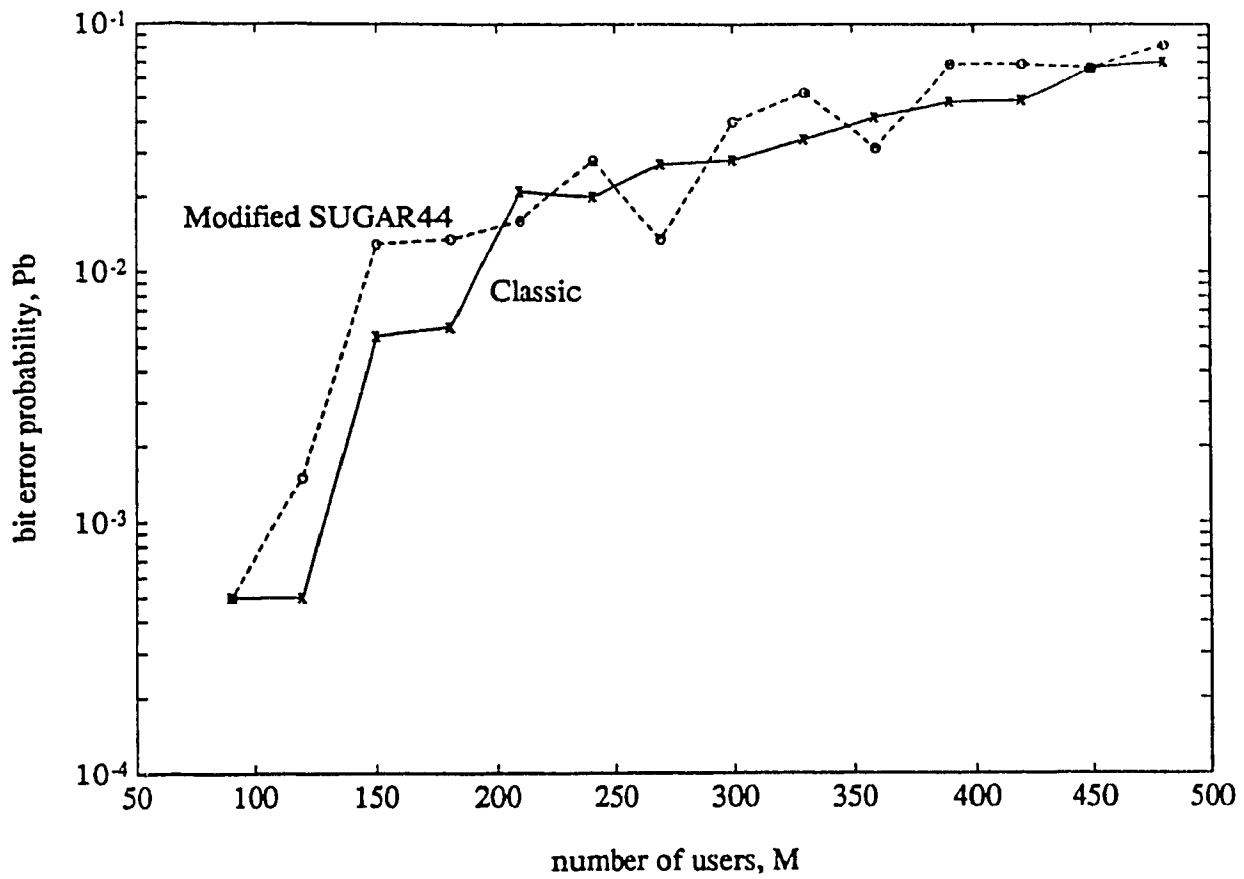


Fig.3.6 Simulation results of Probability of bit error vs. number of users for asynchronous classic Spread Spectrum and Modified SUGAR44 systems for $L=511$ (no coding, no fading)

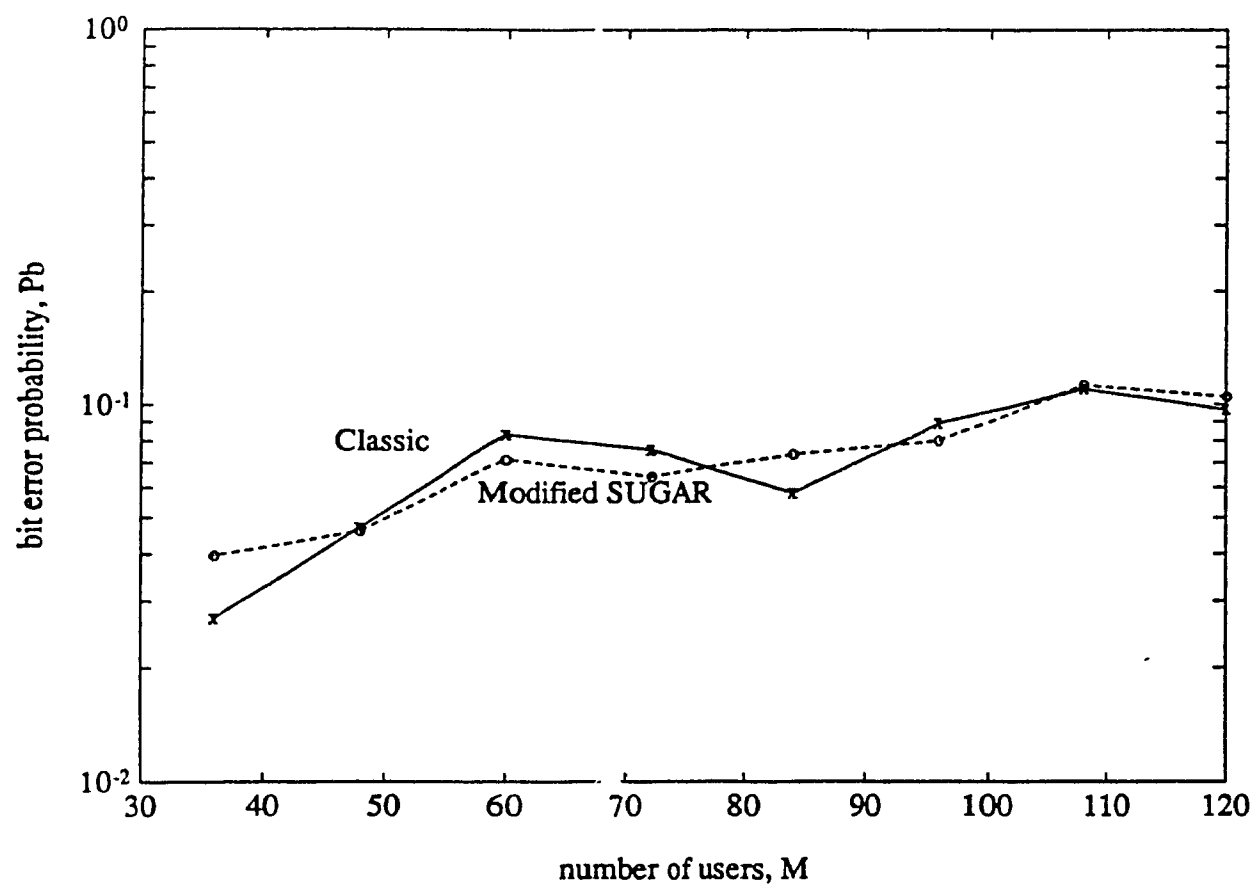


Fig.3.7 Simulation results of Probability of bit error vs. number of users for asynchronous classic Spread Spectrum and Modified SUGAR systems for $L=127$ (Ricean fading, no coding)

Chapter 4

Summary and conclusions

4.1 Conclusions

Spread spectrum communication has long been considered a technique used primarily in military systems. It is not the case since there is a renewed interest in it for commercial applications such as mobile telephony, mobile satellite systems and a few indoor applications. The hardware associated with CDMA-code generators, correlators and matched filters are within the state of the art. In the case of signals transmitted over channels degraded by both multipath and intentional interference and when network synchronization is both a problem and economically infeasible, CDMA is an ideal multiple access technique.

A new Modified SUGAR/DS system has been presented in this thesis. This system has a minimum of 2 dB of SNR improvement over the classic DS system. The superior error and throughput characteristics of the new system have prevailed under various FEC and fading environments.

4.2 Suggestions and Future Work

This thesis has concentrated on three groups case, it is straightforward to extend this work to four or more orthogonal user groups. We have also dealt with PSK modulation in this thesis, however DPSK or MPSK modulation techniques can be easily coupled to this work. It would be interesting to relate the results of this work to the recent efforts in [13], [14], [15], especially under near-far problems, where our Modified SUGAR system is expected to outperform existing efforts (i.e., it needs less sophisticated power control).

In this work codes of various users were assumed to be chip synchronous but otherwise epoch asynchronous. Better gains in SNR are possible if we force epoch syn

chronization, thus achieving complete orthogonality. Future suggested topics include network topology effects, optimal code assignment algorithms over the various user groups as well as multiclass services integration.

REFERENCES

- [1] A. Rahman and A. K. Elhakeem, "Noncoherent Trellis Coding for Frequency Hopping SUGAR Spread Spectrum Multiaccess systems", *Archiv Fur Elektronik und Ubertragungstechnik (AEU)*, Band 44, 1990.
- [2] A. K. Elhakeem, "A new Secure High Capacity Mobile Communication System Employing the SUGARW Principle", A U.S.government disclosure document received March 22,1991.
- [3] A. K. Elhakeem and A. Rahman, "SUGARW, A New Purely Random Spread Spectrum system for Multiaccess", Fourteenth Biennial Symposium on Communication, Queens University at Kingston, Canada.
- [4] K. S. Gilhousein, I. Jacobs, R. Padovani and L. A. Weaver, "Increased Capacity using CDMA for Mobile Satellite Communication", *IEEE J. Select. Areas Commun.*, vol.8, No.4, pp. 503-515, May 1990.
- [5] M. B. Pursley, "Performance Evaluation for Phase-Coded Spread Spectrum Multiple Access Communications - Part I:Systems Analysis", *IEEE Trans. Commun.*, Vol.25, No.8, pp. 795-799, August 1977.
- [6] J. K. Omura, "Spread Spectrum Radios for Personal Communication Services" , IEEE workshop on "Spread Spectrum : Potential Commercial Applications - Myth or Reality?", Montbello, Quebec, Canada, May 1991.
- [7] R. Ziemer and R. Peterson, *Digital Communication and Spread Spectrum Systems*, Macmillan Publishing Company, 1985, pp. 405.
- [8] J. J. Spilker Jr., *Digital Communication by Satellites*, Prentice Hall, 1977, pp. 605.
- [9] J. G. Proakis, *Digital Communications*, McGraw Hill Company, Second Edition, 1989, pp. 718.
- [10] A. C. M. Lee and P. J. McLane, "Convolutionally Interleaved PSK and DPSK

- Trellis Codes for Shadowed, Fast Fading Mobile Satellite Communication Channels", *IEEE Trans. Veh. Technol.*, Vol. 39, No.1, pp. 37-47, Feb. 1990.
- [11] W. W. Wu, D. Haccoun, R. Peile and Y. Hirata, "Coding for Satellite Communication", *IEEE J. Select. Areas Commun.*, vol. SAC-5, No. 4, May 1987.
- [12] J. Hagenauer and E. Lutz, "Forward Error Correction Coding for Fading Compensation in Mobile Satellite Channels", *IEEE J. Select. Areas Commun.*, Vol. SAC-5, No.2, Feb. 1987.
- [13] A.Viterbi, "Very low rate Convolutional Codes for Maximum Theoretical Performance of Spread Spectrum Multiple Access Channels", *IEEE J. Select. Areas Commun.*, vol.8, No.4, May 1990, pp. 641-650.
- [14] M. Nakagawa and T. Hasegawa, "Spread Spectrum for Consumer Communication - Application of Spread Spectrum Communication in Japan", *IEICE Transactions*, Vol.E74, No.5, May 1991.
- [15] A. Polydoros, "Physical Link Access and Topological Level Aspects of Slotted Aloha, Packet Switched Code Division Random Access Networks", IEEE Workshop on "Spread Spectrum: Potential Commercial Applications - Myth or Reality?", Montbello, Quebec, Canada, May 1991.
- [16] A. K. Elhakeem, A. Rahman, P. Balasubramanian and T. LeNgoc, "Modified SUGAR/DS, a new CDMA scheme", *IEEE J. Select. Areas Commun.*, vol. 10, No. 4, May 1992.
- [17] C. L. Weber, G. K. Huth and B. H. Batson, "Performance considerations of CDMA systems", *IEEE Trans. Veh. Technol.*, Vol. VT-30, No. 1, February 1981.
- [18] J. F. Musser, J. N. Daigle, "Derivation of asynchronous CDMA throughput", Bell Systems Technical Journal.
- [19] R. D. J. van Nee, H. S. Misser and R. Prasad, "Direct sequence spread spectrum in a shadowed Rician fading land-mobile satellite channel"*IEEE J. Select. Areas*

Commun., vol. 10, No. 2, Feb. 1992.

- [20] L. Kleinrock, *Queuing Systems - Volume I*, John Wiley & Sons Inc., 1976.
- [21] V. J. Bhargava, D. Haccoun, R. Matyas and P. P. Nuspl, *Digital communications by satellite*, John Wiley & Sons Inc., 1981.
- [22] B. Sklar, *Digital Communications - Fundamentals and Applications*, Prentice Hall, 1988.
- [23] E. A. Geraniotis and M. B. Pursley, "Error probabilities for slow frequency-hopped spread spectrum multiple access communications over fading channels", *IEEE Trans. Commun.*, Vol. Com-30, No. 5, May 1982.
- [24] S. Stein, "Fading channel issues in system engineering", *IEEE J. Select. Areas Commun.*, vol. SAC-5, No. 2, Feb. 1987.
- [25] K. Dessouky and M. Mohamedi, "Multiple access capacity tradeoffs for a Ka-based personal access satellite system", International Mobile Satellite Conference, Ottawa, 1990.
- [26] F.G.Stremmler, *Introduction to Communication Systems*, Addison Wesley Publishing Company, 1990.
- [27] R. C. Dixon, *Spread Spectrum Systems*, John Wiley and Sons, 1984.
- [28] W. W. Peterson and E. J. Weldon, *Error Correction Codes*, MIT Press, Cambridge, Mass., 1972.
- [29] C. E. Cook, F. W. Ellersick, L. B. Milstein and D. L. Schilling, *Spread Spectrum Communications*, IEEE Press, 1983.
- [30] M. K. Simon, J. K. Omura, R. A. Scholtz and B. K. Levitt, *Spread Spectrum Communications*, Computer Science Press, 1985.
- [31] E. A. Geraniotis and M. B. Pursley, "Performance of a coherent direct sequence spread spectrum communication over specular multipath fading channels", *IEEE Trans. Commun.*, Vol. Com.33, No. 6, June 1985.

APPENDIX

Here we evaluate the cross correlation (envelopes) of the switching function in equations (2.10) for a receiver in group 4, as well as other switching function cross correlation for receivers in groups 1,2 to be finally substituted into equations (2.21),(2.22), (2.23).

Taking, for example, the first user of group 4, he will have the reference local switching function $(S_{1,4}(t-jT_b/4))$, in (2.10a) while the interfering k^{th} user of the same group will have the shifted switching function $(S_{k,4}(t-jT_b/4+\tau_{k,4}))$ in (2.10a) which is easily seen to overlap the two data bits duration of the interfering k^{th} user $(d_{k,4}(t-nT_b+\tau_{k,4}))$ of (2.10a). So multiplying the interfering user data with its switching function for different values of $\tau_{k,4}$ with $S_{1,4}(t-jT_b/4)$, we obtain the cross correlation $ff_{4,4}(\tau_{k,4})$ of Fig(A-1) for different values of $\tau_{k,4}$. Needless to say $ff_{4,4}(\tau_{k,4})$ depends on the identity of the overlapping data bits b_0, b_1 . Figures (A-2 to A-4) also show the same results for $[b_0, b_1]=[-1,1]$, for $[b_0, b_1]=[1,1]$ and for $[b_0, b_1]=[-1,-1]$.

It is a simple exercise to repeat the same procedure for the switching cross correlation between users 1 of group 4 (the intended receiver) and user k2 of group 2, we obtain Figures (A-5 to A-8) depending on the identity of $[b_0, b_1]$ as explained. For switching cross correlations between user 1 of group 4 and user k1 of group 1, we obtain Figures (A-9 to A-12).

Figures (A-1)-(A-12) groups are sufficient to evaluate the performance of a typical user in group 4. For purposes of obtaining the performance of a typical user in group 2, we need Figures (A-13 to A16) for $ff_{1,2}(\tau_{k1,2})$ and Figures (A-17 to A20) for $ff_{2,2}(\tau_{k2,2})$ and of course Figures (A-5 to A-8) evaluated previously for $ff_{2,4}(\tau_{k2,4})$. Finally for the performance of a typical user in group 1, we need Figures (A-21 to A-24) on top of Figures (A-13 to A-16) and Figures (A-9 to A-12).

Now the calculation of the average sum over $ff^2(.)$ terms in (2.19)-(2.21) becomes tedious but straight forward given Figs(A-1)-(A-24). For each Figure (conditioned on one bit set $[b_0, b_1]$) we evaluate $\left[\frac{1}{4L} \sum_{\tau=0}^{4L} ff^2(\tau) \right]$. Then we average the 4 results corresponding to the possible values of $[b_0, b_1]$ bits i.e. $[1, -1]$, $[-1, 1]$, $[1, 1]$, $[-1, -1]$ (see for example Figures (A-1 to A-4)). From (A-1 to A-4)), we then obtain

$$\begin{aligned} \left[X_{44} \right]_{1,-1} &= \frac{T_c^2}{4L} \sum_{\tau=0}^{4L} ff_{4,4}^2(\tau) = \frac{T_c^2}{4L} \left\{ 2 \sum_{\tau=0}^{2L/3} (6\tau)^2 + 2 \sum_{\tau=0}^{L/3} (6\tau)^2 + 2 \sum_{\tau=0}^L (2\tau)^2 \right\} \\ &= \frac{T_c^2}{4L} \left\{ 72 \sum_{\tau=0}^{2L/3} \tau^2 + 72 \sum_{\tau=0}^{L/3} \tau^2 + 8 \sum_{\tau=0}^L \tau^2 \right\} \\ &= \frac{T_c^2}{4L} \left\{ \frac{72(2L/3)(2L/3)(4L/3)}{6} + \frac{72(L/3)(L/3)(2L/3)}{6} + \frac{8(L)(L+1)(2L+1)}{6} \right\} \quad (A-1) \end{aligned}$$

$$\left[X_{44} \right]_{-1,1} = \left[X_{44} \right]_{1,-1} = \frac{T_c^2}{L} \left\{ \frac{18L^3}{9} + \frac{L(L+1)(2L+1)}{3} \right\} \approx \frac{8L^2 T_c^2}{3} \quad (A-2)$$

$$\begin{aligned} \left[X_{44} \right]_{-1,-1} &= \left[X_{44} \right]_{1,1} = \frac{T_c^2}{4L} \left\{ 8 \sum_{\tau=0}^{L/2} (8\tau)^2 \right\} \\ &\approx \frac{512}{4L} \left\{ \frac{(L/2)(L/2)(L)}{6} \right\} = \frac{16T_c^2 L^2}{3} \quad (A-3) \end{aligned}$$

From (A-1)-(A-4), we get,

$$\begin{aligned} \frac{1}{4L} \sum_{\tau=0}^{4L} ff_{4,4}^2(\tau) &= \frac{1}{4} \left[\left[X_{44} \right]_{1,-1} + \left[X_{44} \right]_{-1,1} + \left[X_{44} \right]_{1,1} + \left[X_{44} \right]_{-1,-1} \right] \\ &= \frac{T_c^2 \left[\frac{8}{3} L^2 + \frac{16}{3} L^2 \right]}{2} = 4L^2 T_c^2 \quad (A-4) \end{aligned}$$

Similarly for $ff_{2,4}(.)$ from Figures (A-5 to A-8), we get

$$\frac{1}{4L} \sum_{\tau=0}^{4L} ff_{2,4}^2(\tau) = \frac{T_c^2}{4} \left\{ \frac{1}{4L} (2.4.4. \sum_{\tau=0}^L \tau^2) + 0 + 0 + 0 \right\}$$

$$= \frac{T_c^2}{L} \frac{2L(L+1)(2L+1)}{6} = \frac{2L^2 T_c^2}{3} \quad (\text{A-5})$$

$$\begin{aligned} \frac{1}{4L} \sum_{\tau=0}^{4L} f f_{1,4}^2(\tau) &= \frac{T_c^2}{4} \left\{ \frac{1}{4L} (2.4.4) \sum_{\tau=0}^L \tau^2 + 0 + 0 \right\} \\ &= \frac{8L(L+1)(2L+1)}{96L} = \frac{2L^2 T_c^2}{3} \end{aligned} \quad (\text{A-6})$$

$$\begin{aligned} \frac{1}{4L} \sum_{\tau=0}^{4L} f f_{1,2}^2(\tau) &= \frac{T_c^2}{4} \left\{ \frac{1}{4L} (2.2.4) \cdot \sum_{\tau=0}^{2L} \tau^2 + 0 + 0 \right\} \\ &= \frac{32L(2L+1)(4L+1)}{96L} = \frac{8L^2 T_c^2}{3} \end{aligned} \quad (\text{A-7})$$

$$\begin{aligned} \frac{1}{4L} \sum_{\tau=0}^{4L} f f_{2,2}^2(\tau) &= \frac{T_c^2}{4} \left\{ \frac{1}{4L} (2.2.4) \cdot \sum_{\tau=0}^{2L} \tau^2 + 2.4.16 \cdot \sum_{\tau=0}^L \tau^2 \right\} \\ &= T_c^2 \left[\frac{2L(2L+1)(4L+1)}{6L} + \frac{8L(L+1)(2L+1)}{6L} \right] = \frac{16}{3} L^2 T_c^2 \end{aligned} \quad (\text{A-8})$$

$$\begin{aligned} \frac{1}{4L} \sum_{\tau=0}^{4L} f f_{1,1}^2(\tau) &= \frac{T_c^2}{4} \left\{ \frac{1}{4L} (2.2.4) \cdot \sum_{\tau=0}^{2L} \tau^2 + 2.64L^3 \right\} \\ &= T_c^2 \left[\frac{2L(2L+1)(4L+1)}{6L} + 8L^2 \right] = T_c^2 \left[\frac{8}{3} L^2 + 8L^2 \right] = \frac{32}{3} L^2 T_c^2 \end{aligned} \quad (\text{A-9})$$

To find out whether we have performance symmetry i.e. performance of a type 4 receiver is the same as 1 or 2, we assume $M_1 = M_2 = M_4 = \frac{M}{3}$ and compute

$$y_1 = \frac{T_c^2}{4L} \sum f f_{1,1}^2(\tau) + \frac{T_c^2}{4L} \sum f f_{1,2}^2(\tau) + \frac{T_c^2}{4L} \sum f f_{1,4}^2(\tau) \quad (\text{A-10})$$

$$= \frac{\left[\frac{32L^2}{3} + \frac{8L^2}{3} + \frac{2L^2}{3} \right] T_c^2}{3} = \frac{42L^2 T_c^2}{9} \quad (\text{A-11})$$

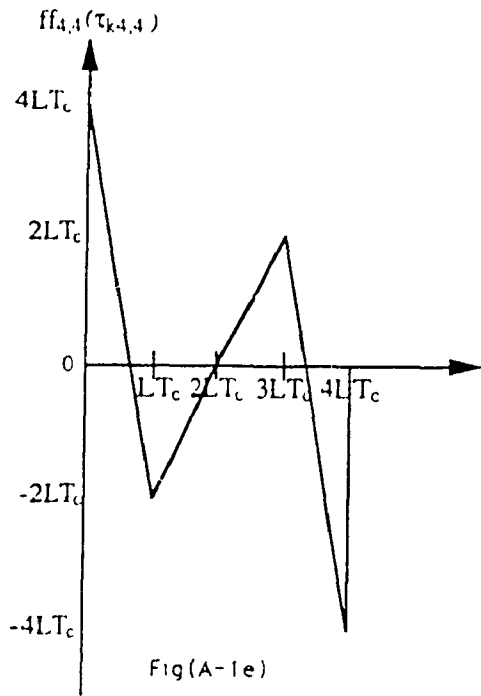
y_1 is the effective envelope of the Gold Codes cross correlation of group 1. Compare to

$y_c = 16L^2 T_c^2$ for the classic system (switching functions are all 1s). Similarly

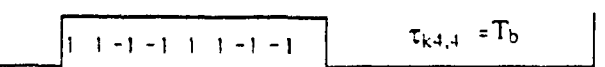
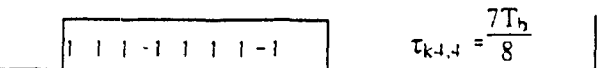
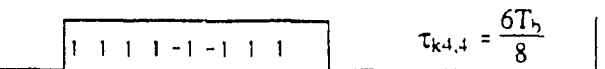
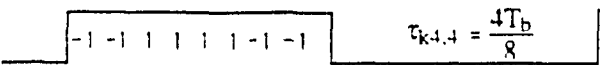
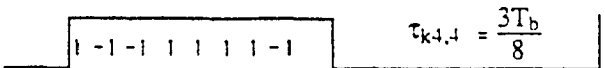
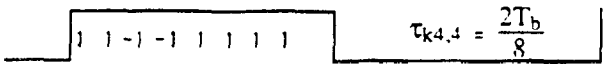
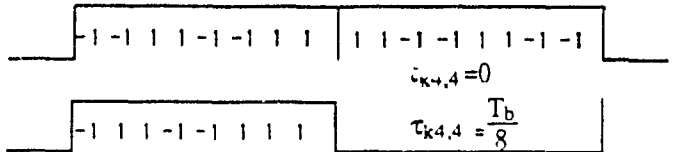
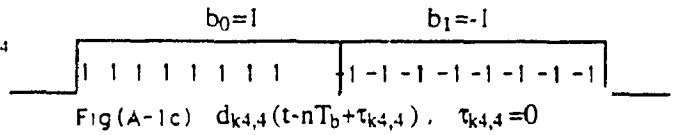
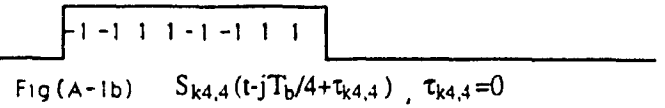
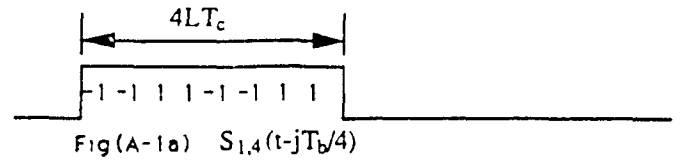
$$\begin{aligned}
 y_2 &= \frac{T_c^2}{4L} \left[\sum ff_{2,1}^2(\tau) + \sum ff_{2,2}^2(\tau) + \sum ff_{2,4}^2(\tau) \right] \\
 &\quad \left[\frac{8L^2}{3} + \frac{16}{3}L^2 + \frac{2L^2}{3} \right] T_c^2 \\
 &= \frac{26}{9} L^2 T_c^2
 \end{aligned} \tag{A-12}$$

$$\begin{aligned}
 y_4 &= \frac{T_c^2}{4L} \sum ff_{1,4}^2(\tau) + \frac{T_c^2}{4L} \sum ff_{2,4}^2(\tau) + \frac{T_c^2}{4L} \sum ff_{4,4}^2(\tau) \\
 &\quad \left[\frac{2L^2}{3} + \frac{2L^2}{3} + 4L^2 \right] T_c^2 \\
 &= \frac{16}{9} L^2 T_c^2
 \end{aligned} \tag{A-13}$$

Evidently $y_4 \neq y_2 \neq y_1$.

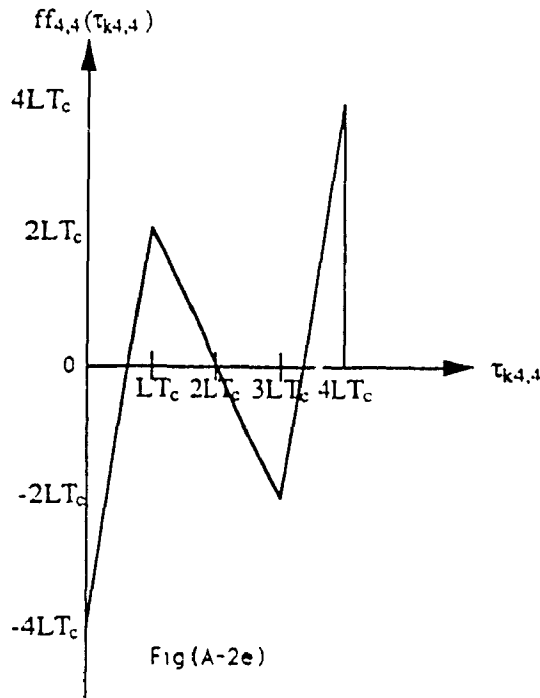


Switching function cross correlation for 2 users in groups 4,4 ($b_0, b_1 = (1, -1)$) are the two data bits of the interfering user k_4 overlapping the received bit of the intended user



Fig(A-1d)

$d_{k4,4}(t-nT_b + \tau_{k4,4})$ $S_{k4,4}(t-jT_b/4 + \tau_{k4,4})$
for various $\tau_{k4,4}$



Switching function cross correlation for 2 users in groups 4,4 ($b_0, b_1 = (-1, 1)$) are the two data bits of the interfering user k_4 overlapping the received bit of the intended user

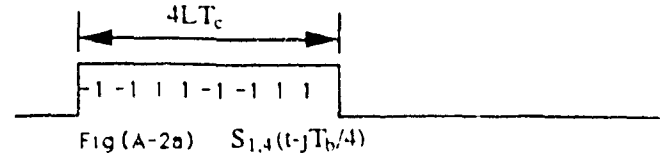


Fig (A-2a) $S_{1,4}(t-jT_b/4)$



Fig (A-2b) $S_{k4,4}(t-jT_b/4 + \tau_{k4,4})$, $\tau_{k4,4} = 0$

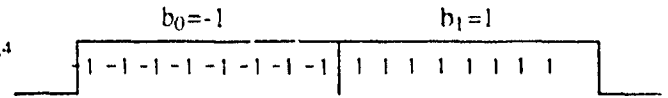
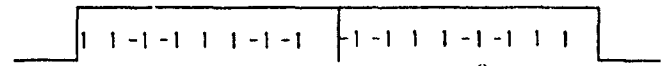


Fig (A-2c) $d_{k4,4}(t-nT_b + \tau_{k4,4})$, $\tau_{k4,4} = 0$



$\tau_{k4,4} = 0$



$\tau_{k4,4} = \frac{T_b}{8}$



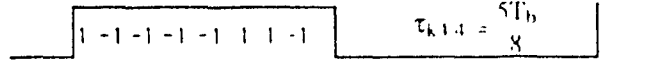
$\tau_{k4,4} = \frac{2T_b}{8}$



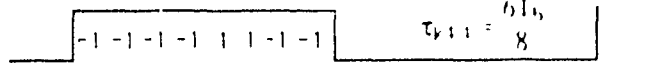
$\tau_{k4,4} = \frac{3T_b}{8}$



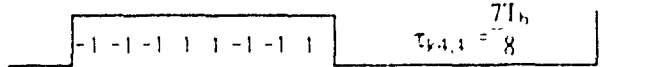
$\tau_{k4,4} = \frac{4T_b}{8}$



$\tau_{k4,4} = \frac{5T_b}{8}$



$\tau_{k4,4} = \frac{6T_b}{8}$



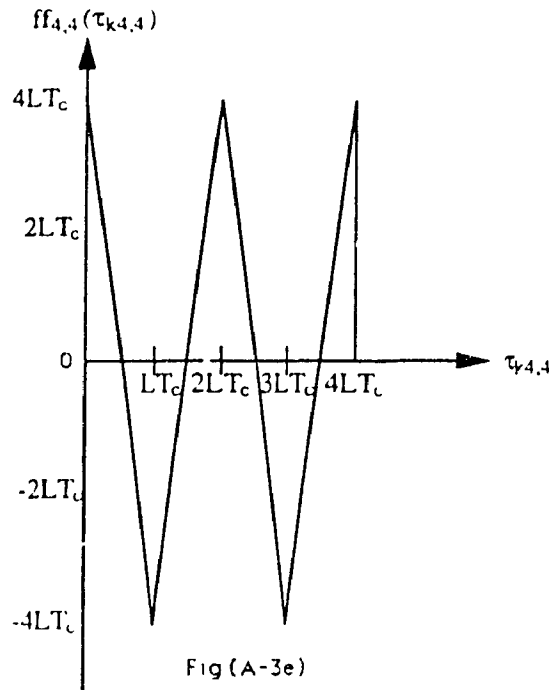
$\tau_{k4,4} = \frac{7T_b}{8}$



$\tau_{k4,4} = T_b$

Fig (A-2d)

$d_{k4,4}(t-nT_b + \tau_{k4,4})$ $S_{r,4,4}(t-jT_b/4 + \tau_{r,4,4})$
for various $\tau_{r,4,4}$



Switching function cross correlation for 2 users in groups 4,4 ($b_0, b_1 = (1, 1)$) are the two data bits of the interfering user k_4 overlapping the received bit of the intended user

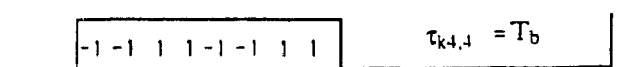
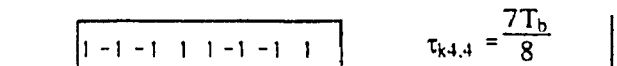
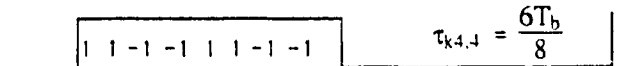
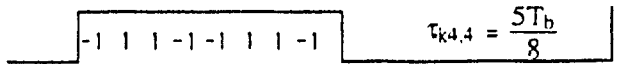
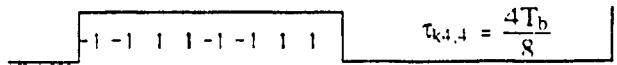
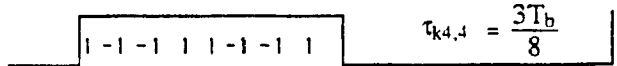
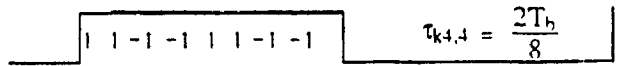
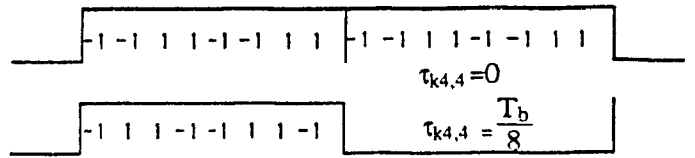
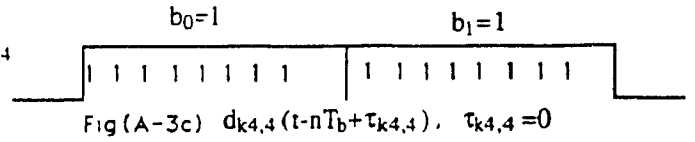
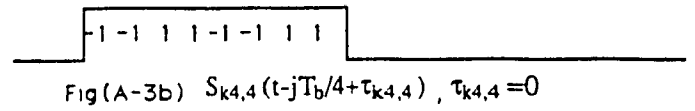
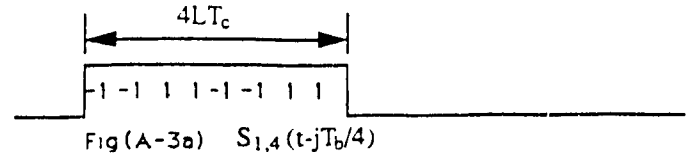
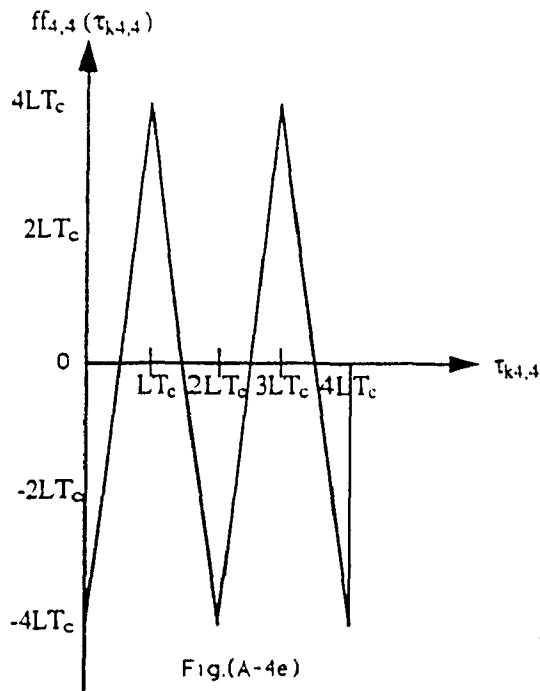


Fig (A-3d)

$d_{k4,4}(t-nT_b+\tau_{k4,4})$ $S_{k4,4}(t-jT_b/4+\tau_{k4,4})$
for various $\tau_{k4,4}$



Switching function cross correlation for 2 users in groups 4,4 ($b_0, b_1 = (-1, -1)$) are the two data bits of the interfering user k_4 overlapping the received bit of the intended user.

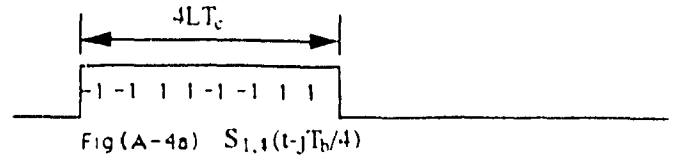


Fig (A-4b) $S_{k4,4}(t-jT_b/4 + \tau_{k4,4})$, $\tau_{k4,4} = 0$

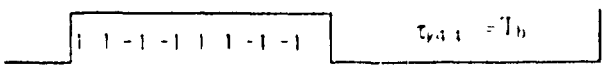
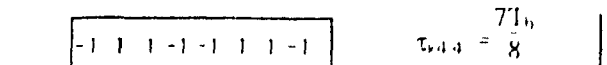
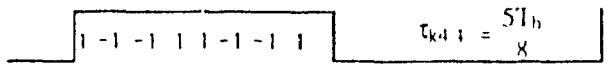
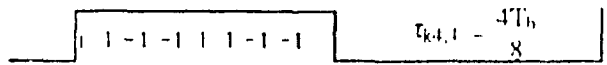
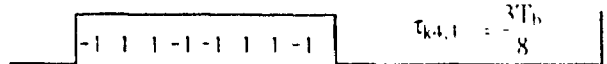
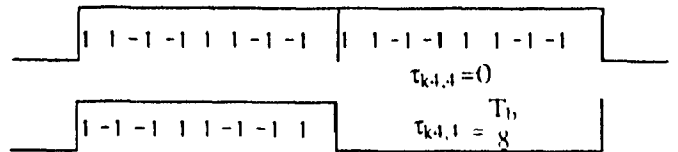
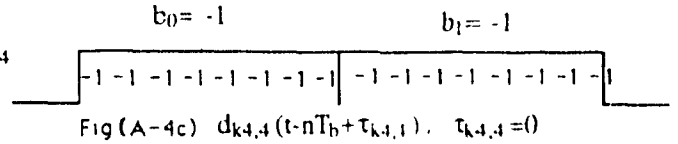
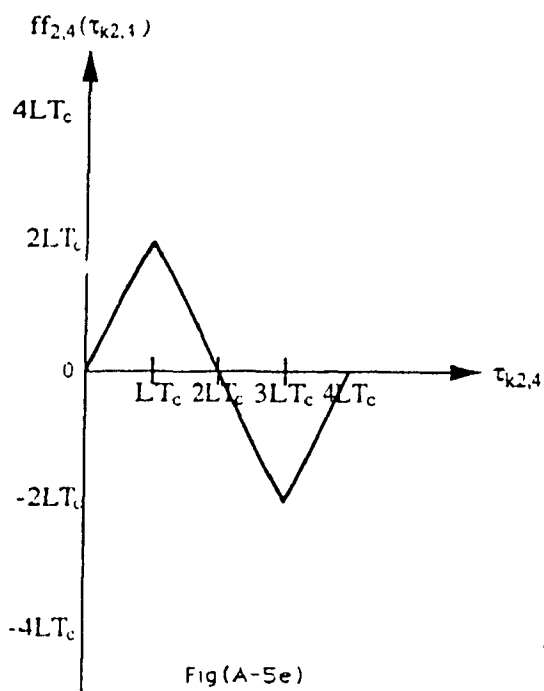
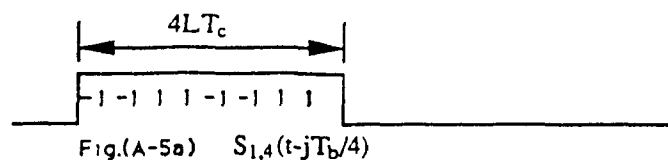


Fig (A-4d)
 $d_{k4,4}(t-nT_b + \tau_{k4,4})$ $S_{k4,4}(t-jT_b/4 + \tau_{k4,4})$
for various $\tau_{k4,4}$



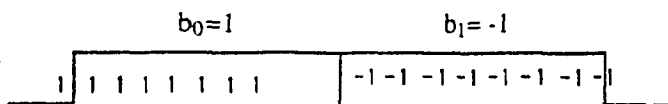
Fig(A-5e)
Switching function cross correlation
for 2 users in groups 4,2
($b_0, b_1 = (1, -1)$) are the two
data bits of the interfering user k2
overlapping the received bit of the
intended user



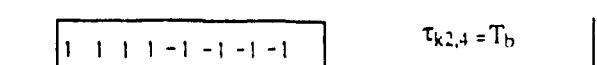
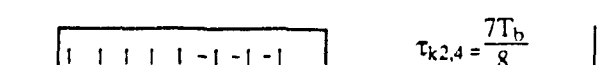
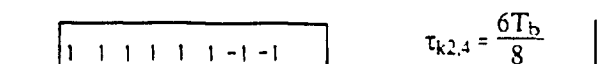
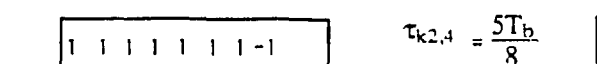
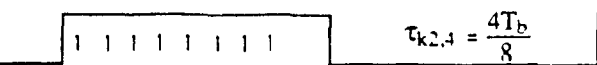
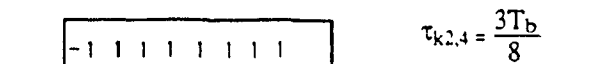
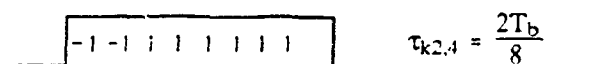
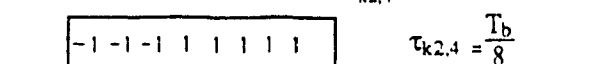
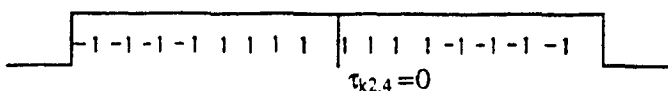
Fig(A-5a) $S_{1,4}(t-jT_b/4)$



Fig(A-5b) $S_{k2,2}(t-jT_b/4+\tau_{k2,4}), \tau_{k2,4}=0$

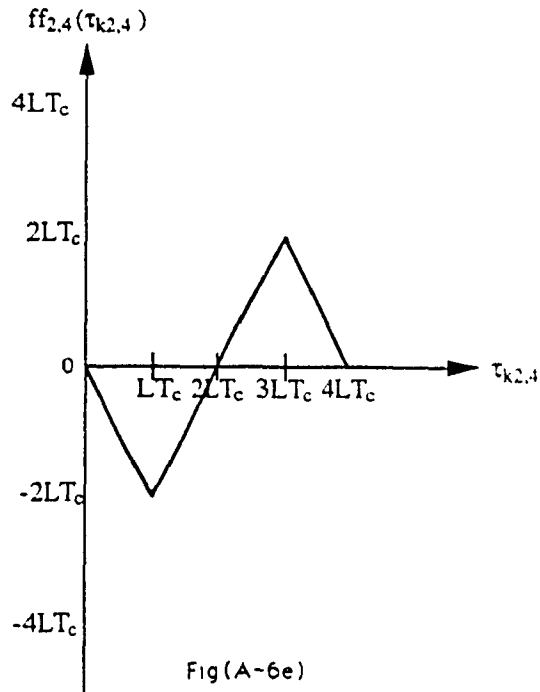


Fig(A-5c) $d_{k2,2}(t-nT_b+\tau_{k2,4}), \tau_{k2,4}=0$



Fig(A-5d)

$d_{k2,2}(t-nT_b+\tau_{k2,4})$ $S_{k2,2}(t-jT_b/4+\tau_{k2,4})$
for various $\tau_{k2,4}$



Switching function cross correlation for 2 users in groups 4,2 ($b_0, b_1 = (-1, 1)$) are the two data bits of the interfering user $k2$ overlapping the received bit of the intended user

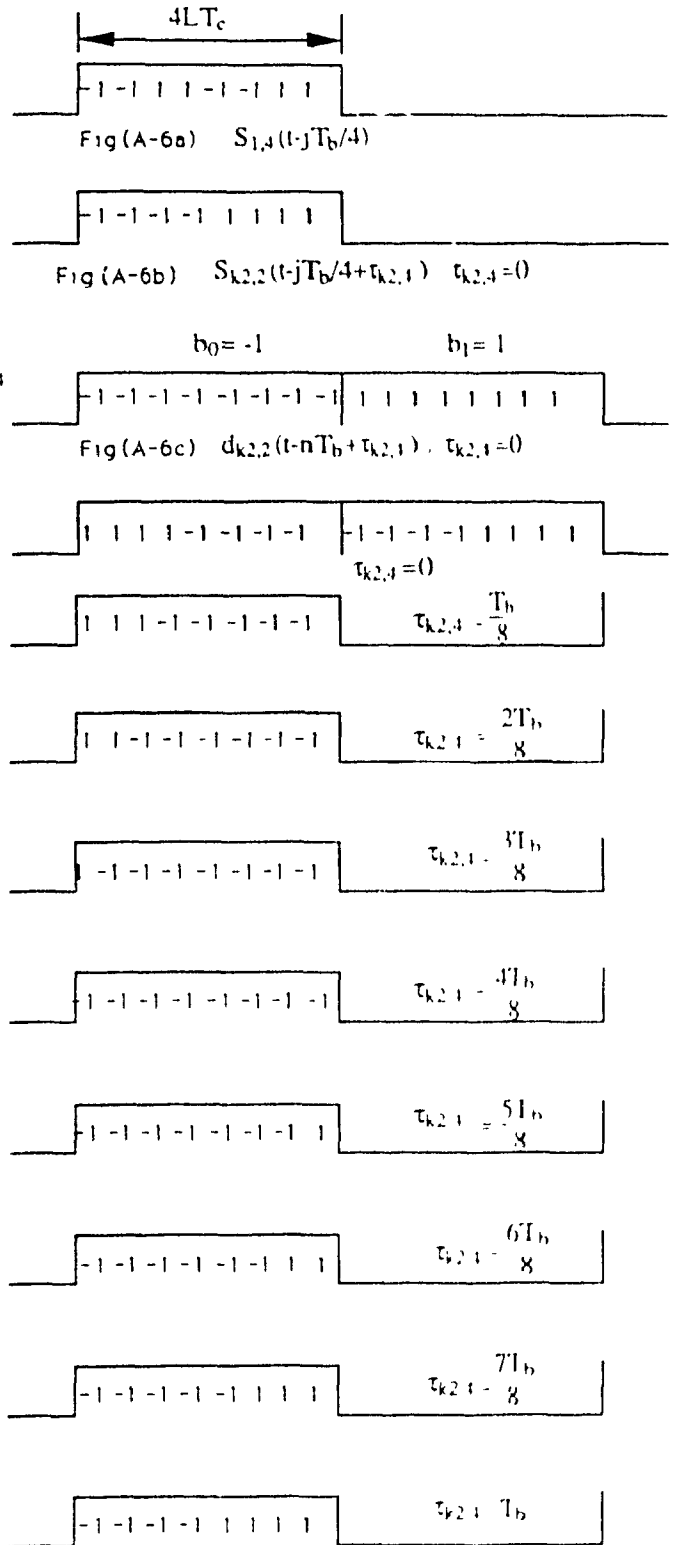
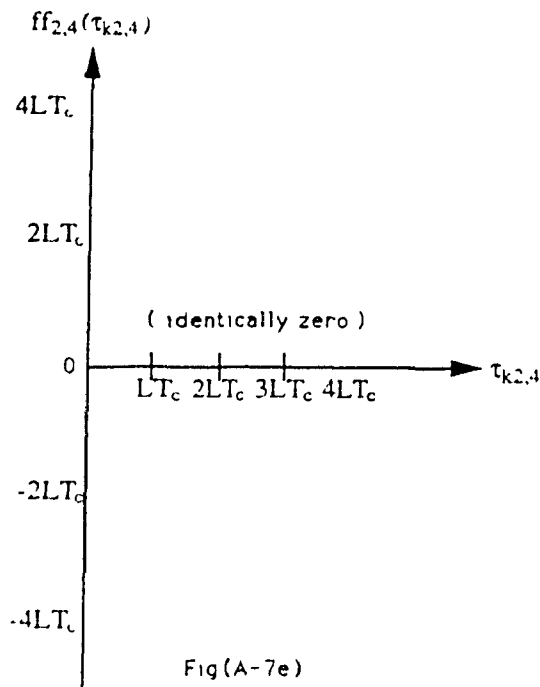


Fig (A-6d)

$d_{k2,2}(t-nT_b + \tau_{k2,4}) \quad S_{k2,2}(t-jT_b/4 + \tau_{k2,4})$
for various $\tau_{k2,4}$



Switching function cross correlation for 2 users in groups 4,2 ($b_0, b_1 = (1,1)$) are the two data bits of the interfering user $k2$ overlapping the received bit of the intended user

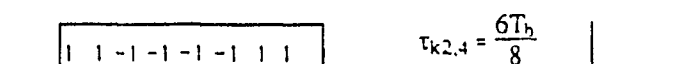
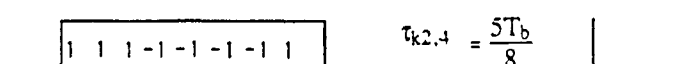
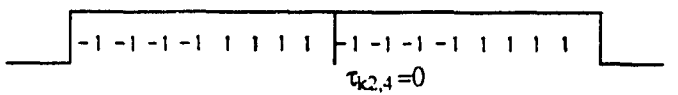
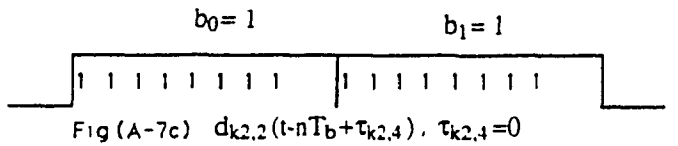
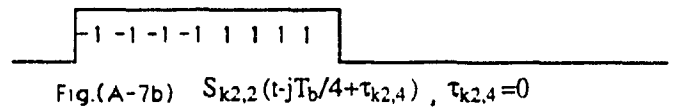
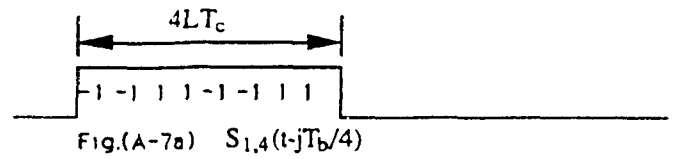
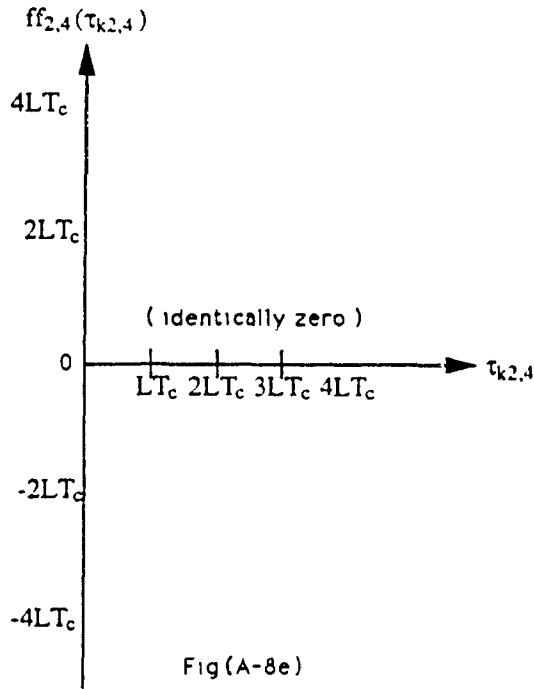
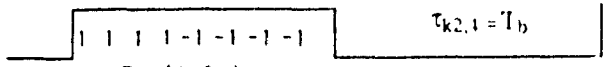
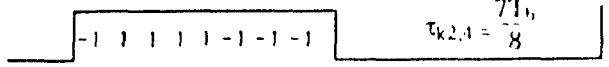
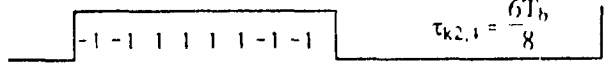
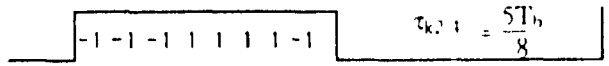
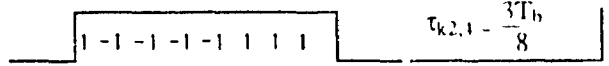
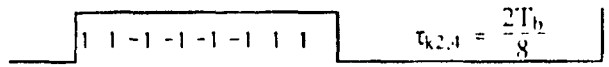
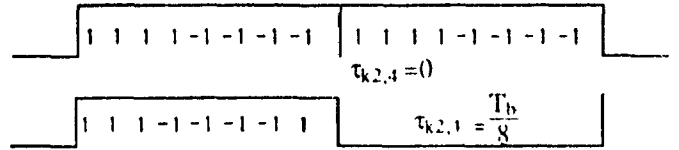
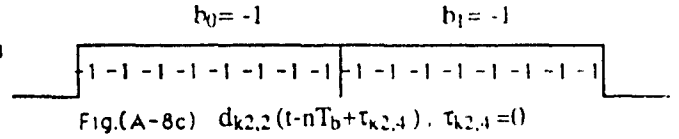
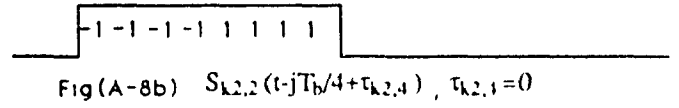
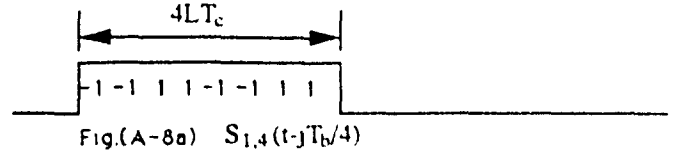


Fig (A-7a)
 $d_{k2,2}(t-nT_b+\tau_{k2,4}) \cdot S_{k2,2}(t-jT_b/4+\tau_{k2,4})$
for various $\tau_{k2,4}$



Switching function cross correlation for 2 users in groups 2,4 ($b_0, b_1 = (-1, -1)$) are the two data bits of the interfering user k_2 overlapping the received bit of the intended user



$d_{k2,2}(t-nT_b+\tau_{k2,4})$ $S_{k2,2}(t-jT_b/4+\tau_{k2,4})$
for various $\tau_{k2,4}$

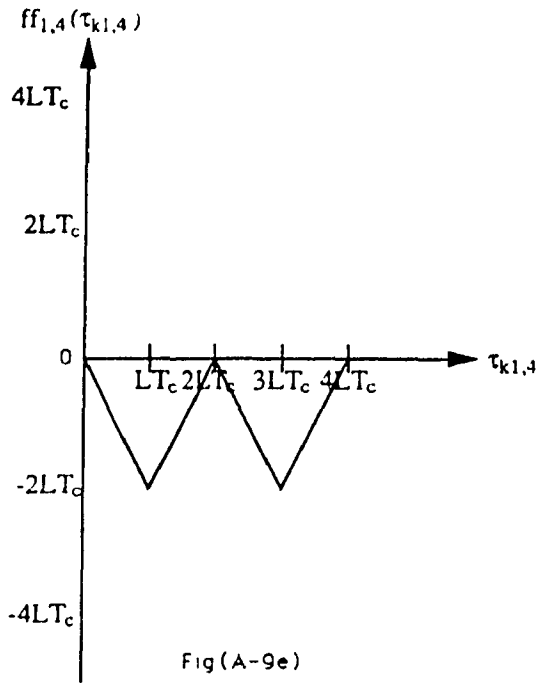


Fig (A-9e)
Switching function cross correlation
for 2 users in groups 1,4
($b_0, b_1 = \{1, -1\}$) are the two
data bits of the interfering user $k1$
overlapping the received bit of the
intended user

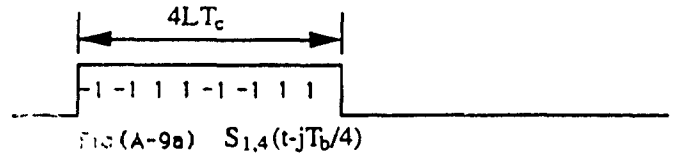


Fig (A-9a) $S_{1,4}(t-jT_b/4)$



Fig (A-9b) $S_{k1,1}(t-jT_b/4+\tau_{k1,4}), \tau_{k1,4}=0$

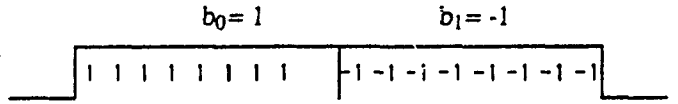


Fig (A-9c) $d_{k1,1}(t-nT_b+\tau_{k1,4}), \tau_{k1,4}=0$

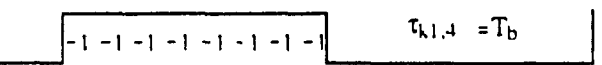
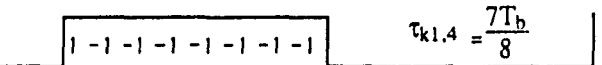
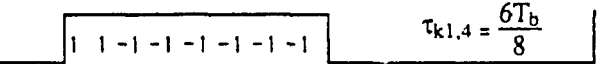
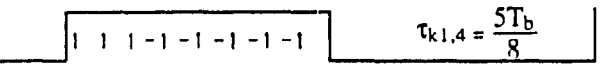
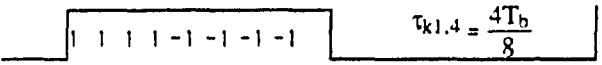
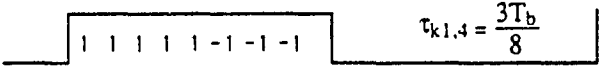
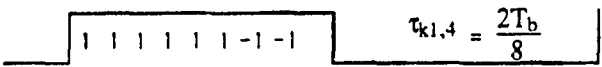
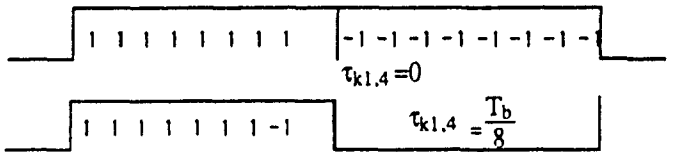
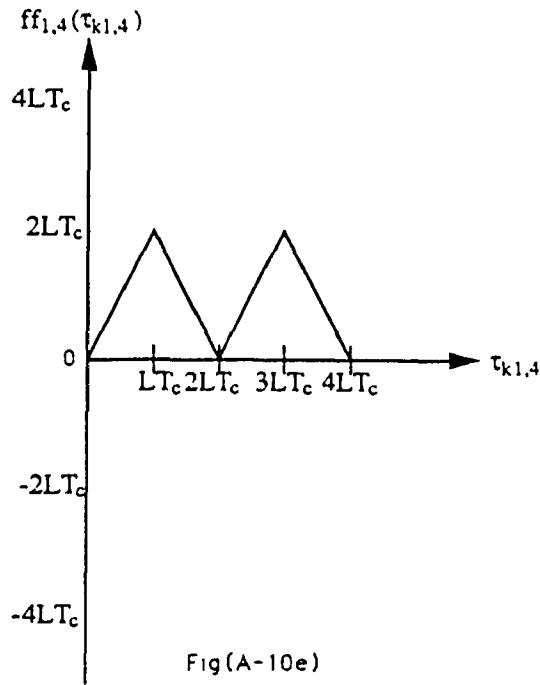


Fig (A-9d)

$d_{k1,1}(t-nT_b+\tau_{k1,4}) S_{k1,1}(t-jT_b/4+\tau_{k1,4})$
for various $\tau_{k1,4}$



Switching function cross correlation for 2 users in groups 1,4 ($b_0, b_1 = (-1, 1)$) are the two data bits of the interfering user k_1 overlapping the received bit of the intended user.

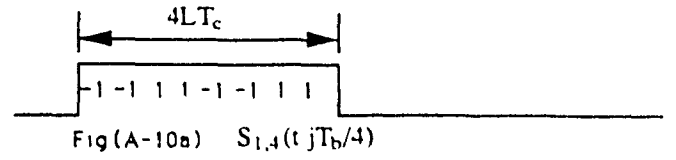
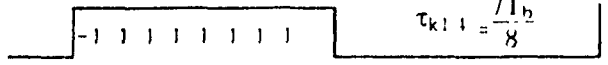
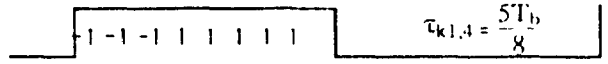
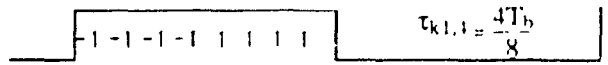
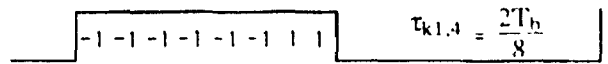
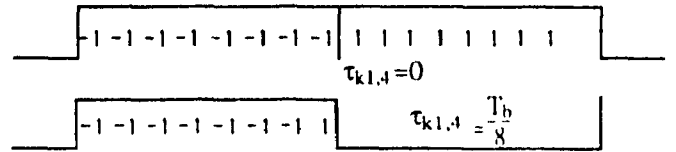
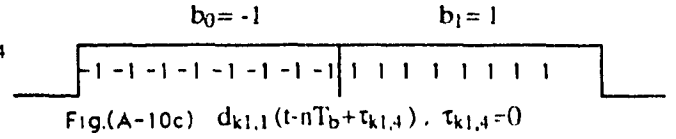
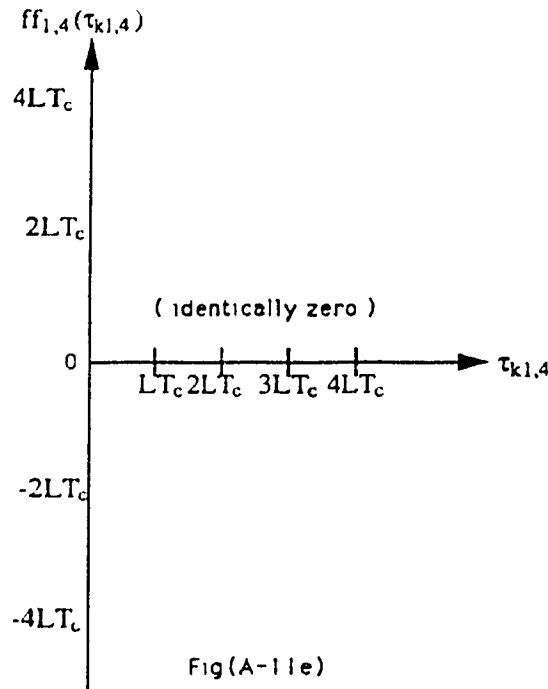


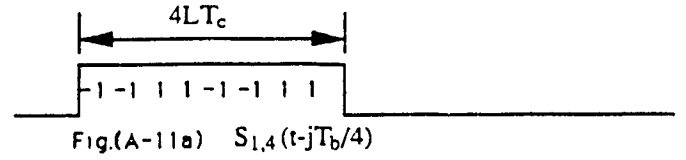
Fig.(A-10b) $S_{k1,1}(t-jT_b/4+\tau_{k1,4})$, $\tau_{k1,4}=0$



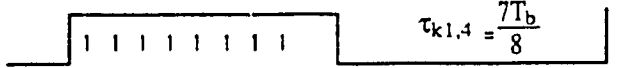
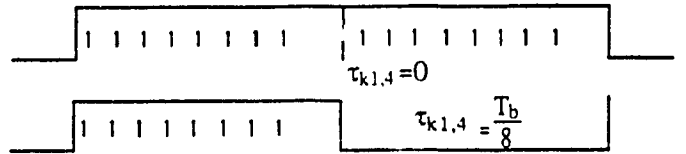
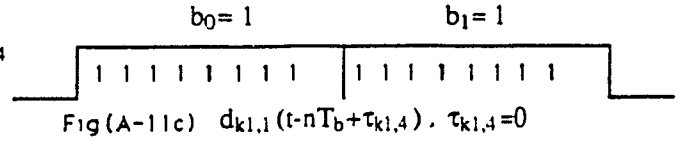
Fig(A-10d) $d_{k1,1}(t-nT_b+\tau_{k1,4}) S_{k1,1}(t-jT_b/4+\tau_{k1,4})$ for various $\tau_{k1,4}$



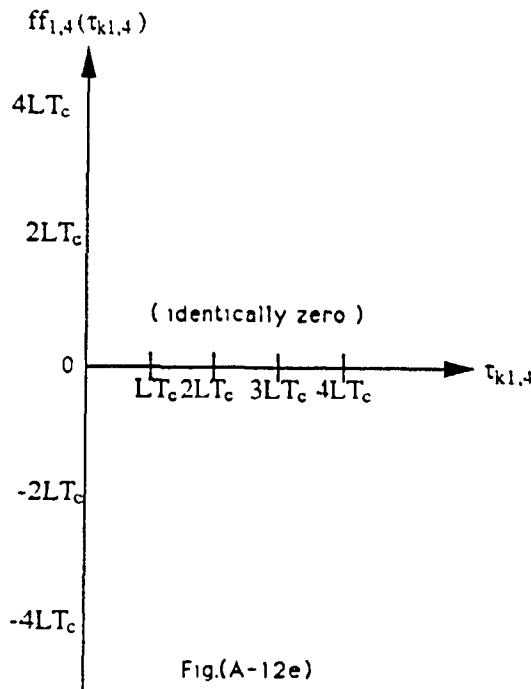
Switching function cross correlation for 2 users in groups 1,4 ($b_0, b_1 = (1,1)$) are the two data bits of the interfering user $k1$ overlapping the received bit of the intended user



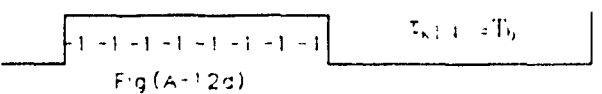
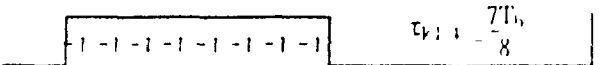
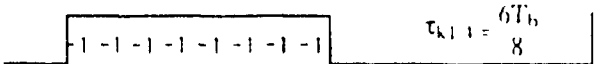
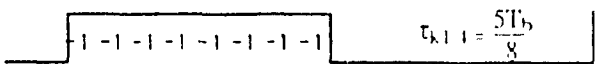
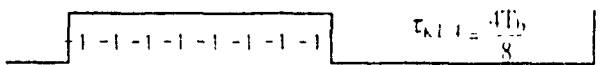
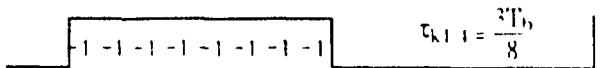
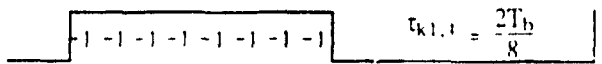
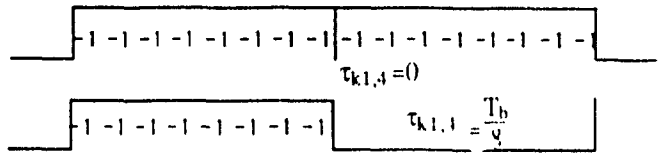
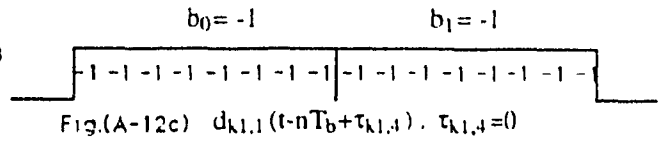
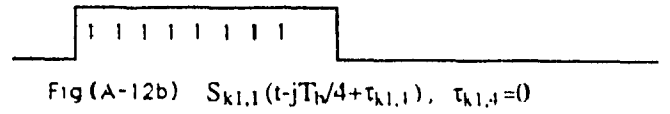
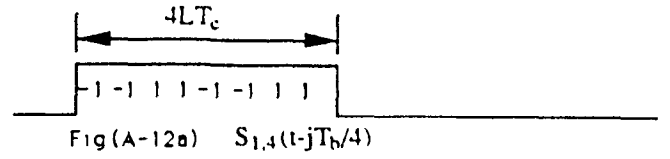
Fig(A-11b) $S_{k1,1}(t-jT_b/4+\tau_{k1,4}), \tau_{k1,4}=0$



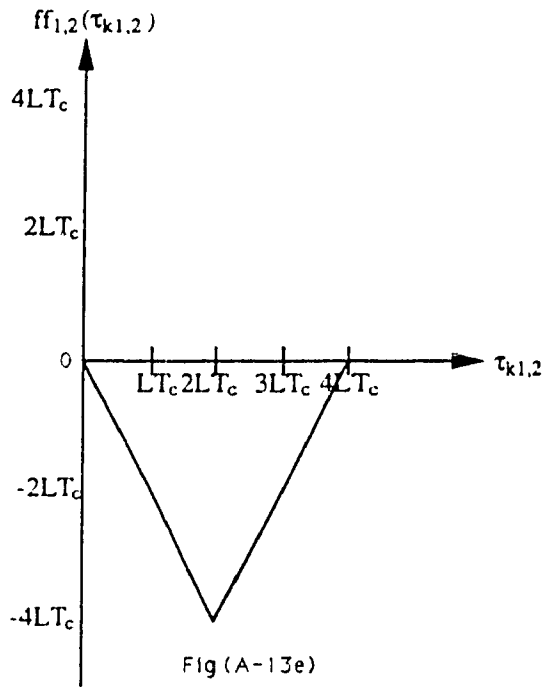
Fig(A-11d)
 $d_{k1,1}(t-nT_b+\tau_{k1,4}) S_{k1,1}(t-jT_b/4+\tau_{k1,4})$
for various $\tau_{k1,4}$



Switching function cross correlation for 2 users in groups 1,4 ($b_0, b_1 = -1, -1$) are the two data bits of the interfering user $k1$ overlapping the received bit of the intended user



Fig(A-12d)
 $d_{k1,1}(t-nT_b+\tau_{k1,1}), S_{1,4}(t-jT_b/4+\tau_{k1,1})$
for various $\tau_{k1,1}$



Switching function cross correlation for 2 users in groups 1,2 (b_0, b_1) = (1, -1) are the two data bits of the interfering user $k1$ overlapping the received bit of the intended user

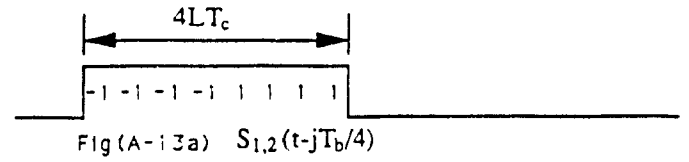


Fig (A-13b) $S_{k1,1}(t-jT_b/4+\tau_{k1,2})$, $\tau_{k1,2}=0$

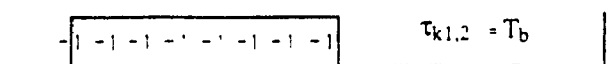
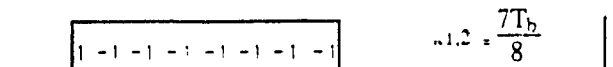
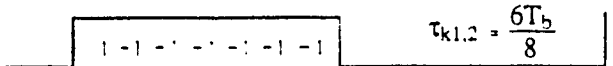
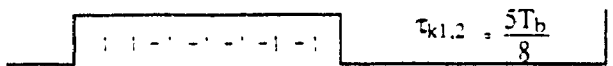
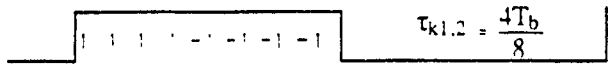
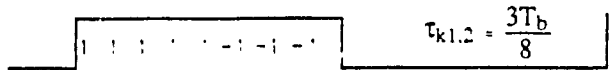
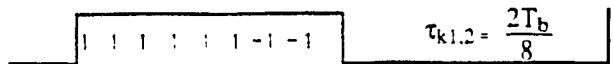
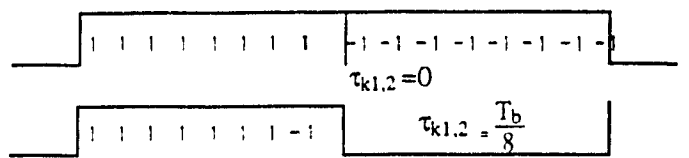
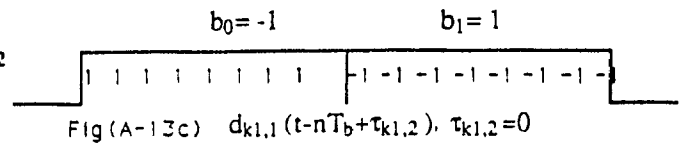
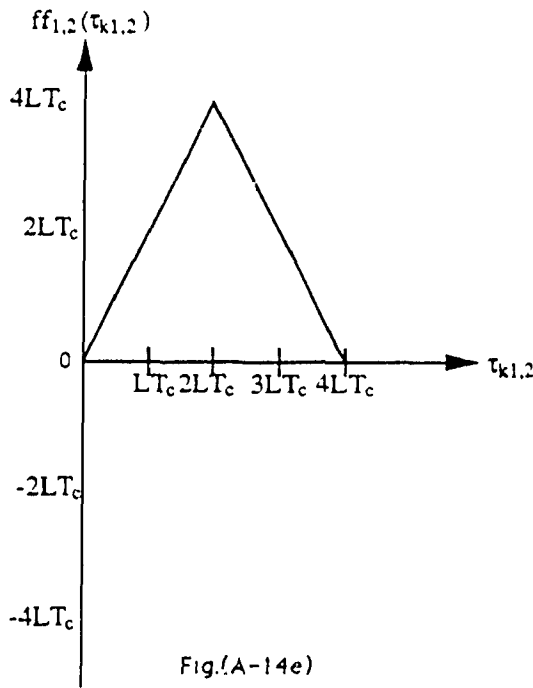


Fig (A-13d)

$d_{k1,1}(t-nT_b+\tau_{k1,2}) S_{k1,1}(t-jT_b/4+\tau_{k1,2})$ for various $\tau_{k1,2}$



Switching function cross correlation for 2 users in groups 1,2 ($b_0, b_1 = (-1, 1)$) are the two data bits of the interfering user $k1$ overlapping the received bit of the intended user

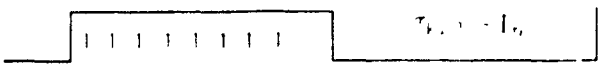
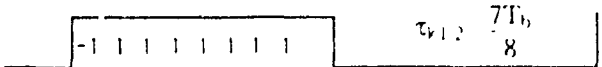
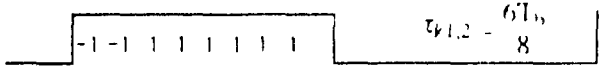
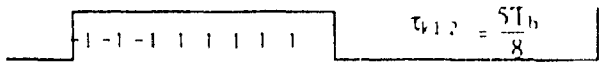
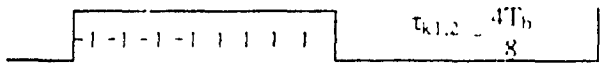
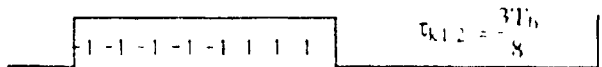
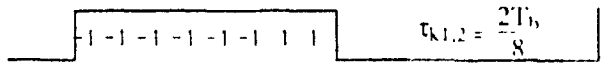
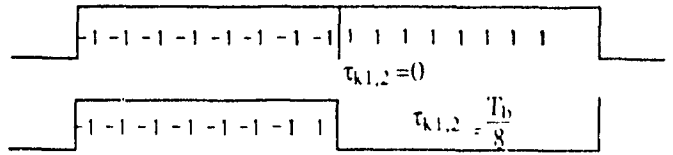
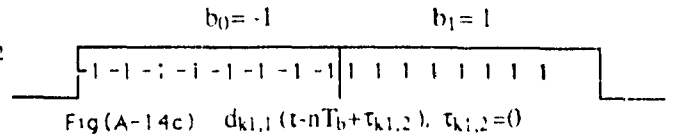
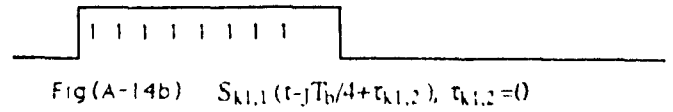
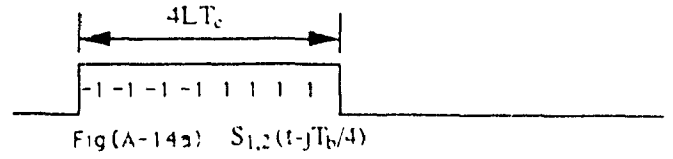
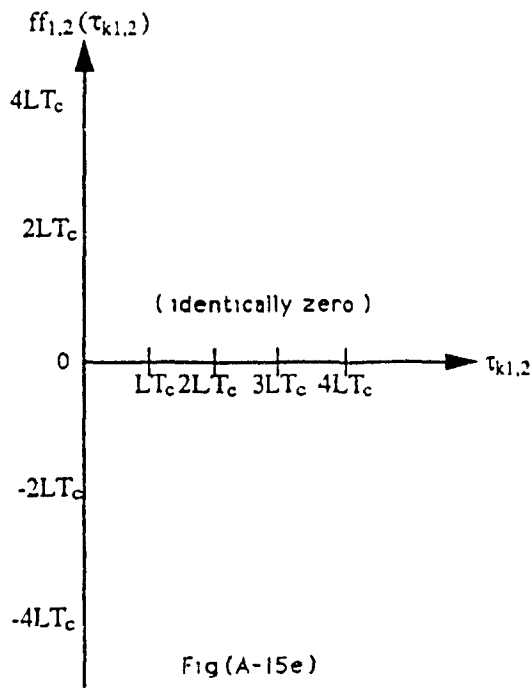


Fig (A-14d)
 $d_{k1,1}(t-nT_b + \tau_{k1,2}) = S_{k1,1}(t-jT_b/4 + \tau_{k1,2})$
for various $\tau_{k1,2}$



Switching function cross correlation for 2 users in groups 1,2 ($b_0, b_1 = (1, 1)$) are the two data bits of the interfering user $k1$ overlapping the received bit of the intended user.

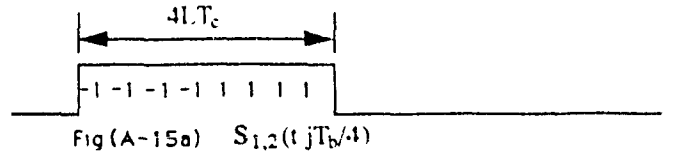


Fig (A-15a) $S_{1,2}(t-jT_b/4)$



Fig (A-15b) $S_{k1,1}(t-jT_b/4+\tau_{k1,2}), \tau_{k1,2}=0$

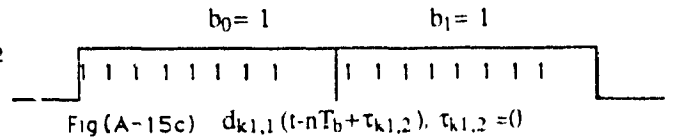


Fig (A-15c) $d_{k1,1}(t-nT_b+\tau_{k1,2}), \tau_{k1,2}=0$

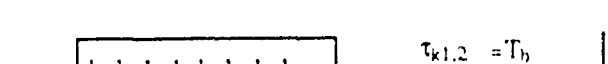
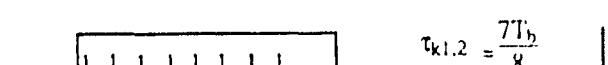
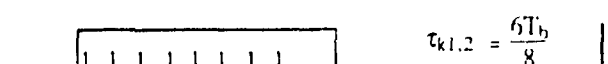
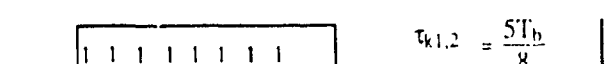
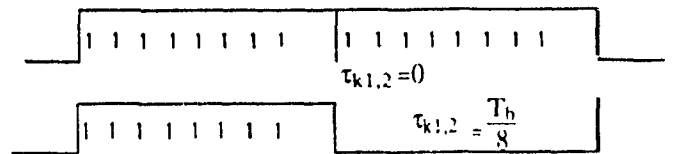
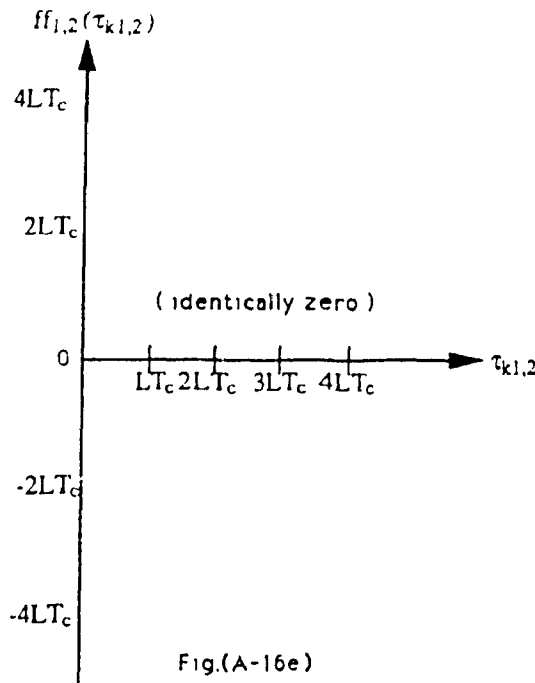
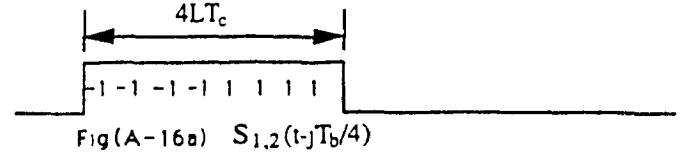


Fig (A-15d)

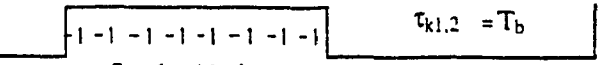
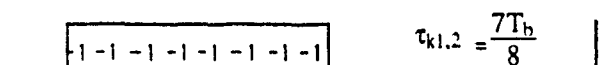
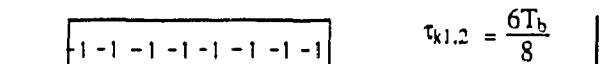
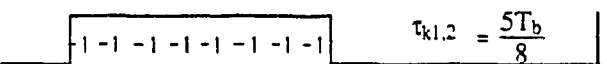
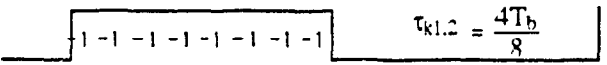
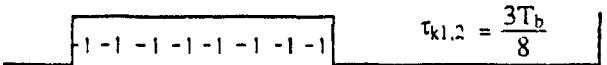
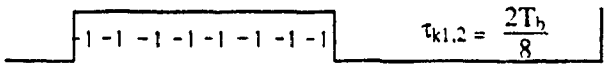
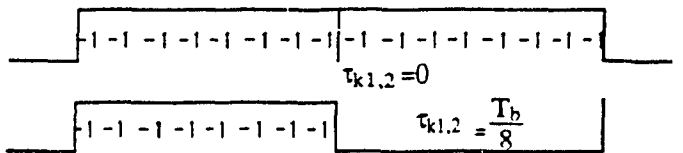
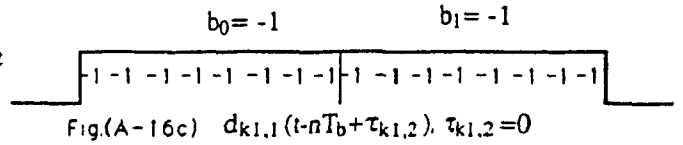
$d_{k1,1}(t-nT_b+\tau_{k1,2})$ $S_{k1,1}(t-jT_b/4+\tau_{k1,2})$
for various $\tau_{k1,2}$



Switching function cross correlation
for 2 users in groups 1,2
($b_0, b_1 = (-1, -1)$) are the two
data bits of the interfering user $k1$
overlapping the received bit of the
intended user



Fig(A-16b) $S_{k1,1}(t-jT_b/4+\tau_{k1,2}), \tau_{k1,2}=0$



Fig(A-16a)

$d_{k1,1}(t-nT_b+\tau_{k1,2}) S_{k1,1}(t-jT_b/4+\tau_{k1,2})$
for various $\tau_{k1,2}$

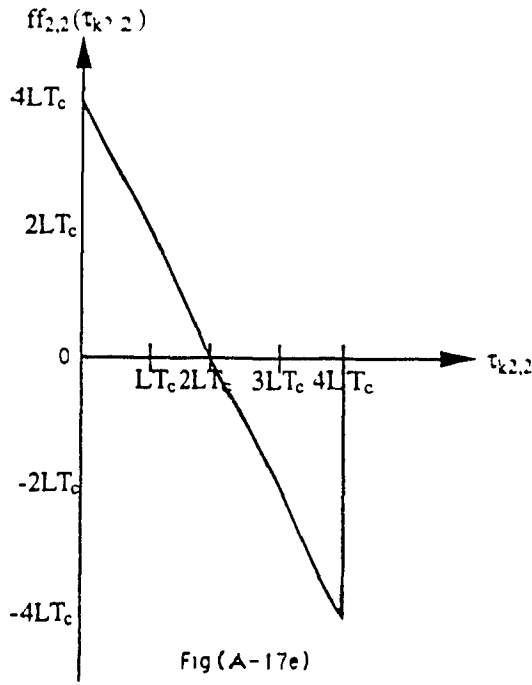


Fig (A-17e)
Switching function cross correlation for 2 users in groups 2,2 ($b_0, b_1 = (1, -1)$) are the two data bits of the interfering user k2 overlapping the received bit of the intended user

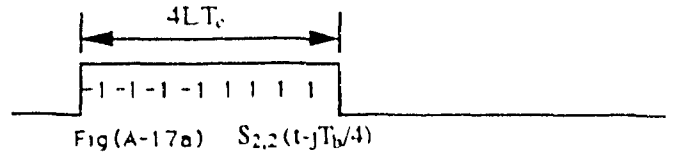


Fig (A-17a) $S_{2,2}(t-jT_b/4)$



Fig (A-17b) $S_{k2,2}(t-jT_b/4+\tau_{k2,2}), \tau_{k2,2}=0$

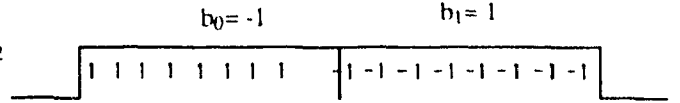


Fig (A-17c) $d_{k2,2}(t-nT_b/4+\tau_{k2,2}), \tau_{k2,2}=0$

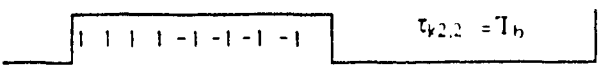
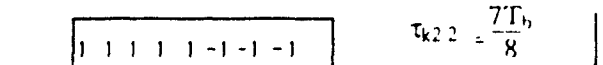
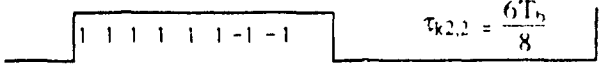
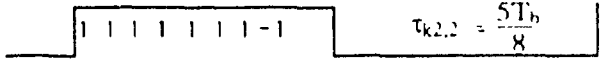
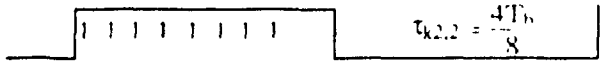
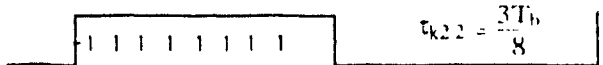
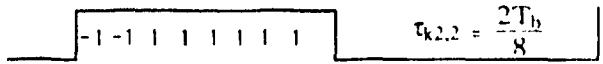
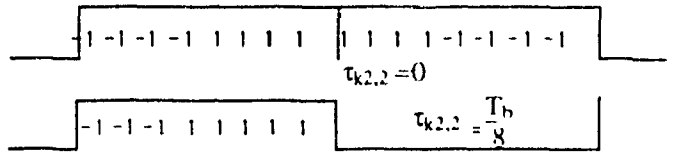
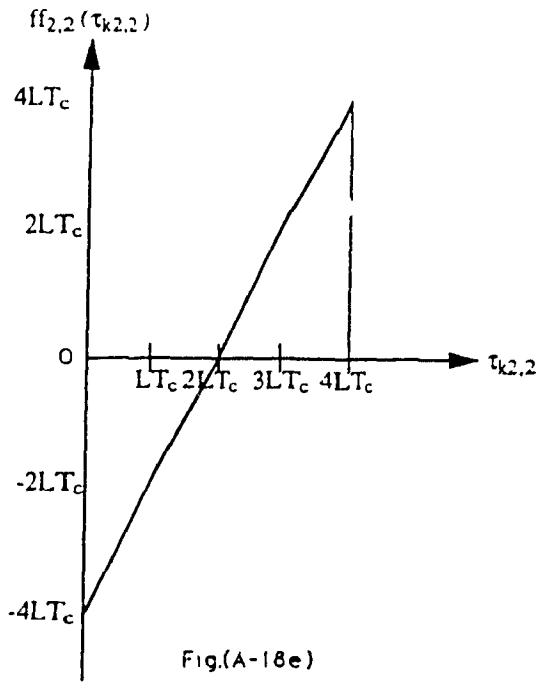
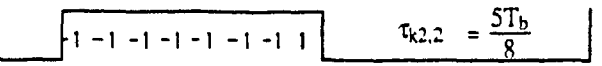
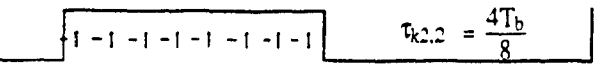
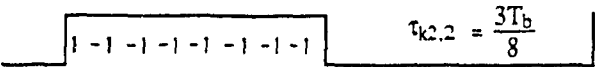
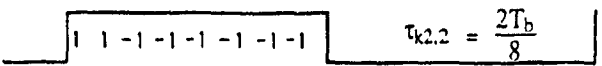
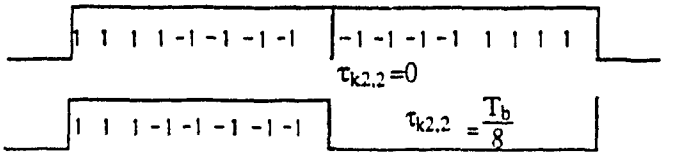
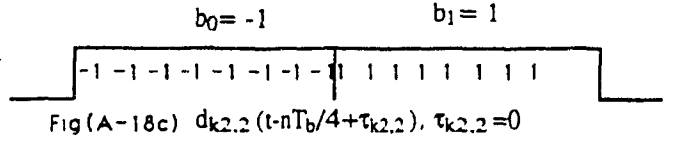
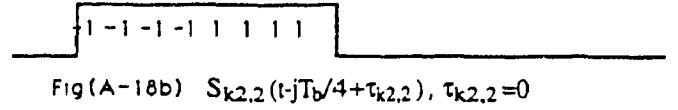
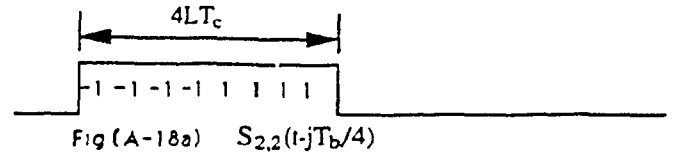


Fig (A-17d)

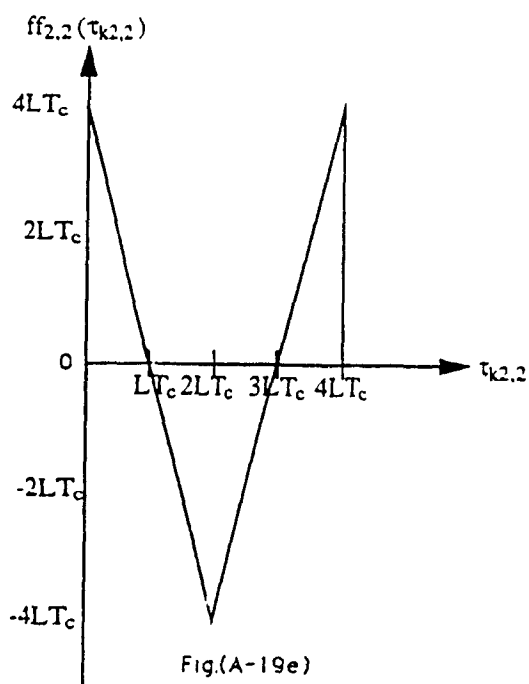
$d_{k2,2}(t-nT_b/4+\tau_{k2,2}) S_{k2,2}(t-jT_b/4+\tau_{k2,2})$
for various $\tau_{k2,2}$



Switching function cross correlation for 2 users in groups 2,2 ($b_0, b_1 = (-1, 1)$) are the two data bits of the interfering user k_2 overlapping the received bit of the intended user



Fig(A-18d)
 $d_{k2,2}(t-nT_b/4+\tau_{k2,2}) S_{k2,2}(t-jT_b/4+\tau_{k2,2})$
for various $\tau_{k2,2}$



Switching function cross correlation for 2 users in groups 2,2 ($b_0, b_1 = (1, 1)$) are the two data bits of the interfering user k_2 overlapping the received bit of the intended user

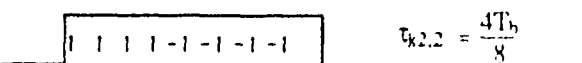
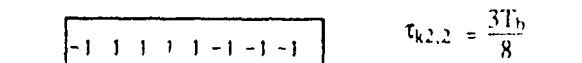
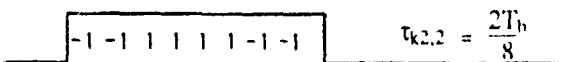
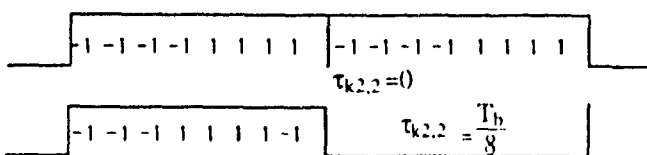
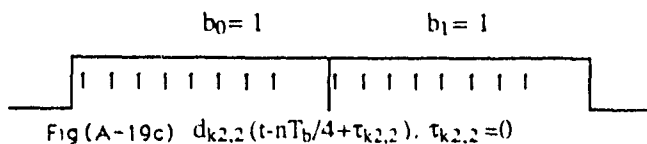
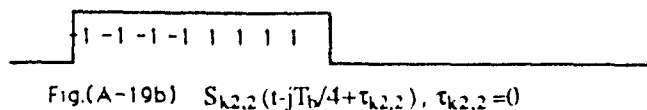
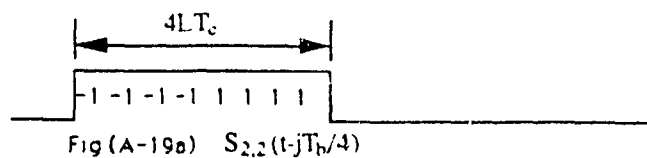
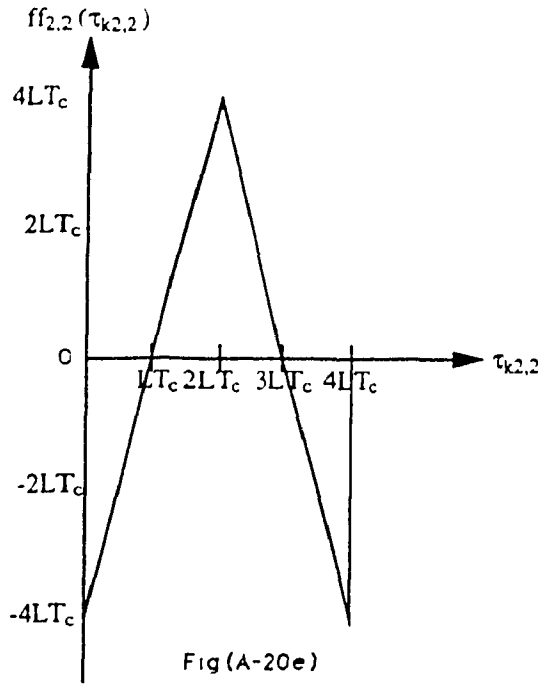


Fig (A-19d)

$d_{k2,2}(t-nT_b/4+\tau_{k2,2})$ $S_{k2,2}(t-jT_b/4+\tau_{k2,2})$
for various $\tau_{k2,2}$



Switching function cross correlation for 2 users in groups 2,2 ($b_0, b_1 = (-1, -1)$) are the two data bits of the interfering user k_2 overlapping the received bit of the intended user.

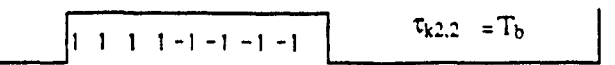
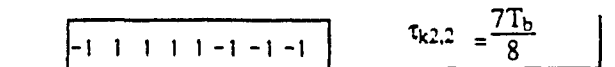
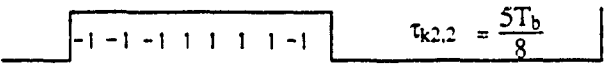
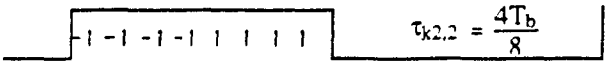
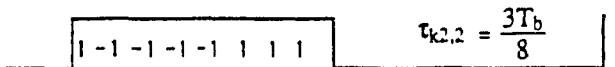
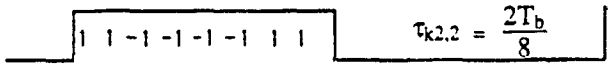
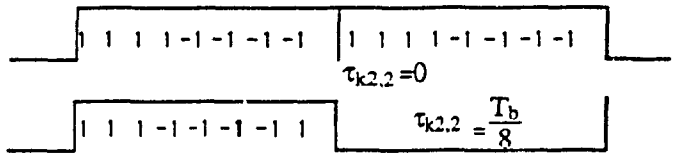
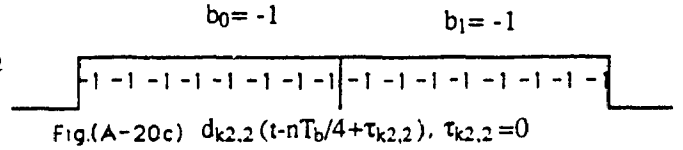
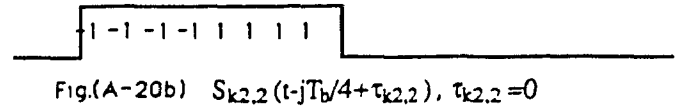
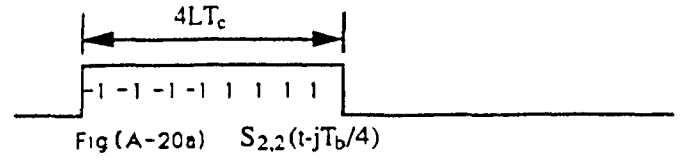
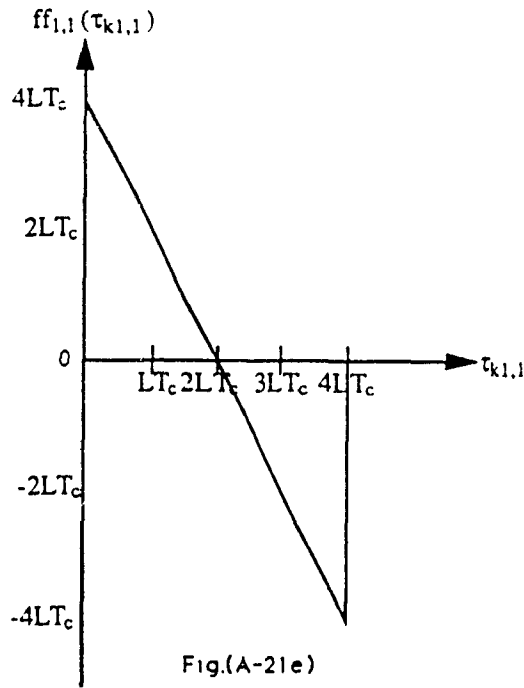
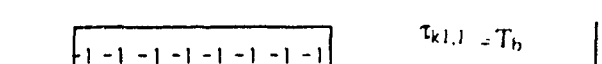
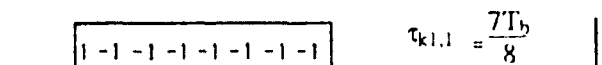
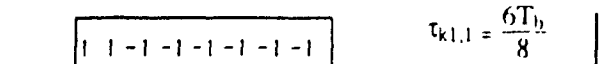
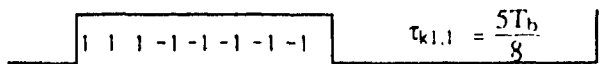
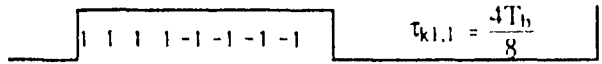
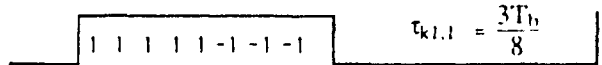
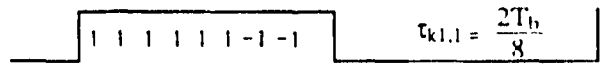
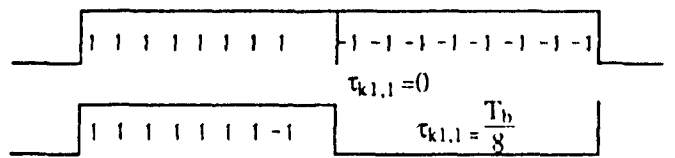
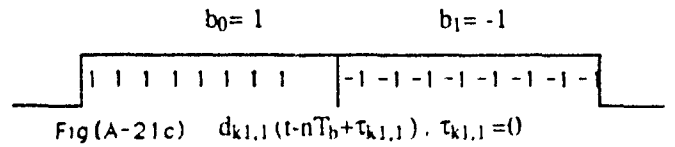
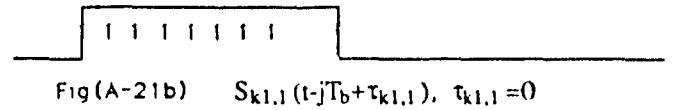
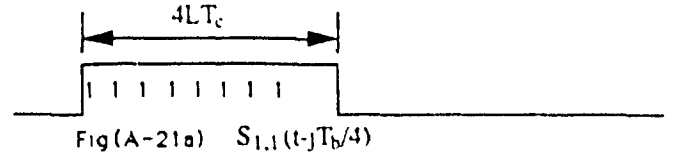


Fig (A-20d)

$d_{k2,2}(t-nT_b/4+\tau_{k2,2})$ $S_{k2,2}(t-jT_b/4+\tau_{k2,2})$
for various $\tau_{k2,2}$



Switching function cross correlation for 2 users in groups 1,1 ($b_0, b_1 = (1, -1)$ are the two data bits of the interfering user $k1$ overlapping the received bit of the intended user



Fig(A-21d)
 $d_{k1,1}(t-nT_b+\tau_{k1,1}) S_{k1,1}(t-jT_b+\tau_{k1,1})$
for various $\tau_{k1,1}$

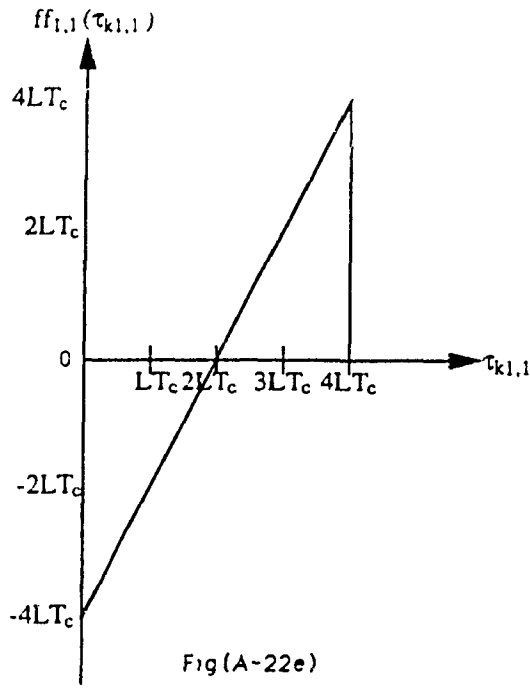


Fig (A-22e)
Switching function cross correlation for 2 users in groups 1,1 ($b_0, b_1 = (-1, 1)$) are the two data bits of the interfering user $k1$ overlapping the received bit of the intended user.

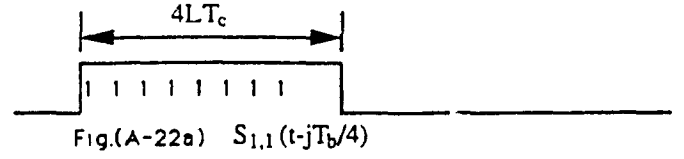


Fig (A-22b) $S_{k1,1}(t-jT_b+\tau_{k1,1}), \tau_{k1,1}=0$

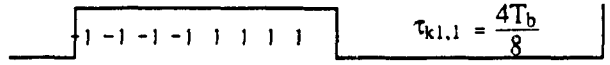
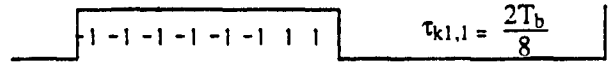
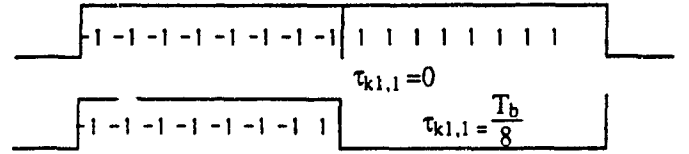
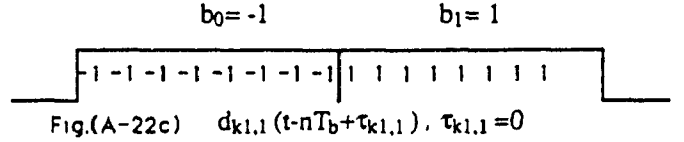
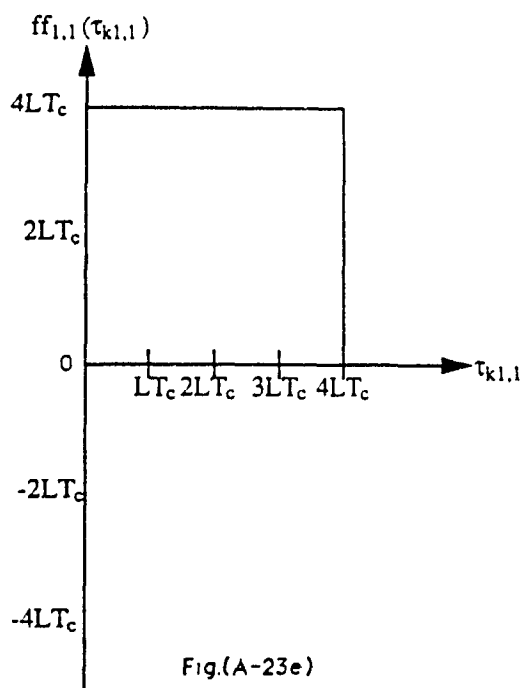


Fig.(A-22d)

$d_{k1,1}(t-nT_b+\tau_{k1,1}) S_{k1,1}(t-jT_b+\tau_{k1,1})$
for various $\tau_{k1,1}$



Switching function cross correlation for 2 users in groups 1,1 ($b_0, b_1 = 1, 1$) are the two data bits of the interfering user $k1$ overlapping the received bit of the intended user

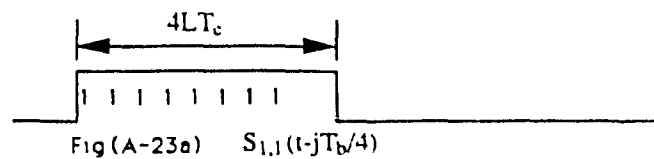


Fig (A-23a) $S_{1,1}(t-jT_b/4)$



Fig (A-23b) $S_{k1,1}(t-jT_b+\tau_{k1,1})$, $\tau_{k1,1}=0$

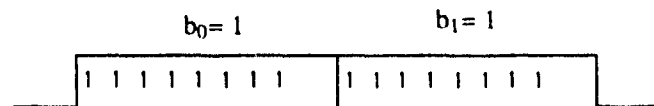


Fig (A-23c) $d_{k1,1}(t-nT_b+\tau_{k1,1})$, $\tau_{k1,1}=0$

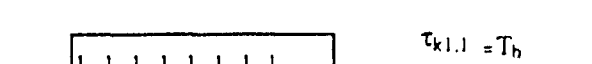
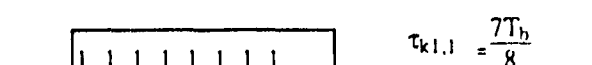
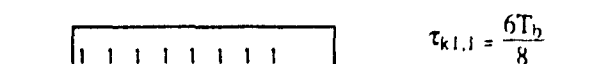
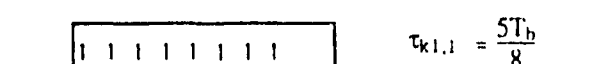
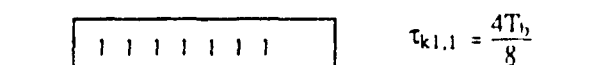
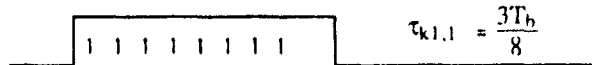
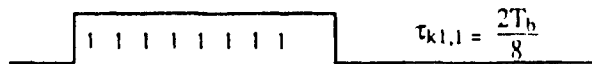
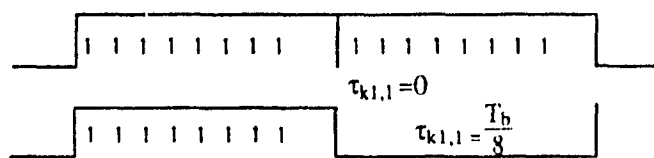


Fig (A-23d)

$d_{k1,1}(t-nT_b+\tau_{k1,1})$ $S_{k1,1}(t-jT_b+\tau_{k1,1})$
for various $\tau_{k1,1}$

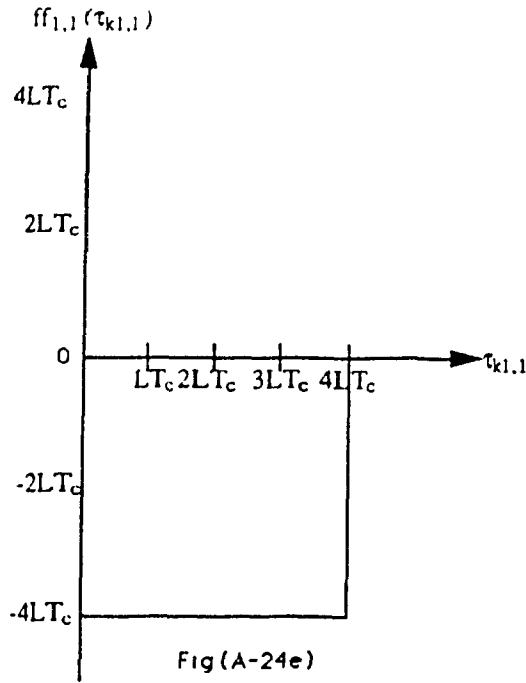


Fig (A-24e)
Switching function cross correlation for 2 users in groups 1,1 ($b_0, b_1 = (-1, -1)$) are the two data bits of the interfering user $k1$ overlapping the received bit of the intended user.

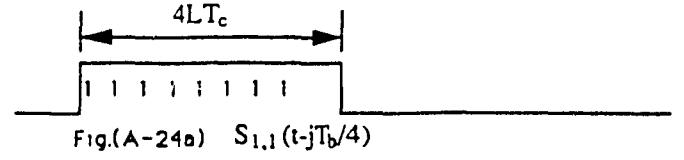


Fig.(A-24b) $S_{k1,1}(t-jT_b+\tau_{k1,1}), \tau_{k1,1}=0$

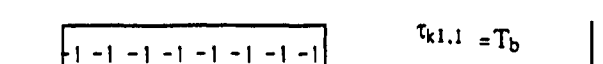
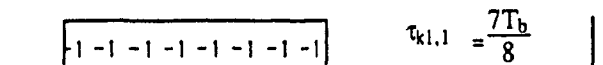
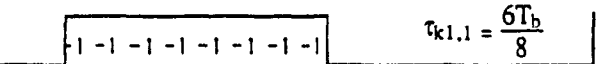
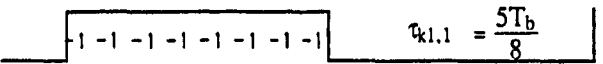
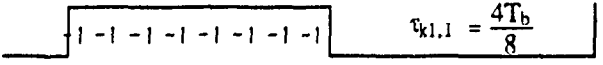
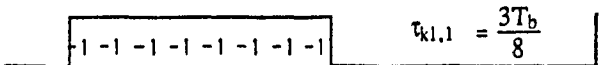
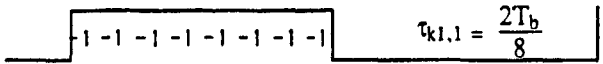
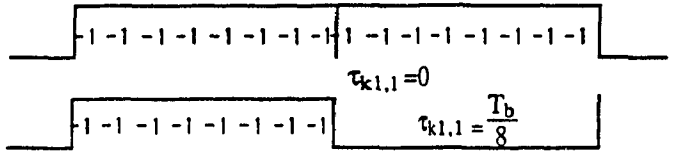
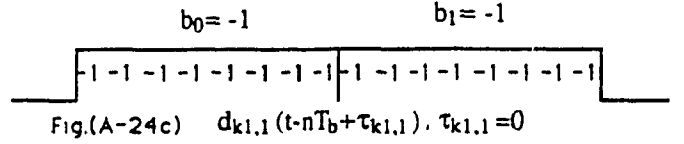


Fig (A-24d)

$d_{k1,1}(t-nT_b+\tau_{k1,1}) \cdot S_{k1,1}(t-jT_b+\tau_{k1,1})$
for various $\tau_{k1,1}$